

**STUDIES ON SOME NONLINEAR  
SCHRÖDINGER TYPE EQUATIONS  
DESCRIBING PULSE PROPAGATION  
THROUGH OPTICAL FIBERS**



**Thesis Submitted**  
in partial fulfilment of the requirements  
for the award of the DEGREE of  
**DOCTOR OF PHILOSOPHY**

**M.N. VINOJ**

**DEPARTMENT OF PHYSICS  
COCHIN UNIVERSITY OF SCIENCE AND TECHNOLOGY  
KOCHI - 682 022**

**November 2003**

To

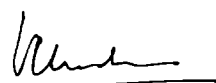
My parents

## CERTIFICATE

Certified that the work presented in this thesis is the bonafide work done by Mr. M. N. Vinoj, under my guidance in the Department of Physics, Cochin University of Science and Technology and that this work has not been included in any other thesis submitted previously for the award of any degree.

Kochi-682 022

November 2003



Dr. V. C. Kuriakose

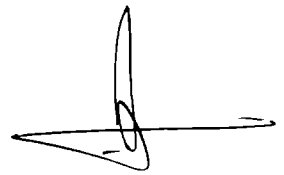
Supervising Teacher

## DECLARATION

I here by declare that the work presented in this thesis is based on the original work done by me under the guidance of Dr. V. C. Kuriakose, Professor, in the Department of Physics, Cochin University of Science and Technology and has not been included in any other thesis submitted previously for the award of any degree.

Kochi-682 022

November 2003

A handwritten signature in black ink, consisting of a vertical stroke on the right, a horizontal stroke extending to the left, and a loop at the bottom.

M. N. Vinoj

## PREFACE

The work presented in this thesis has been carried out by the author at the Department of Physics, Cochin University of Science and Technology during the period 1998-2003.

The discovery of the soliton is considered to be one of the most significant events of the twentieth century. The term soliton refers to special kinds of waves that can propagate undistorted over long distances and remain unaffected even after collision with each other. Solitons have been studied extensively in many fields of physics. In the context of optical fibers, solitons are not only of fundamental interest but also have potential applications in the field of optical fiber communications. This thesis is devoted to the theoretical study of soliton pulse propagation through single mode optical fibers.

Chapter one provides a general introduction to various linear and nonlinear propagation effects in single mode optical fibers. Derivation of the nonlinear Schrödinger (NLS) equation describing the wave propagation of the envelope of the optical field in nonlinear dispersive media and various methods for the analysis of integrable nonlinear equations are also presented in this chapter.

Chapter two focuses on the higher-order dispersive and nonlinear effects that occur when ultra-short pulse propagates through birefringent single mode fibers. Condition for the propagation of stable soliton pulse in presence of higher-order effects are discussed. The fundamental and higher-order solitons are then introduced by solving coupled higher-order nonlinear Schrödinger equation (CHNLS) with Hirota's method. The interaction of solitons are also studied.

Chapter three is devoted to the study of propagation of initially unchirped

pulse through lossy fiber. In soliton communication system, input pulse launched into the fiber should be unchirped. Integrability condition required for the formation of soliton in the presence of frequency chirping and damping is derived. Fundamental soliton solution is then constructed by using linear eigen value problem and Bäcklund transformation technique. Effect of initial frequency chirp on soliton propagation is also presented.

Chapter four considers the effect of electro-optic phase modulation, fiber loss, and gain on the formation of solitons, both in the anomalous and normal dispersive regimes. Integrability of such system is verified in both regimes by constructing linear eigen value problem. Bright and dark soliton solutions are generated using Hirota's method. Influence of electro-optic phase modulation, fiber loss, and gain on soliton pulse compression is also analyzed.

Chapter five is devoted to study the effect of dispersion-decreasing fibers (DDFs) on soliton propagation. Requirement for the existence of soliton in DDF is discussed at first. Various dispersion-decreasing profiles have been considered. Effect of various profiles on soliton pulse compression has been analyzed. Pulse propagation through birefringent single mode fiber with variable dispersion has also been discussed.

Chapter six considers the influence of both DDFs and fiber loss on pulse propagation. Integrability analysis of the system is presented. Variable transformations are introduced to transform the nonuniform NLS equation to the well-known uniform NLS equation. Effect of fiber loss in different dispersion-decreasing profiles are studied. Compression achieved by the soliton pulse during its propagation through various profiles have also been discussed. Study is also extended to the birefringent DDFs.

Chapter seven deals with the major results and overall conclusions of the

thesis work.

A part of the present investigations has been appeared in the form of following publications.

1. Multisoliton solutions and integrability aspects of coupled higher-order nonlinear Schrödinger equations, M. N. Vinoj and V. C. Kuriakose, *Phys. Rev. E*, 62, 8719 (2000)
2. Optical soliton with damping and frequency chirping in fiber media, M. N. Vinoj, V. C. Kuriakose and K. Porsezian, *Chaos, Solitons, and Fractals*, 12, 2569 (2001)
3. Nonlinear compression of optical solitons, M. N. Vinoj and V. C. Kuriakose, *Pramana-J. Phys.*, 57, 987 (2001)
4. Optimum dispersion profile and pedestal free soliton pulse compression in dispersion-decreasing fiber, M. N. Vinoj, A. U. Seema and V. C. Kuriakose, *J. of Nonlinear Optical Physics and Materials* (to appear)
5. Generation of pedestal free ultrashort soliton pulses and optimum dispersion profile in real dispersion-decreasing fiber, M. N. Vinoj and V. C. Kuriakose, *J. Opt. A: Pure Appl. Opt.* (to appear)
6. Pedestal free soliton compression and optimum dispersion profile in a birefringent single-mode fiber, M. N. Vinoj and V. C. Kuriakose, *Opt. Commun.* (to appear)
7. Compression of soliton pulses in a single mode birefringent dispersion-decreasing fiber, M. N. Vinoj and V. C. Kuriakose, *Pramana-J. Phys* (submitted)

A part of the present investigations has been presented in the following seminars/workshops.

1. Generation of pedestal free ultra-short soliton pulses in a dispersion-decreasing fiber, M. N. Vinoj and V C. Kuriakose, International Workshop on Optical Solitons: Theory and Experiments, Cochin University of Science and Technology, Cochin-682 022, January 24-29 (2002)



## ACKNOWLEDGEMENTS

It gives me great pleasure to express my sincere gratitude to Dr. V C. Kuriakose for his guidance and valuable suggestions. His overwhelming patience, constant encouragement, and ever-helpful attitude helped me a lot during the period of my research work.

I am extremely thankful to Prof. K. P. Vijayakumar, Head of the Department of Physics. Prof. Elizebath Mathai, and Prof. K. P. Rajappan Nair, former Heads of Department of Physics, for providing the necessary facilities for the successful completion of my research work.

I am also thankful to Prof. K. Babu Joseph, Prof. M. Sabir and Dr. T. Ramesh Babu for their constant encouragement.

I am greatly indebted to Prof. M. Lakshmanan, The Head, Center for Non-linear Dynamics and Department of Physics, Bharathidasan University, Dr. K. Porsezian, Raman School of Physics, Pondicherry University, Prof. K. Thyagarajan, Department of Physics, Indian Institute of Technology, Delhi, and Prof. K. J. Blow, Aston University, UK for the useful and informative discussions I had with them.

I am very happy to express my thanks to Dr. R. Ganapathy, C. D. Ravikumar, P. D. Shaju, Minu Joy, M. Sivakumar, P. I. Kuriakose, S. Shaji, M. C. Santhosh Kumar and A. P. Jayadevan for all their help and cooperation extended during my research work.

I also acknowledge the help and constant encouragement I received from all my friends pursuing research in the Department of Physics, Cochin University of Science and Technology.

I express my gratitude to The Head and Staff members of Physics Department, St. Peter's College.

I am overwhelmed with love and joy for the affection and inspiration received from my parents and other members of the family in my pursuit of this research work.

The moral support and encouragement extended by my wife Mrs. Seema deserves special mention here.

I gratefully acknowledge the Council of Scientific and Industrial Research (CSIR), Govt. of India for the award of fellowship in the form of JRF and SRF to carry out the research work.

M N Vinoj

# Table of Contents

<b>Table of Contents</b>	<b>vii</b>
<b>1 Introduction</b>	<b>1</b>
1.1 Optical fiber	2
1.2 Linear effects	5
1.2.1 Optical loss	6
1.2.2 Dispersion	6
1.3 Nonlinear effects	8
1.3.1 Nonlinear refraction	9
1.3.2 Four-wave mixing	10
1.3.3 Self-steepening	10
1.3.4 Stimulated inelastic scattering	11
1.4 Wave propagation in single-mode optical fibers	12
1.5 Soliton solution for the nonlinear Schrödinger equation.	23
1.6 Dispersion decreasing fibers	27
1.7 Analysis of nonlinear partial differential equations	27
1.7.1 Painleve' analysis	28
1.7.2 Inverse Scattering Transform (IST)	29
1.7.3 AKNS Method	30
1.7.4 Hirota's method	31
1.7.5 Bäcklund transformation	32
<b>2 Soliton propagation in a fiber with higher-order dispersive and nonlinear effects</b>	<b>33</b>
2.1 Introduction	33
2.2 NLSE in the presence of third order dispersion	34
2.3 NLSE with Self-Steepening and Delayed Nonlinear Response	34
2.4 NLSE in the presence of all higher-order effects	35
2.5 Integrability analysis of CHNLS equations	37
2.6 Hirota bilinearization and soliton solutions	40

2.6.1	One-soliton solutions	43
2.6.2	Two-soliton solutions	45
2.7	Asymptotic analysis	47
2.8	Lax pair for CHNLS equations	48
2.9	Conclusion	50
<b>3</b>	<b>Effect of frequency chirping on soliton formation</b>	<b>51</b>
3.1	Introduction	51
3.2	Formulation of the problem	52
3.3	Singularity structure analysis	52
3.4	Linear eigen value problem	56
3.5	Soliton solution	57
3.6	Compression factor	60
3.7	Conclusion	62
<b>4</b>	<b>Soliton propagation in a real fiber with amplification and effective phase modulation</b>	<b>63</b>
4.1	Introduction	63
4.2	Formulation of the problem	64
4.3	Linear eigen value problem	65
4.4	Hirota bilinearization and soliton solution	66
4.5	Pulse propagation in normal dispersive regime	69
4.6	Integrability analysis	69
4.7	Dark solitons	71
4.8	Conclusion	73
<b>5</b>	<b>Propagation of soliton pulse through dispersion-decreasing fiber</b>	<b>74</b>
5.1	Introduction	74
5.2	Mathematical formulation of the problem	75
5.3	Singularity analysis and soliton solution	76
5.4	Analysis of pulse propagation through different profiles	80
5.5	Compression factor	86
5.6	Pulse propagation through birefringent DDF	87
5.7	Adiabatic soliton pulse compression in DDF with various dispersion profiles	90
5.8	Conclusion	96
<b>6</b>	<b>Soliton propagation through dispersion-decreasing fiber with fiber loss</b>	<b>97</b>
6.1	Introduction	97
6.2	Basic equation	97

6.3	Linear eigenvalue problem and soliton solution	98
6.4	Soliton pulse propagation through various profiles	101
6.4.1	Critical fiber loss	101
6.4.2	Compression factor	102
6.5	Pulse propagation through a birefringent DDF	110
6.6	Lax pairs and soliton solutions	111
6.7	Critical loss and optimum dispersion profile	113
6.8	Results and Discussions	122
<b>7</b>	<b>Conclusion</b>	<b>123</b>
	<b>Bibliography</b>	<b>126</b>

# Chapter 1

## Introduction

Optical solitons in fibers attract interest from wide area of science and technology. Among solitons which exist in various areas of physics, chemistry and biology, the optical solitons behave most ideally in that the behavior can be described by mathematical models which take into account for proper physical properties of fibers and applied perturbations. This property is very effective in exploiting the soliton for engineering purposes in particular for applying it to ultra high speed optical communication [1-7]. The advent of high intense laser sources and optical fibers having very low fiber loss have further paved the way for efficient and fast transmission of ultrashort soliton pulses through high mode fibers that form the basis of high speed communication systems [6,7]. In addition, the ideal phase property of solitons makes them ideal bits for application to ultrashort switching and processing based on interferometric techniques [8-10]. The advantage of using solitons is that they do not change their shapes even on interaction with other pulses. Another very important application of optical solitons is pulse compression [11-13]. The production of ultrashort soliton pulses are needed in different branches of science and technology which have been using

nanosecond and picosecond pulses. The another interesting and useful application of the soliton-formation capability of optical fibers is in the development of soliton lasers [14-17]. Recently solitons in dispersion-managed fibers have increased the transmission capacity of the fiber against the fiber dispersion and fiber nonlinearity with minimum loss [18]. These potential applications of optical solitons have promoted extensive research studies to explore the important properties of optical solitons taking into account for the proper physical properties of the high mode optical fibers.

In this chapter, the various physical properties of optical fibers, their behavior during the propagation of high-intensity optical pulses, and different methods for the analysis of propagation equations are presented.

## 1.1 Optical fiber

The simplest optical fiber is a cylindrical structure consisting of central core of doped silica ( $\text{SiO}_2$ ) surrounded by a concentric cladding of pure silica. Such a fiber is referred to as a step index fiber to distinguish them from graded-index fibers in which the refractive index of the core decreases gradually from center to the core boundary. Figure 1.1 shows schematically the cross-section and refractive index profile of a step-index fiber. The refractive index of the core ( $n_1$ ) is slightly greater than that of the cladding ( $n_2$ ). To understand light guidance in an optical fiber, consider a ray entering the fiber as shown in Fig. 1.2. If the angle of incidence  $\theta$ , is greater than the critical angle:

$$\phi_c = \sin^{-1}(n_2/n_1), \quad (1.1.1)$$

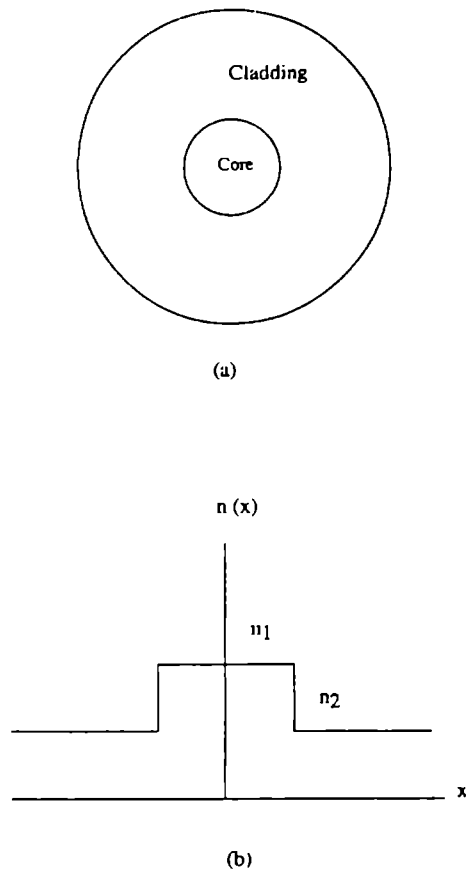


Fig. 1.1: Schematic illustration of (a) the cross-section and (b) the refractive index profile of a step-index fiber

the ray will undergo total internal reflection at the interface and will be guided by the core.

There are mainly two types of fibers: multimode fibers and single mode fibers



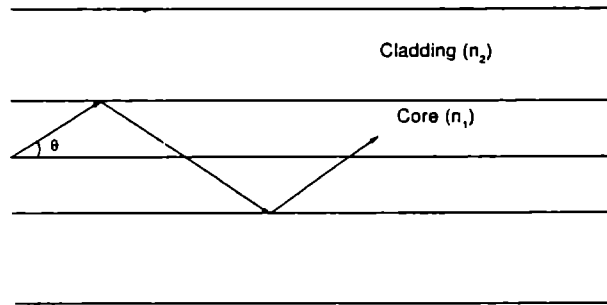


Fig. 1.2: A glass fiber that consist of a cylindrical central core, clad. Light rays impinging on the core-cladding interface at an angle greater than critical angle are trapped inside the core of the waveguide.

[19]. Multimode fibers are characterized by core diameters of  $50 \mu m$  and cladding diameter of  $125 \mu m$  while single mode fibers have typically core diameters of 9 to  $10 \mu m$  and cladding diameter of  $125 \mu m$ . There are two main varieties of multimode fibers namely step index and graded index fibers. Step index fibers are characterized by a homogeneous core of constant refractive index while graded index fibers have an inhomogeneous core in which refractive index decreases in an almost parabolic fashion from the center of the core to the core cladding interface as shown in Fig. 1.3.

Among all the types of communication systems, optical fiber communication (OFC) systems have many advantages like low loss, no electromagnetic interference, signal security, wide band width and so on. Though the OFC systems have several advantages, in order to utilize fiber in an effective manner, one has to overcome the effects of optical loss, dispersion, amplifier induced noise and

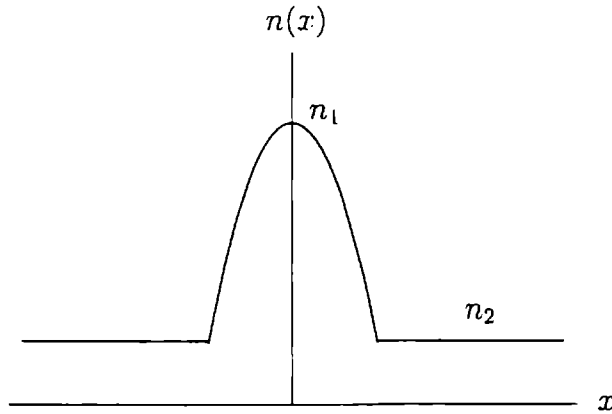


Fig. 1.3: Variation of refractive index in a graded index fiber.

nonlinearity. In short distance communication, these effects can be ignored. Various effects which influence the propagation of pulse through optical fibers are discussed in the following sections.

## 1.2 Linear effects

The linear effects of an optical system arises from the linear susceptibility  $\chi^{(1)}$ . The refractive index  $n$  of the system can be expressed as

$$n = \sqrt{1 + \chi^{(1)}} \quad (1.2.1)$$

and is a function of optical frequency ( $\omega$ ) and is a complex quantity in general. The real and imaginary parts of  $n$  represent dispersion effects and optical losses respectively [2].

### 1.2.1 Optical loss

Measurement of power loss during transmission of optical signals through the fiber is an important fiber parameter. If  $P_0$  is the power launched at the input of a fiber of length  $L$ , the transmitted power  $P_T$  is given by [2]

$$P_T = P_0 \exp(-\alpha L) \quad (1.2.2)$$

where  $\alpha$  is the attenuation constant, referred to as the fiber loss.

Among the several factors contributing to the losses, material absorption and Rayleigh scattering are the major ones. Material absorption arises due to the presence of several impurities inside the core medium. The major impurity constituent is the presence of hydroxyl ions. These hydroxyl ions are absorbed by the silica material during the manufacturing process. Depending upon the vibrational absorption characteristics of hydroxyl ion impurities, the loss profile due to material dispersion is formed. By taking precautions during the fiber-fabrication process [20], impurity level can be reduced.

Rayleigh scattering arises due to random density fluctuations of frozen silica materials formed at the time of manufacturing. Loss due to Rayleigh scattering varies inversely as the fourth power of optical wavelength. Other losses are those which occur due to bending and coupling which can be minimized by taking suitable care during installation [19].

### 1.2.2 Dispersion

When an electromagnetic wave interacts with bound electrons of a dielectric, the medium response depends on the optical frequency  $\omega$ . As a result, index of

refraction becomes frequency dependent and this phenomenon is referred to as dispersion [1,2]. This fiber dispersion plays a crucial role in the propagation of optical pulses since different spectral components associated with the pulse travel at different speeds given by  $c/n(\omega)$ . Mathematically, the effect of fiber dispersion is accounted for by expanding the mode propagation constant  $\beta$  in a Taylor series about the center frequency  $\omega_0$ :

$$\beta(\omega) = \beta_0 + (\omega - \omega_0) \beta_1 + \frac{1}{2} (\omega - \omega_0)^2 \beta_2 + \frac{1}{6} (\omega - \omega_0)^3 \beta_3 + \dots \quad (1.2.3)$$

where

$$\beta_m = \left( \frac{d^m \beta}{d\omega^m} \right)_{\omega=\omega_0} \quad (m = 0, 1, 2, \dots) \quad (1.2.4)$$

The parameter  $\beta_2$  is responsible for pulse broadening and is generally referred to as group-velocity dispersion (GVD) parameter. The most notable feature is that  $\beta_2$  vanishes at a particular wavelength. The wavelength at which  $\beta_2 = 0$  is often referred to as zero-dispersion wavelength  $\lambda_d$ . Variation of  $\beta_2$  with wavelength for silica is shown in Fig. 1.4.

For wavelength such that  $\lambda < \lambda_d$ ,  $\beta_2 > 0$  and fiber is said to exhibit normal dispersion. In the normal dispersion regime, the higher frequency components of an optical pulse travel slower than lower frequency components. By contrast, the opposite occurs in the so-called anomalous dispersion regime in which  $\beta_2 < 0$ . Because of this, the spectrum of the pulse gets broadened in the time domain during its propagation through fibers [2].

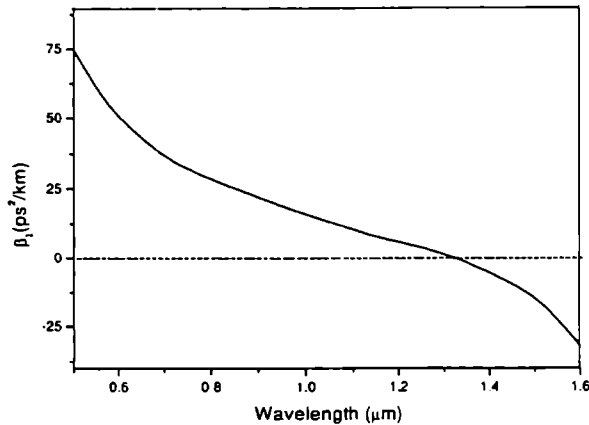


Fig. 1.4: Variation of  $\beta_2$  with wavelength.

### 1.3 Nonlinear effects

Linear effects of dielectric materials depend only on the frequency of optical pulse. But, for very intense electromagnetic fields, all dielectrics behave nonlinearly. Origin of the nonlinear response is related to anharmonic motion of bound electrons under the influence of an applied field. As a result, the induced polarization  $\mathbf{P}$  from the electric dipoles is not linear in the electric field  $\mathbf{E}$ , but satisfies the more general relation [21-22]:

$$P = \epsilon_0 [\chi^{(1)} E + \chi^{(2)} E^2 + \chi^{(3)} E^3 + \dots] \quad (1.3.1)$$

where  $\epsilon_0$  is the vacuum permittivity and  $\chi^{(j)}$  ( $j = 1, 2, \dots$ ) is the  $j^{\text{th}}$  order susceptibility. In a centrosymmetric molecule, all the even order susceptibility vanish in the dipole approximation [22]. Since silica fiber made up of  $\text{SiO}_2$  is a symmetric molecule, the lowest dominant nonlinearity is due to  $\chi^{(3)}$ . The lowest order nonlinear effects are nonlinear refraction, four-wave mixing, and third harmonic

generation [22]. The other nonlinear effects such as self-steepening and stimulated inelastic scattering belong to the class of higher-order nonlinear effects [22-24].

### 1.3.1 Nonlinear refraction

The phenomenon of nonlinear refraction is due to the intensity dependence of refractive index and is also called Kerr nonlinearity or simply Kerr effect [21]. Intensity dependent refractive index of the fiber is given by

$$n(\omega, |E|^2) = n_0(\omega) + n_2 |E|^2 \quad (1.3.2)$$

where  $n_0(\omega)$  is the linear index of refraction,  $|E|^2$  is the optical intensity inside the fiber, and  $n_2$  is the nonlinear-index coefficient also called Kerr coefficient.

The intensity dependent refractive index introduces a phase shift given by

$$\phi = nk_0L = (n_0 + n_2 |E|^2)k_0L \quad (1.3.3)$$

where  $k_0 = 2\pi/\lambda$  and  $L$  is the length of the fiber. The intensity dependent nonlinear phase shift  $\phi_{NL} = n_2 k_0 L |E|^2$  is due to Kerr effect [21, 22]. Since the optical field experiences a self-induced phase due to Kerr nonlinearity during its propagation, it is called self phase modulation (SPM). SPM leads to the generation of new frequency components and as a result, spectrum of the pulse gets broadened in frequency domain during its propagation [21-25].

In the case of an ideal fiber made up of isotropic material and of perfect geometry, degenerative modes would not couple during propagation. But, in actual case, when two optical waves having frequencies  $\omega_1$  and  $\omega_2$  polarized along a given axis copropagate inside a fiber, they can interact with each other through the fiber

nonlinearity. The fiber nonlinearity thus provides a coupling between degenerative modes and this phenomenon is referred to as cross-phase modulation (XPM) [26]. As a result, nonlinear phase shift of an optical field will be induced by a copropagating field at a different wavelength. The nonlinear phase shift for the field at  $\omega_1$  is given by

$$\phi_{NL} = n_2 k_0 L (|E_1|^2 + 2|E_2|^2) \quad (1.3.4)$$

The two terms on the right-hand side of Eq. (1.3.4) are due to SPM and XPM respectively.

### 1.3.2 Four-wave mixing

Let  $\omega_1$ ,  $\omega_2$ , and  $\omega_3$  be the frequencies of three waves incident in an optical fiber. Third order nonlinearity of the fiber, which is more predominant, would lead to the generation of a nonlinear polarization, say  $\omega_4$  given by  $\omega_4 = \omega_3 + \omega_2 - \omega_1$ . The nonlinear polarization, can under some circumstances, leads to the generation of electromagnetic waves at the new frequency  $\omega_4$ . This phenomenon is referred to as four wave mixing [27].

### 1.3.3 Self-steepening

The channel handling capacity of a fiber system can be increased by propagating Ultra Short Pulses (USP). When the width of the pulse is too narrow, effects of higher order nonlinear effects are to be considered. Two different phenomena come under this higher-order nonlinear effects are Kerr dispersion or otherwise called self-steepening (SS) and stimulated inelastic scattering. These are considered as important perturbations of pulses.

Self-steepening is due to the intensity dependent group velocity [28]. This causes the peak of the pulse to travel slower than the wings. So during propagation, the pulse will become steeper and steeper because of its own intensity and hence the name self-steepening. There is also a possibility of breaking up of the pulse due to instability. As this phenomenon is basically due to the variation in the group velocity (with respect to the intensity), this is also referred as Kerr dispersion. Due to Kerr-dispersion, pulse gets broadened in the frequency domain and is asymmetrical in nature [29].

### 1.3.4 Stimulated inelastic scattering

The nonlinear effects governed by the third-order susceptibility  $\chi^{(3)}$  are elastic in nature. Second class of nonlinear effect results from stimulated inelastic scattering in which the optical field transfers part of its energy to the nonlinear medium [30]. Two important nonlinear effects in optical fibers in this category are stimulated Raman scattering (SRS) and stimulated Brillouin scattering (SBS). The main difference between the two is that optical phonons participate in SRS while acoustic phonons participate in SBS. In both cases, a photon of incident field (often called the pump) is annihilated to create a photon at the downshifted stokes frequency and a phonon with appropriate energy and momentum to conserve the energy and momentum. A higher energy photon can also be created provided a phonon of appropriate energy and momentum is available for absorption. Even though SRS and SBS are very similar in their origin, different dispersion relations for acoustic and optical phonons lead to some basic difference between the two. A fundamental difference is that SBS in optical fibers can occur only in the backward direction whereas SRS dominates in the forward direction. The effect of



SRS produces a self-frequency shift, which can cause a decay in the pulse. This will cause splitting up of the pulse. The phenomenon of SRS is used for the amplification of pulses. Higher frequency light pulses are periodically pumped into the fiber. The SRS of the pump wave gives the necessary amplification for the propagating pulses. SRS also gives asymmetrical broadening of the pulse in the frequency domain [22].

## 1.4 Wave propagation in single-mode optical fibers

When short pulses with width ranging from  $\sim 10$  ns to  $\sim 10$  fs propagate through a fiber, in addition to dispersive effect, nonlinear effects will also come into play. Like all other electromagnetic phenomena, the propagation of such optical pulses is also governed by Maxwell's equation [31, 32]. In this section, nonlinear envelope equation taking into account for the linear, nonlinear, and dissipation effects has been derived.

Maxwell's equations in a conducting medium are [33]

$$\nabla \times \mathbf{E} = -\frac{\partial \mathbf{B}}{\partial t}, \quad (1.4.1)$$

$$\nabla \times \mathbf{H} = \mathbf{J}_f + \frac{\partial \mathbf{D}}{\partial t}, \quad (1.4.2)$$

$$\nabla \cdot \mathbf{D} = \rho_f, \quad (1.4.3)$$

$$\nabla \cdot \mathbf{B} = 0, \quad (1.4.4)$$

where  $\mathbf{E}$  and  $\mathbf{H}$  are electric and magnetic vectors respectively, and  $\mathbf{D}$  and  $\mathbf{B}$  are the corresponding electric and magnetic flux densities. The current density vector  $\mathbf{J}_f$  and charge density  $\rho_f$  represent the source for the electromagnetic field.

In the absence of free charges in a medium such as optical fibers,  $\mathbf{J}_f = 0$  and  $\rho_f = 0$ . The flux densities  $\mathbf{D}$  and  $\mathbf{B}$  arise in response to the electric and magnetic fields  $\mathbf{E}$  and  $\mathbf{H}$  propagating inside a medium and are related to them through the constitutive relations given by [32]

$$\mathbf{D} = \epsilon_0 \mathbf{E} + \mathbf{P} \quad (1.4.5)$$

$$\mathbf{E} = \mu_0 \mathbf{H} + \mathbf{M} \quad (1.4.6)$$

where  $\epsilon_0$  is the vacuum permittivity,  $\mu_0$  is the vacuum permeability, and  $\mathbf{P}$  and  $\mathbf{M}$  are the induced electric and magnetic polarizations. For a nonmagnetic medium such as optical fibers,  $\mathbf{M} = 0$ . Maxwell's equations can be used to obtain the wave equation that describes light propagation in optical fibers. By taking the curl of Eq. (1.4.1) and using Eqs. (1.4.2), (1.4.3), and (1.4.4), one can eliminate  $\mathbf{B}$  and  $\mathbf{D}$  in favor of  $\mathbf{E}$  and  $\mathbf{P}$  and obtain

$$\nabla \times \nabla \times \mathbf{E} = -\frac{1}{c^2} \frac{\partial^2 \mathbf{E}}{\partial t^2} - \mu_0 \frac{\partial^2 \mathbf{P}}{\partial t^2} \quad (1.4.7)$$

or

$$-\nabla^2 \mathbf{E} = -\frac{1}{c^2} \frac{\partial^2 \mathbf{E}}{\partial t^2} - \mu_0 \frac{\partial^2 \mathbf{P}}{\partial t^2} \quad (1.4.8)$$

where  $\nabla \cdot \mathbf{D} = \epsilon \nabla \cdot \mathbf{E} = 0$  in a dielectric medium such as an optical fiber,  $\mu_0 \epsilon_0 = 1/c^2$  and  $c$  is the velocity of light in vacuum. When nonlinear effects governed by  $\chi^{(3)}$  are considered, the induced polarization consists of two parts such that

$$\mathbf{P}(\mathbf{r}, t) = \mathbf{P}_L(\mathbf{r}, t) + \mathbf{P}_{NL}(\mathbf{r}, t) \quad (1.4.9)$$

where the linear part  $\mathbf{P}_L$  and nonlinear part  $\mathbf{P}_{NL}$  are related to the electric field by the relations [21, 34]

$$\mathbf{P}_L(\mathbf{r}, t) = \varepsilon_0 \int_{-\infty}^{\infty} \chi^{(1)}(t - t') \mathbf{E}(\mathbf{r}, t') dt' \quad (1.4.10)$$

$$\mathbf{P}_{NL}(\mathbf{r}, t) = \varepsilon_0 \int \int_{-\infty}^{\infty} \int \chi^{(3)}(t - t_1, t - t_2, t - t_3) \mathbf{E}(\mathbf{r}, t_1) \mathbf{E}(\mathbf{r}, t_2) \mathbf{E}(\mathbf{r}, t_3) dt_1 dt_2 dt_3 \quad (1.4.11)$$

These relations are valid in the electric-dipole approximation such that the medium response is local. Equations (1.4.8-1.4.11) provide a general formalism for treating the lowest-order nonlinear effects in optical fibers. By using Eq. (1.4.9), Eq. (1.4.8) can be written as

$$\nabla^2 \mathbf{E} - \frac{1}{c^2} \frac{\partial^2 \mathbf{E}}{\partial t^2} = -\mu_0 \frac{\partial^2 \mathbf{P}_L}{\partial t^2} - \mu_0 \frac{\partial^2 \mathbf{P}_{NL}}{\partial t^2} \quad (1.4.12)$$

The following assumptions are made to solve the above equation. First,  $\mathbf{P}_{NL}$  is treated as a small perturbation to  $\mathbf{P}_L$ . Second, the optical field is assumed to maintain its polarization along the fiber length so that a scalar approach is valid. Third, the optical field is assumed to be quasi-monochromatic, i.e., its spectrum, centered at  $\omega_0$ , has a spectral width  $\Delta\omega$  such that  $\Delta\omega / \omega_0 \ll 1$ . Since  $\omega_0 \sim 10^{15} \text{ s}^{-1}$ , the last assumption is valid for pulses whose width is  $\geq 0.1$  ps ( $\Delta\omega \leq 10^{13} \text{ s}^{-1}$ ). In the slowly varying envelope approximation, it is useful to separate the rapidly varying part of the electric field by writing it in the form

$$E(r, t) = \frac{1}{2} \hat{x} [E(\mathbf{r}, t) \exp(-i\omega_0 t) + c.c.] \quad (1.4.13)$$

where c.c stands for complex conjugate.  $\hat{x}$  is the polarization unit vector of the

light assumed to be linearly polarized along the x axis,  $E(\mathbf{r}, t)$  is a slowly varying function of time. The polarization components  $\mathbf{P}_L$  and  $\mathbf{P}_{NL}$  can also be expressed in a similar way by writing

$$\mathbf{P}_L(r, t) = \frac{1}{2} \hat{x} [\mathbf{P}_L(\mathbf{r}, t) \exp(-i\omega_0 t) + c.c.] \quad (1.4.14)$$

$$\mathbf{P}_{NL}(r, t) = \frac{1}{2} \hat{x} [\mathbf{P}_{NL}(\mathbf{r}, t) \exp(-i\omega_0 t) + c.c.] \quad (1.4.15)$$

The linear component  $\mathbf{P}_L$  can be obtained by substituting Eq. (1.4.14) in Eq. (1.4.10) and is given by

$$P_L(r, t) = \varepsilon_0 \int_{-\infty}^{\infty} \chi_{xx}^{(1)}(t - t') \mathbf{E}(\mathbf{r}, t') \exp[i\omega_0(t - t')] dt' \quad (1.4.16)$$

$$= \varepsilon_0 \int_{-\infty}^{\infty} \tilde{\chi}_{xx}^{(1)}(\omega) \tilde{\mathbf{E}}(\mathbf{r}, \omega - \omega_0) \exp[-i(\omega - \omega_0)t] d\omega$$

where  $\tilde{\mathbf{E}}(\mathbf{r}, \omega)$  is the Fourier transform of  $\mathbf{E}(\mathbf{r}, t)$ . The nonlinear component  $\mathbf{P}_{NL}(r, t)$  is obtained by substituting Eq. (1.4.15) in Eq. (1.4.11). Equation (1.4.11) then reduces to

$$\mathbf{P}_{NL}(\mathbf{r}, t) = \varepsilon_0 \chi^{(3)} \mathbf{E}(\mathbf{r}, t) \mathbf{E}(\mathbf{r}, t) \mathbf{E}(\mathbf{r}, t) \quad (1.4.17)$$

The assumption of instantaneous nonlinear response amounts to neglecting the contribution of molecular vibrations to  $\chi^{(3)}$ . In general, both electrons and nuclei respond to the optical field in a nonlinear manner. The nuclei response is inherently slower compared with the electronic response. For silica fibers, the vibrational or Raman response occurs over a time scale 60-70 fs. Thus, Eq. (1.4.17) is approximately valid for pulse width  $>1$  ps. When Eq. (1.4.13) is substituted in Eq. (1.4.17),  $\mathbf{P}_{NL}(\mathbf{r}, t)$  is found to have a term oscillating at  $\omega_0$  and another

term oscillating at the third-harmonic frequency  $3\omega_0$ . The latter term is generally negligible in optical fibers. By making use of Eq. (1.4.15),  $\mathbf{P}_{NL}(\mathbf{r}, t)$  is given by

$$\mathbf{P}_{NL}(\mathbf{r}, t) = \varepsilon_0 \varepsilon_{NL} \mathbf{E}(\mathbf{r}, t) \quad (1.4.18)$$

where  $\varepsilon_{NL}$  is the nonlinear contribution to the dielectric constant and is defined by

$$\varepsilon_{NL} = \frac{3}{4} \chi_{\chi\chi\chi}^{(3)} |\mathbf{E}(\mathbf{r}, t)|^2 \quad (1.4.19)$$

To obtain the wave equation for the slowly varying amplitude  $\mathbf{E}(\mathbf{r}, t)$ , it is more convenient to work in Fourier domain. This is generally not possible as Eq. (1.4.12) is nonlinear because of the intensity dependence of  $\varepsilon_{NL}$ . In one approach,  $\varepsilon_{NL}$  is treated as a constant during the derivation of the propagation equation for  $\mathbf{E}(\mathbf{r}, t)$  [35, 36]. The approach is justified in view of the slowly varying envelope approximation and perturbative nature of  $\mathbf{P}_{NL}$ . By substituting Eqs. (1.4.13)-(1.4.15) in Eq. (1.4.12), the Fourier transform  $\tilde{\mathbf{E}}(\mathbf{r}, \omega - \omega_0)$ , defined by

$$\tilde{\mathbf{E}}(\mathbf{r}, \omega - \omega_0) = \int_{-\infty}^{\infty} \mathbf{E}(\mathbf{r}, t) \exp[i(\omega - \omega_0)t] dt \quad (1.4.20)$$

is found to satisfy

$$\nabla^2 \tilde{\mathbf{E}} + \varepsilon(\omega) k_0^2 \tilde{\mathbf{E}} = 0 \quad (1.4.21)$$

where  $k_0 = \omega/c$  and

$$\varepsilon(\omega) = 1 + \tilde{\chi}_{\chi\chi}^{(1)}(\omega) + \varepsilon_{NL} \quad (1.4.22)$$

is the dielectric constant whose nonlinear part  $\varepsilon_{NL}$  is given by Eq. (1.4.19). The

dielectric constant can be used to define refractive index  $\tilde{n}$  and the absorption coefficient  $\tilde{\alpha}$  become intensity dependent because of  $\varepsilon_{NL}$ . Therefore

$$\tilde{n} = n_0 + n_2 |E|^2 \quad \tilde{\alpha} = \alpha + \alpha_2 |E|^2 \quad (1.4.23)$$

Using  $\varepsilon = (\tilde{n} + i\tilde{\alpha}/2k_0)^2$  and Eqs. (1.4.19) and (1.4.22), the nonlinear-index coefficient  $n_2$  and the two-photon absorption coefficient  $\alpha_2$  are given by

$$n_2 = \frac{3}{8n} \text{Re}(\chi_{xxxx}^{(3)}) \quad \alpha_2 = \frac{3\omega_0}{4nc} \text{Im}(\chi_{xxxx}^{(3)}) \quad (1.4.24)$$

The linear index  $n_0$  and the absorption coefficient  $\alpha$  are related to the real and imaginary parts of  $\hat{\chi}_{xx}^{(1)}$ . Since  $\alpha_2$  is relatively small for silica fibers,  $\tilde{\alpha} \approx \alpha$ . Equation (1.4.21) can be solved using the method of separation of variables. The solution is assumed to be:

$$\tilde{\mathbf{E}}(\mathbf{r}, \omega - \omega_0) = F(x, y) \tilde{A}(z, \omega - \omega_0) \exp(i\beta_0 \xi) \quad (1.4.25)$$

$\tilde{A}(\xi, \omega)$  is a slowly varying function of  $\xi$  and  $\beta_0$  is the wavenumber to be determined. Equation (1.4.21) leads to the following two equations for  $F(x, y)$  and  $\tilde{A}(\xi, \omega)$

$$\frac{\partial^2 F}{\partial x^2} + \frac{\partial^2 F}{\partial y^2} + [\varepsilon(\omega) k_0^2 - \tilde{\beta}^2] F = 0 \quad (1.4.26)$$

$$2i\beta_0 \frac{\partial \tilde{A}}{\partial \xi} + (\tilde{\beta}^2 - \beta_0^2) \tilde{A} = 0 \quad (1.4.27)$$

Equation (1.4.27) is obtained by neglecting the second derivative  $\frac{\partial^2 \tilde{A}}{\partial \xi^2}$  since  $\tilde{A}(\xi, \omega)$  is assumed to be a slowly varying function of  $\xi$ . The wavenumber  $\tilde{\beta}$  is determined by solving the eigenvalue Eq. (1.4.26). The dielectric constant  $\varepsilon(\omega)$  in

Eq. (1.4.26) can be approximated by

$$\varepsilon = (n_0 + \Delta n)^2 \simeq n_0^2 + 2n_0\Delta n \quad (1.4.28)$$

where  $\Delta n$  is a small perturbation given by

$$\Delta n = n_2 |E|^2 + \frac{i\alpha}{2k_0} \quad (1.4.29)$$

Equation (1.4.26) can be solved by using first-order perturbation theory [37]. At first,  $\varepsilon$  is replaced by  $n^2$  and obtain the modal distribution  $F(x, y)$  and the corresponding wavenumber  $\beta(\omega)$ . For a single-mode fiber,  $F(x, y)$  corresponds to the modal distribution of the fundamental fiber mode  $HE_{11}$ . Then the effect of  $\Delta n$  is included in Eq. (1.4.26). In the first-order perturbation theory,  $\Delta n$  doesn't affect the modal distribution  $F(x, y)$ . The eigenvalue  $\tilde{\beta}$  is given by

$$\tilde{\beta}(\omega) = \beta(\omega) + \Delta\beta \quad (1.4.30)$$

where

$$\Delta\beta = \frac{k_0 \int_{-\infty}^{\infty} \int_{-\infty}^{\infty} \Delta n |F(x, y)|^2 dx dy}{\int_{-\infty}^{\infty} \int_{-\infty}^{\infty} |F(x, y)|^2 dx dy} \quad (1.4.31)$$

This step completes the formal solution of Eq. (1.4.12) to the lowest order in perturbation  $P_{NL}$ . Using Eqs. (1.4.13) and (1.4.23), the electric field  $\mathbf{E}(\mathbf{r}, t)$  is given by

$$\mathbf{E}(\mathbf{r}, t) = \hat{x} \frac{1}{2} \{ F(x, y) A(\xi, t) \exp[i(\beta_0 \xi - \omega_0 t)] + c.c. \} \quad (1.4.32)$$

The Fourier transform  $\tilde{A}(\xi, \omega - \omega_0)$  of the slowly varying amplitude  $A(\xi, t)$  satisfies Eq. (1.4.27) which can be written as

$$\frac{\partial \tilde{A}}{\partial \xi} = i[\beta(\omega) + \Delta\beta - \beta_0] \tilde{A} \quad (1.4.33)$$

where Eq. (1.4.30) is used and approximated  $\tilde{\beta}^2 - \beta_0^2$  by  $2\beta_0(\tilde{\beta} - \beta_0)$ . The inverse Fourier transform of Eq. (1.4.33) provides the propagation equation for  $A(\xi, t)$ . For this purpose, it is useful to expand  $\beta(\omega)$  in a Taylor series about the carrier frequency  $\omega_0$ , i.e.,

$$\beta(\omega) = \beta_0 + (\omega - \omega_0)\beta_1 + \frac{1}{2}(\omega - \omega_0)^2\beta_2 + \frac{1}{6}(\omega - \omega_0)^3\beta_3 + \dots \quad (1.4.34)$$

where

$$\beta_n = \left( \frac{d^n \beta}{d\omega^n} \right)_{\omega=\omega_0} \quad (1.4.35)$$

The cubic and higher-order terms in this expansion are generally negligible if the spectral width  $\Delta\omega \ll \omega_0$  which is consistent with quasi-monochromatic assumption used in the derivation of Eq. (1.4.33) and limits its validity to pulse width  $\geq 0.1$  ps. If  $\beta_2 \simeq 0$  for some specific values of  $\omega_0$ , it may be necessary to include the cubic term. Substituting Eq. (1.4.34) in Eq. (1.4.33) and taking the inverse Fourier transform:

$$A(\xi, t) = \frac{1}{2\pi} \int_{-\infty}^{\infty} \tilde{A}(\xi, \omega - \omega_0) \exp[-i(\omega - \omega_0)t] d\omega \quad (1.4.36)$$

During the Fourier-transform operation,  $\omega - \omega_0$  is replaced by the differential



operator  $i(\partial/\partial t)$  and the result is

$$\frac{\partial A}{\partial \xi} = -\beta_1 \frac{\partial A}{\partial t} - \frac{i}{2} \beta_2 \frac{\partial^2 A}{\partial \xi^2} + i \Delta \beta A \quad (1.4.37)$$

The term with  $\Delta \beta$  includes the effect of fiber loss and nonlinearity. By using Eqs. (1.4.29) and (1.4.31),  $\Delta \beta$  can be evaluated and substituted in Eq. (1.4.37).

The result is

$$\frac{\partial A}{\partial \xi} + \beta_1 \frac{\partial A}{\partial t} + \frac{i}{2} \beta_2 \frac{\partial^2 A}{\partial \xi^2} = i \gamma |A|^2 A \quad (1.4.38)$$

where the nonlinearity or Kerr coefficient  $\gamma$ , responsible for SPM, is defined by

$$\gamma = \frac{n_2 \omega_0}{c A_{eff}}. \quad (1.4.39)$$

The parameter  $A_{eff}$  is known as the effective core area and is given by

$$A_{eff} = \frac{\left( \int_{-\infty}^{\infty} \int_{-\infty}^{\infty} |F(x, y)|^2 dx dy \right)^2}{\int_{-\infty}^{\infty} \int_{-\infty}^{\infty} |F(x, y)|^4 dx dy}. \quad (1.4.40)$$

The effective core area depends on the fiber parameters such as the core radius and core-cladding index difference. By making the transformation:

$$T = t - \xi/v_g = t - \beta_1 \xi \quad (1.4.41)$$

and using Eq. (1.4.38):

$$i \frac{\partial A}{\partial \xi} + \frac{i}{2} \alpha A - \frac{1}{2} \beta_2 \frac{\partial^2 A}{\partial T^2} + \gamma |A|^2 A = 0 \quad (1.4.42)$$

where  $A(\xi, T)$  is the slowly varying amplitude of the pulse envelope,  $\beta_2$  is the

GVD parameter. The last three terms in the above equation govern respectively the effect of fiber loss, dispersion, and nonlinearity on the pulse propagation inside optical fibers. If the fiber loss is ignored, i.e.  $\alpha = 0$ , the above equation takes the form:

$$i \frac{\partial A}{\partial \xi} - \frac{i}{2} \beta_2 \frac{\partial^2 A}{\partial T^2} + \gamma |A|^2 A = 0 \quad (1.4.43)$$

and is referred to as the nonlinear Schrödinger equation (NLSE) which describes the propagation of optical pulses having widths  $\geq 1$  ps. The above equation can be normalized by introducing:

$$U = 2^{-1/3} \frac{A}{\sqrt{P_0}}, \quad z = 2^{-1/3} \frac{\xi}{L_D}, \quad t = 2^{1/3} \frac{T}{T_0} \quad (1.4.44)$$

and obtain

$$i \frac{\partial U}{\partial z} - \text{sgn}(\beta_2) \frac{\partial^2 U}{\partial t^2} + 2N^2 |U|^2 U = 0 \quad (1.4.45)$$

where  $P_0$  is the peak power,  $T_0$  is the width of the incident pulse, and  $\text{sgn}(\beta_2) = \pm 1$  depending on the sign of the GVD parameter  $\beta_2$ . The parameter  $N$  is defined by

$$N^2 = \frac{L_D}{L_{NL}} = \frac{\gamma P_0 T_0^2}{|\beta_2|} \quad (1.4.46)$$

and

$$L_D = \frac{T_0^2}{|\beta_2|}, \quad L_{NL} = \frac{1}{\gamma P_0} \quad (1.4.47)$$

where the dispersion length  $L_D$  and nonlinear length  $L_{NL}$  provide the length scales over which the dispersive or nonlinear effects become important for pulse evolution along a fiber of length  $L$ . Depending on the relative magnitude of  $L$ ,  $L_D$ ,

and  $L_{NL}$ , the propagation behavior can be classified in the following categories. When the fiber length  $L$  is such that  $L \ll L_{NL}$  and  $L \ll L_D$  neither dispersive nor nonlinear effects play a significant role during pulse propagation. As a result, the pulse maintains its shape during propagation. The fiber plays a passive role in this regime and act as a mere transporter of optical pulses. This regime is useful for optical communication systems. When the fiber length is such that  $L \ll L_{NL}$  but  $L > L_D$ , the last term in Eq. (1.4.45) is negligible compared to the other two. The pulse evolution is then governed by GVD and the nonlinear effects play a minor role. The effect of GVD leads to the broadening of pulse in the time domain. When the fiber length  $L$  is such that  $L \ll L_D$  but  $L \gg L_{NL}$ , the dispersion term in Eq. (1.4.45) is negligible compared to the nonlinear term. In that case, pulse evolution in the fiber is governed by SPM that leads to the broadening of the pulse in the frequency domain. But when the fiber length  $L$  is comparable to both  $L_{NL}$  and  $L_D$ , dispersion and nonlinearity act together as pulse propagates along the fiber. The interplay of the GVD and SPM effects can lead to a qualitatively different behavior compared with that expected from GVD or SPM alone. As a result of the combined action, pulse becomes highly stable and undergoes elastic collisions. Such a pulse is known as optical soliton. In the anomalous-dispersive regime ( $sgn(\beta_2) < 0$ ), optical soliton in the fiber is known as bright soliton [38, 39]. In the normal-dispersive regime ( $sgn(\beta_2) > 0$ ), the corresponding soliton is known as dark soliton [40].

## 1.5 Soliton solution for the nonlinear Schrödinger equation.

In the case of anomalous GVD,  $\text{sgn}(\beta_2) = -1$ . The parameter  $N$  can be eliminated from Eq. (1.4.45) by defining

$$q = NU = \left( \frac{\gamma T_0^2}{|\beta_2|} \right) A \quad (1.5.1)$$

Equation (1.4.45) then takes the following standard form of the nonlinear Schrödinger equation (NLSE):

$$i \frac{\partial q}{\partial z} + \frac{\partial^2 q}{\partial t^2} + 2|q|^2 q = 0 \quad (1.5.2)$$

Solution for the above equation can be obtained by using linear eigen value problem [41] auto-Bäcklund transformation technique [42].

Let  $\Psi \equiv \begin{pmatrix} \Psi_1 \\ \Psi_2 \end{pmatrix}$  be a two component wave function of the Zakharov-Shabat-Ablowitz-Kaup-Newell-Segur (ZS/AKNS) scattering problem for the NLSE. The space and time evolution of the wavefunction  $\Psi$  are defined by the linear eigen value problem given by [41]

$$\Psi_t = Q_1 \Psi \quad \Psi_z = V \psi \quad \Psi = (\Psi_1 \Psi_2)^T \quad (1.5.3)$$

where

$$Q_1 = \begin{pmatrix} -i\lambda & q \\ -q^* & i\lambda \end{pmatrix} \quad (1.5.4)$$

$$Q_2 = 2i\lambda^2 \begin{pmatrix} -1 & 0 \\ 0 & 1 \end{pmatrix} + 2\lambda \begin{pmatrix} 0 & q \\ -q^* & 0 \end{pmatrix} + i \begin{pmatrix} |q|^2 & q_\tau \\ q_\tau^* & -|q|^2 \end{pmatrix} \quad (1.5.5)$$

such that the relation  $Q_{1z} - Q_{2t} + [Q_1, Q_2] = 0$  gives rise to Eq. (1.5.2). Thus in effect, NLSE is presented as a linear eigen value problem with eigen value  $\lambda$  [42]. The above mentioned wave function refers to the  $(n - 1)^{th}$  - soliton problem [42], i.e.,

$$\Psi_1 \equiv \Psi_1(n - 1)$$

$$\Psi_2 \equiv \Psi_2(n - 1) \tag{1.5.6}$$

$$u \equiv u(n - 1)$$

In a similar way, the  $(n)^{th}$  - soliton problem can be represented in the form:

$$\Psi'_1 \equiv \Psi'_1(n)$$

$$\Psi'_2 \equiv \Psi'_2(n) \tag{1.5.7}$$

$$u' \equiv u(n)$$

and have the same form as Eqs. (1.5.3-1.5.5) and where all the terms are primed. To generate soliton solution of Eq. (1.5.2), a pseudopotential  $\Gamma$  is introduced such that

$$\Gamma = \frac{\Psi_1}{\Psi_2} \tag{1.5.8}$$

Differentiating Eq. (1.5.8) and on simplifying using Eqs. (1.5.3) and (1.5.4) gives

$$\Gamma_t = -2i\lambda\Gamma + q + \Gamma^2 q^* \Psi_z \tag{1.5.9}$$

The transformations  $\lambda \rightarrow \lambda^*$  and  $q \rightarrow q'$  in Eq. (1.5.9) leads

$$\Gamma_t = -2i\lambda^*\Gamma + q' + \Gamma^2 q'^* \quad (1.5.10)$$

Simplification of Eqs. (1.5.9) and (1.5.10) gives

$$q - q' = \frac{-4\Gamma\lambda_2}{1 + |\Gamma|^2} \quad (1.5.11)$$

where  $\lambda = \lambda_1 + i\lambda_2$ .  $\lambda_1$  and  $\lambda_2$  are real, denoting the soliton velocity and amplitude parameters respectively. The above equation is a recurrence relation in which primed and unprimed quantities represent  $n^{\text{th}}$  and  $(n-1)^{\text{th}}$  – soliton solutions respectively. For the trivial case, i.e.  $q = 0$ , the above equation becomes

$$q' = \frac{4\Gamma\lambda_2}{1 + |\Gamma|^2} \quad (1.5.12)$$

From the expression  $\Psi_t = Q_1\Psi$  in Eq. (1.5.3), the following results are obtained:

$$\Psi_1 = c_1(z) \exp(-i\lambda t) \quad (1.5.13)$$

$$\Psi_2 = c_2(z) \exp(i\lambda t)$$

where  $c_1(z)$  and  $c_2(z)$  are integration constants depend on  $z$ . The expression  $\Psi_z = Q_2\Psi$  in Eq. (1.5.3) gives

$$\Psi_{1z} = -2i\lambda^2\Psi_1 \quad (1.5.14)$$

$$\Psi_{2z} = 2i\lambda^2\Psi_2$$

Substituting Eq. (1.5.13) in Eq. (1.5.14) gives

$$\Psi_1 = c_1(0) \exp(-2i\lambda^2 z - i\lambda t) \quad (1.5.15)$$

$$\Psi_2 = c_2(0) \exp(2i\lambda^2 z + i\lambda t)$$

Then Eq. (1.5.8) becomes

$$\Gamma = \frac{c_1(0)}{c_2(0)} \exp(-2i\lambda_1 t - 4i(\lambda_1^2 - \lambda_2^2)z) \exp(2\lambda_2 t + 8\lambda_1 \lambda_2 z) \quad (1.5.16)$$

On substituting Eq. (1.5.16) in (1.5.12), the solution of Eq. (1.5.2) is obtained as

$$q = 2\lambda_2 \chi \exp(-2i\lambda_1 t - 4i(\lambda_1^2 - \lambda_2^2)z) \operatorname{sech}(2\lambda_2 t + 8\lambda_1 \lambda_2 z + \theta) \quad (1.5.17)$$

where  $\theta = \frac{1}{2} \ln \left( \frac{|c_1(0)|^2}{|c_2(0)|^2} \right)$  and  $\chi = \sqrt{\frac{|c_2(0)|^2}{|c_1(0)|^2}}$ . The single soliton solution is plotted in Fig. 1.5 depicts the undistorted soliton propagation along the fiber length. This is due to the exact balance between the group velocity dispersion and self-phase modulation.

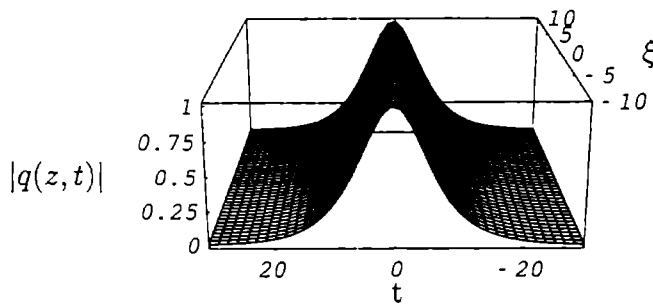


Fig. 1.5: Evolution of bright soliton described in Eq. (1.5.17)

## 1.6 Dispersion decreasing fibers

In dispersion-decreasing fibers, magnitude of the GVD parameter  $|\beta_2|$  decreases along the direction of propagation of optical pulses [43, 44]. Such fibers can be made by tapering the core diameter at the manufacturing stage since the waveguide contribution to the GVD parameter  $\beta_2$  depends on the core size. Pulse propagation through DDF can be explained mathematically by using the NLS equation of the form:

$$i \frac{\partial q}{\partial z} + p(z) \frac{\partial^2 q}{\partial t^2} + 2|q|^2 q = 0 \quad (1.6.1)$$

where the parameter  $p(z) = |\beta_2(z)/\beta_2(0)|$  governs dispersion variation along the fiber length.

DDFs can be effectively used for pulse compression. The pulse-compression mechanism of dispersion-decreasing fibers has been used to generate train of ultrashort pulses [45-47]. The basic idea consists of injecting a continuous wave (CW) beam, with weak sinusoidal modulation imposed on it, into an optical fiber. As the sinusoidal signal propagates, individual pulse are also compressed. The combined effect of GVD, SPM, and decreasing GVD is to convert a nearly CW signal into high-quality train of ultrashort solitons [44].

## 1.7 Analysis of nonlinear partial differential equations

There are different methods for the analysis of nonlinear partial differential equations (NPDEs). NPDEs in general are not integrable and hence they do not possess soliton solutions. For the system to be completely integrable, it must



possess (i) Painleve' property, (ii) infinite conservation laws (iii) N soliton solutions (iv) Lax pairs etc. In this section, some of the mathematical tools useful for studying NPDEs are discussed.

### 1.7.1 Painleve' analysis

Painleve' analysis is one of the most powerful and frequently applied method in nonlinear dynamics to see whether a given nonlinear evolution equation is integrable in general and if not for what parametric restrictions, the system is integrable. The Painleve' analysis of nonlinear partial differential equations (NLPDEs) is proposed by Weiss, Tabor, and Carnevale with a suitable simplification by Kruskal and this method is also known as WTC method [48,49]. This analysis ensures that general solutions of NLPDEs are single valued in the neighborhood of non-characteristics, movable singularity manifold when expressed locally as a Laurent series.

Let  $q(z, t)$  satisfy the nonlinear evolution equation.

$$q_t = k[q, q_z, \dots] \quad (1.7.1)$$

and let

$$\phi(z, t) = 0 \quad (1.7.2)$$

be the manifold (the singular or pole manifold) on which  $q(z, t)$  is singular. The basic ideas of WTC method is that the Laurent expansion:

$$q(z, t) = \frac{1}{\phi^\alpha} \sum_{j=0}^{\infty} q_j(z, t) \phi^j \quad (1.7.3)$$

be single valued. This requires that (i)  $\alpha$  is an integer, (ii)  $\phi$  is analytic in  $z$  and  $t$ , and (iii) the equation for the coefficients  $q_j$  have self-consistent solutions. If all these conditions are satisfied, Eqn. (1.7.3) can be considered to be a Laurent expansion of the solution in the neighborhood of singular manifold and nonlinear evolution equation satisfying  $q(z, t)$  is said to possess Painleve property. Apart from providing the integrability property of a given nonlinear partial differential equations, P analysis also provides information about Bäcklund transformation(BT), Lax pair, Hirota's bilinear representation, special and rational solutions, etc. Many of these results are obtained by truncating the Laurent series at a constant level term [50].

### 1.7.2 Inverse Scattering Transform (IST)

It is one of the powerful methods to prove the integrability of a given nonlinear partial differential equations (NPDEs). This method was first introduced by Gardner, Green, Kruskal and Miura (GGKM) [51] based on the context of quantum mechanical scattering theory. The goal of the inverse method is to solve the NPDEs. It essentially consists of three steps. First step is known as direct scattering method. In this method, from the initial condition  $q = q(z, 0)$  solve direct scattering problem, i.e., treat  $q(z, 0)$  as a potential in the Schrodinger equation and find all the associated eigen values and eigen functions. Next, in step 2, as  $q$  evolves as a function of  $t$ , associated scattering data will also evolve. In step 3, one can uniquely constructs  $q(z, t)$  from the scattering data.

The inverse method is easily described by a flowchart given in Fig. 1.6.

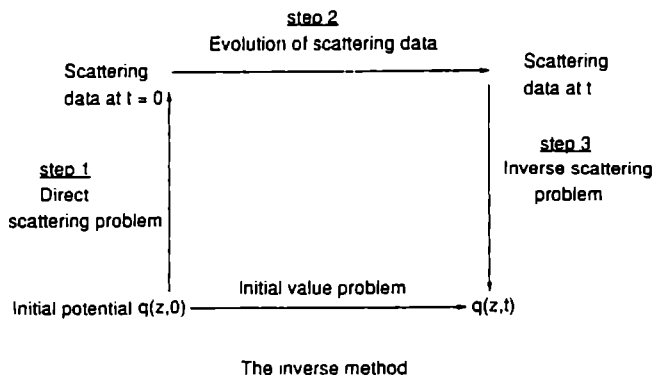


Fig. 1.6: Flow chart of IST

### 1.7.3 AKNS Method

In this section, the method to generate soliton possessing equations is explained. The main idea of this method was due to Lax [52] and hence the resulting operators in this formalism are called Lax operators or Lax pair. Actually, the method given by Lax, may not be applicable to many soliton possessing nonlinear evolution equations (NEEs) because of the differential form and the assumption on one of the operators. To overcome these problems, AKNS proposed a method which can be used to describe many soliton possessing NEEs [53].

Consider the  $3 \times 3$  eigen value problem

$$\Phi_t = U\Phi \tag{1.7.4}$$

$$\Phi_z = V\Phi$$

where  $\Phi = (\Phi_1 \Phi_2 \Phi_3)^T$

$$U = \begin{pmatrix} -i\lambda & q & q^* \\ -q^* & i\lambda & 0 \\ -q & 0 & i\lambda \end{pmatrix} \quad (1.7.5)$$

$$V_{ij} = \sum_{n=0}^N V_{ij}^n \lambda^n \quad (1.7.6)$$

The integrability condition for Eq. (1.7.4) is

$$U_z - V_t + [U, V] = 0 \quad (1.7.7)$$

The integrability condition leads to soliton possessing equations.

#### 1.7.4 Hirota's method

Since the discovery of IST and its subsequent developments, it has been possible to obtain large number of completely integrable NPDEs by reconstructing the potential whose spectrum consists of  $N$  discrete eigen values. However, if one is interested only in obtaining these solutions, then a more straightforward and widely applicable Hirota's direct method is suitable. This method has been used to obtain exact  $N$ -soliton solutions to a large number of NPDEs [54].

This method involves few steps. In the first step, one or two functions, say  $f(z, t)$  and  $g(z, t)$ , are introduced in place of  $q(z, t)$  through some nonlinear transformations. The objective of this transformation is to convert the given nonlinear equation into a homogeneous equation involving only the quadratic terms. In the next step, the homogeneous equation is decoupled into bilinear form. Finally a

power series expansion is given to the functions  $f(z, t)$  and  $g(z, t)$  such that exact solutions are obtained.

### 1.7.5 Bäcklund transformation

Bäcklund transformation originated in the study of surfaces of constant negative curvature. Application of Bäcklund transformation to NEEs is extended by Lamb. It relates the solution of original equation to that of another which is easier to solve. It also relates solution of given equation to another which may already be known through a simple algebraic relation. It helps to construct multisoliton solutions starting from a single soliton solution [55].

# Chapter 2

## Soliton propagation in a fiber with higher-order dispersive and nonlinear effects

### 2.1 Introduction

Dispersion-induced pulse broadening is due to the lowest order GVD term proportional to  $\beta_2$ . Contribution of this term dominates in most practical cases and hence the propagation Eq. (1.5.2) has been successful in explaining many phenomena. But, it is sometimes necessary to include higher-order dispersion term proportional to  $\beta_3$  in the expansion (1.4.34). If the pulse wavelength nearly coincides with the zero-dispersion wavelength  $\lambda_D$ ,  $\beta_2 \simeq 0$ , or for the propagation of ultrashort pulses (USP) with width  $T_0 \leq 100$  fs, it is often necessary to include  $\beta_3$  term even when  $\beta_2 \neq 0$  [56]. In addition to the higher-order dispersion effects, also called third-order dispersion, higher-order nonlinear effects will also come into play during the propagation of USPs [29, 57-60]. The important higher-order nonlinear effects are self-steepening and delayed nonlinear response.

## 2.2 NLSE in the presence of third order dispersion

Normally the effect of the third order dispersion (TOD) is negligible when compared to the GVD. Only in the zero dispersion wavelength,  $\beta_2 \simeq 0$ ; the effect of TOD will give considerable broadening to the optical pulses. Even in the anomalous dispersion regime, the effect of TOD is faced as a perturbation by ultra-short pulses (USP). Pulse broadening due to TOD is asymmetrical in nature. NLSE which governs the wave propagation with the effect of TOD takes the form [1]

$$i \frac{\partial q}{\partial z} + \frac{\partial^2 q}{\partial t^2} + 2|q|^2 q + i\varepsilon\delta_1 \frac{\partial^3 q}{\partial t^3} = 0 \quad (2.2.1)$$

The parameter  $\delta_1$  governs TOD which is proportional to  $\beta_3$  in the expansion (1.4.34) and is given by

$$\delta_1 = \frac{\beta_3}{6|\beta_2|T_0} \quad (2.2.2)$$

## 2.3 NLSE with Self-Steepening and Delayed Nonlinear Response

Self-steepening is the most important nonlinear effect due to the intensity dependent group velocity [28]. It creates an optical shock on the trailing edge of the pulse in the absence GVD effects [61, 62]. This causes the peak of the pulse to travel slower than the wings. So during propagation, pulse will become steeper and steeper. Self-steepening gives asymmetrical broadening to the optical pulse [63, 64]. In the presence of self-steepening, wave propagation in a fiber is governed

by the equation of the form [62]:

$$i \frac{\partial q}{\partial z} + \frac{\partial^2 q}{\partial t^2} + 2|q|^2 q + i\varepsilon\delta_2 \frac{\partial}{\partial t} (|q|^2 q) = 0 \quad (2.3.1)$$

The parameter  $\delta_2$  describes the effect of self-steepening. It is given by

$$\delta_2 = 1/T_0\omega_0 \quad (2.3.2)$$

Equation (2.3.1) is called mixed derivative NLS (MDNLS) equation [65]. In the presence of delayed nonlinear response, NLS equation takes the form

$$i \frac{\partial q}{\partial z} + \frac{\partial^2 q}{\partial t^2} + 2|q|^2 q + i\varepsilon\delta_3 q \frac{\partial}{\partial t} |q|^2 = 0 \quad (2.3.3)$$

The effect of a delayed nonlinear response is governed by the last term proportional to  $\delta_3$  in Eq. (2.3.3) [66, 67] and is given by

$$\delta_3 = \frac{T_R}{T_0} \quad (2.3.4)$$

The qualitative behavior of delayed nonlinear response is similar to the case of self-steepening. An important difference is that relatively smaller values of  $\delta_3$  compared with  $\delta_2$  can induce soliton decay over a given distance [66,67].

## 2.4 NLSE in the presence of all higher-order effects

From Eqs. (2.3.2), (2.3.4), and (2.3.6), it is obvious that all the higher-order parameters vary inversely with the pulse width  $T_0$ . So, for USPs, it is necessary



to include all the higher-order terms in Eq. (1.5.2) and the equation takes the form [29]

$$i \frac{\partial q}{\partial z} + \frac{\partial^2 q}{\partial t^2} + 2 |q|^2 q + i\varepsilon \left\{ \delta_1 \frac{\partial^3 q}{\partial t^3} + \delta_2 \frac{\partial}{\partial t} (|q|^2 q) + \delta_3 q \frac{\partial}{\partial t} |q|^2 \right\} = 0 \quad (2.4.1)$$

When an ultrashort optical field propagates through birefringent fiber media, its state of polarization changes during propagation. As a result, they interact through fiber nonlinearity known as cross-phase modulation. The propagation of ultrashort optical field through birefringent single mode fiber in the anomalous dispersive regime can be described by coupled higher-order nonlinear Schrödinger (CHNLS) equation of the form:

$$i q_{1z} + q_{1tt} + 2 (|q_1|^2 + |q_2|^2) q_1 + i\varepsilon [\delta_1 q_{1ttt} + \delta_2 (\{|q_1|^2 + |q_2|^2\} q_1)_t + \delta_3 (|q_1|^2 + |q_2|^2)_t q_1] = 0 \quad (2.4.2)$$

$$i q_{2z} + q_{2tt} + 2 (|q_1|^2 + |q_2|^2) q_2 + i\varepsilon [\delta_1 q_{2ttt} + \delta_2 (\{|q_1|^2 + |q_2|^2\} q_2)_t + \delta_3 (|q_1|^2 + |q_2|^2)_t q_2] = 0$$

In general, the above equations do not give soliton solutions. However, if some restrictions are imposed on the parametric values, one can obtain several integrable, soliton-possessing NLS-type equations: (i)  $\varepsilon = 0$ , NLS; (ii)  $\delta_1 = \delta_2 = \delta_3 = 0$ ,  $\delta_1 = \delta_2 = 1$ , derivative NLS [65]; (iii)  $\delta_1 = \delta_2 = \delta_3 = 0$ ,  $\delta_1 = \delta_2 = 1$ , derivative mixed NLS [65]; (iv)  $\delta_1 = \delta_2 = \delta_3 = 1$ ,  $\delta_1 = \delta_2 = 6$ ,  $\delta_3 = 0$ , the Hirota equation [68] and (v)  $\delta_1 = \delta_2 = \delta_3 = 1$ ,  $\delta_1 = \delta_2 = 6$ ,  $\delta_3 = 3$ , Sasa-Satsuma equation [69]. For the parametric values

$\delta_1 = 1, \delta_2 = 6, (\delta_2 + \delta_3) = 3$ . [69-71], Eq. (2.4.2) becomes

$$\begin{aligned}
 & i q_{1z} + q_{1tt} + 2 (|q_1|^2 + |q_2|^2) q_1 \\
 & + i \varepsilon [q_{1ttt} + 6 (|q_1|^2 + |q_2|^2) q_{1t} + 3 (|q_1|^2 + |q_2|^2)_t q_1] = 0
 \end{aligned} \tag{2.4.3}$$

$$\begin{aligned}
 & i q_{2z} + q_{2tt} + 2 (|q_1|^2 + |q_2|^2) q_2 \\
 & + i \varepsilon [q_{2ttt} + 6 (|q_1|^2 + |q_2|^2) q_{2t} + 3 (|q_1|^2 + |q_2|^2)_t q_2] = 0
 \end{aligned}$$

## 2.5 Integrability analysis of CHNLS equations

In this section, Painlevé (P) analysis of Eq. (2.4.3) is studied. The motivation behind this exercise is that P condition is a necessary one for studying the integrability of nonlinear partial differential equations and helps to construct solutions. The integrability analysis of Eq. (2.4.3) is carried out by following WTC method with a suitable simplification proposed by Kruskal [48, 49]. This analysis ensures that the general solution of Eq. (2.4.3) is single valued around any movable non-characteristic singular manifold when expressed locally as a Laurent series. For this purpose, assume a solution of Eq. (2.4.3) in the form:

$$q_1(z, t) = \phi^\alpha \sum_{j=0}^{\infty} q_{1j}(z) \phi^j(z, t), q_{10} \neq 0 \tag{2.5.1}$$

$$q_2(z, t) = \phi^\alpha \sum_{j=0}^{\infty} q_{2j}(z) \phi^j(z, t), q_{20} \neq 0$$

with

$$\phi(z, t) = t + \psi(z) = 0 \tag{2.5.2}$$

where  $\psi(z)$  is an arbitrary analytic function of  $t$ ,  $q_{1j}(z)$  and  $q_{2j}(z)$  ( $j = 0, 1, 2, \dots$ ), in the neighborhood of a noncharacteristic movable singularity manifold defined

by  $\phi = 0$ .

In order to investigate the integrability properties of Eq. (2.4.3), it is rewritten in terms of four complex functions  $a$ ,  $b$ ,  $c$  and  $d$  by defining  $q_1 = a$ ,  $q_1^* = b$ ,  $q_2 = c$ ,  $q_2^* = d$ . Then Eq. (2.4.3) becomes:

$$\begin{aligned}
 ia_z + a_{tt} + 2(ab + cd)a + i\varepsilon[a_{ttt} + 6(ab + cd)a_t + 3(ab + cd)_t a] &= 0 \\
 -ib_z + b_{tt} + 2(ab + cd)b - i\varepsilon[b_{ttt} + 6(ab + cd)b_t + 3(ab + cd)_t b] &= 0 \\
 ic_z + c_{tt} + 2(ab + cd)c + i\varepsilon[c_{ttt} + 6(ab + cd)c_t + 3(ab + cd)_t c] &= 0 \\
 -id_z + d_{tt} + 2(ab + cd)d - i\varepsilon[d_{ttt} + 6(ab + cd)d_t + 3(ab + cd)_t d] &= 0
 \end{aligned}
 \tag{2.5.3}$$

Looking at the leading order behavior, substitute  $a \simeq a_0\phi^{\alpha_1}$ ,  $b \simeq b_0\phi^{\alpha_2}$ ,  $c \simeq c_0\phi^{\alpha_3}$ ,  $d \simeq d_0\phi^{\alpha_4}$  in Eqs. (2.5.3) and balancing the dominant terms, gives:

$$\alpha_1 = \alpha_2 = \alpha_3 = \alpha_4 = -1,
 \tag{2.5.4}$$

$$a_0 b_0 + c_0 d_0 = -\frac{1}{2}.$$

For finding the powers at which the arbitrary functions can enter into the series, substitute the expressions:

$$a = a_0\phi^{-1} + a_j\phi^{j-1}, b = b_0\phi^{-1} + b_j\phi^{j-1}
 \tag{2.5.5}$$

$$c = c_0\phi^{-1} + c_j\phi^{j-1}, d = d_0\phi^{-1} + d_j\phi^{j-1}$$

into Eq. (2.5.3), and comparing the lowest-order terms, a system of four linear

algebraic equations in  $(a_j, b_j, c_j, d_j)$  are obtained. In matrix form, it may be conveniently written as

$$[A(j)][X] = 0 \quad (2.5.6)$$

where  $[X] = (a_j, b_j, c_j, d_j)^T$

and

$$[A(j)] = \begin{bmatrix} B & D & E & F \\ G & B & H & I \\ I & F & C & J \\ H & E & K & C \end{bmatrix}$$

where

$$B = (j-1)(j-2)(j-3) - 3(j-1) - 6a_0b_0 + 3(j-2) + 3,$$

$$C = (j-1)(j-2)(j-3) - 3(j-1) - 6c_0d_0 + 3(j-2) + 3$$

$$D = -6a_0^2 + 3a_0^2(j-2), E = -6a_0d_0 + 3a_0d_0(j-2)$$

$$F = -6a_0c_0 + 3a_0c_0(j-2), G = -6b_0^2 + 3b_0^2(j-2)$$

$$H = -6b_0d_0 + 3b_0d_0(j-2), I = -6b_0c_0 + 3b_0c_0(j-2)$$

$$J = -6c_0^2 + 3c_0^2(j-2), K = -6d_0^2 + 3d_0^2(j-2)$$

Condition for non-trivial solution for  $a_j, b_j, c_j$  and  $d_j$  is that

$$\det A(j) = 0 \quad (2.5.7)$$

On solving Eq. (2.5.7), the resonance values are obtained as  $j = -1, 0, 0, 0, 2, 2, 2, 3, 4, 4, 4, 4$ . The resonance at  $j = -1$  corresponds to the arbitrariness of  $\psi(z, t)$

On equating the coefficients of  $\psi^{-4}$ , a unique equation defining  $a_0, b_0, c_0$  and  $d_0$  is obtained:

$$a_0 b_0 + c_0 d_0 = -\frac{1}{2}. \quad (2.5.8)$$

This shows that any three of the four functions  $a_0, b_0, c_0$  and  $d_0$  are arbitrary which correspond to  $j = 0, 0, 0$ . Proceeding further and equating the coefficients of  $(\psi^{-3}, \psi^{-3}, \psi^{-3}, \psi^{-3})$  gives:

$$a_1 = -\frac{a_0}{3iz}, \quad b_1 = \frac{b_0}{3iz}, \quad c_1 = -\frac{c_0}{3iz}, \quad d_1 = \frac{d_0}{3iz}. \quad (2.5.9)$$

The coefficients of  $(\psi^{-2}, \psi^{-2}, \psi^{-2}, \psi^{-2})$  gives rise to a single equation:

$$b_0 a_2 + a_0 b_2 + d_0 c_2 + c_0 d_2 = -\frac{\psi_t}{6z} \quad (2.5.10)$$

From the above equation, it is clear that any three of the four functions  $a_2, b_2, c_2$  and  $d_2$  are arbitrary which correspond to  $j = 2, 2, 2$ . Similarly from the powers of  $(\psi^{-1}, \psi^{-1}, \psi^{-1}, \psi^{-1})$  and  $(\psi^{-0}, \psi^{-0}, \psi^{-0}, \psi^{-0})$ , it is clear that Eq. (2.5.3) admit the sufficient number of arbitrary functions and hence Eq. (2.4.3) possesses the Painlevé property.

## 2.6 Hirota bilinearization and soliton solutions

Hirota's bilinear method [54] is one of the most direct and elegant methods available to generate multi-soliton solutions of nonlinear partial differential equations. In the present form, it is difficult to construct multi-soliton solutions of Eq. (2.4.3). So, to avoid mathematical complexities, a suitable transformation is

introduced as:

$$q_1(z, t) = Q_1(Z, T) \exp \left[ i \left( \frac{Z}{3\epsilon} + \frac{T}{27\epsilon^2} \right) \right], q_2(z, t) = Q_2(Z, T) \exp \left[ i \left( \frac{Z}{3\epsilon} + \frac{T}{27\epsilon^2} \right) \right]$$

$$z = T, Z = t - \frac{z}{3\epsilon} \quad (2.6.1)$$

Using the above transformations in Eq.(2.4.3), the resulting equation is obtained in the form:

$$Q_{1Z} + \epsilon \left[ Q_{1TTT} + 6(|Q_1|^2 + |Q_2|^2) Q_{1T} + 3Q_1 (|Q_1|^2 + |Q_2|^2)_T \right] = 0 \quad (2.6.2)$$

$$Q_{2Z} + \epsilon \left[ Q_{2TTT} + 6(|Q_1|^2 + |Q_2|^2) Q_{2T} + 3Q_2 (|Q_1|^2 + |Q_2|^2)_T \right] = 0$$

The above equation is called complex modified K-dV (cmK-dV) equation. In order to construct Hirota's bilinear form, following bilinear transformations are introduced.

$$Q_1 = \frac{G}{F} \quad Q_2 = \frac{H}{F} \quad (2.6.3)$$

where  $G(Z, T)$  and  $H(Z, T)$  are complex functions and  $F(Z, T)$  is a real function. Now using the transformations given in Eq. (2.6.3), Eq. (2.6.2) can be rewritten as

$$\begin{aligned}
& F^2 [(D_Z + \varepsilon D_T^3)(G.F)] + \varepsilon\{-3D_T^2(F.F)D_T + 12(|G|^2 + |H|^2)D_T\}(G.F) \\
& + 3GFD_T(G.G^*) + 3H^*FD_T(H.G) - 3HFD_T(G.H^*) = 0 \\
& F^2 [(D_Z + \varepsilon D_T^3)(H.F)] + \varepsilon\{-3D_T^2(F.F)D_T + 12(|G|^2 + |H|^2)D_T\}(H.F) \\
& + 3HFD_T(H.H^*) - 3G^*FD_T(H.G) + 3GFD_T(H.G^*) = 0
\end{aligned} \tag{2.6.4}$$

where the Hirota bilinear operators  $D_z$  and  $D_t$  are defined as

$$D_Z^m D_T^n G(Z, T) F(Z', T') = \left( \frac{\partial}{\partial Z} - \frac{\partial}{\partial Z'} \right)^m \left( \frac{\partial}{\partial T} - \frac{\partial}{\partial T'} \right)^n G(Z, T) F(Z', T') \Big|_{Z=Z', T=T'} \tag{2.6.5}$$

Equation (2.6.4) can be decoupled into a set of bilinear equations as

$$(D_Z + \varepsilon D_T^3)(G.F) = 0, \quad (D_Z + \varepsilon D_T^3)(H.F) = 0$$

$$D_T^2(F.F) = 4(|G|^2 + |H|^2) \tag{2.6.6}$$

$$D_T(G.G^*) = 0, D_T(H.H^*) = 0, D_T(G.H^*) = 0,$$

$$D_T(H.G^*) = 0, D_T(G.H) = 0$$

To obtain soliton solutions, a power series expansion is given to the variables  $F$ ,

$G$ , and  $H$ . i.e.

$$F = 1 + \eta^2 f_2 + \eta^4 f_4 + \dots, \quad G = \eta g_1 + \eta^3 g_3 + \eta^5 g_5 + \dots, \quad H = \eta h_1 + \eta^3 h_3 + \eta^5 h_5 + \dots \quad (2.6.7)$$

### 2.6.1 One-soliton solutions

For one-soliton solution (1SS):

$$F = 1 + \eta^2 f_2 \quad G = \eta g_1 \quad H = \eta h_1 \quad (2.6.8)$$

since higher-order terms get truncated. On substituting Eq.(2.6.8) in Eq.(2.6.6) and then collecting the coefficients of terms with same powers in  $\eta$ :

$\eta$

$$(D_Z + \varepsilon D_T^3)(g_1 \cdot 1) = 0 \quad (D_Z + \varepsilon D_T^3)(h_1 \cdot 1) = 0 \quad (2.6.9)$$

$\eta^2$

$$D_T^2(1 \cdot f_2 + f_2 \cdot 1) = 4(g_1 \cdot g_1^* + h_1 \cdot h_1^*)$$

$$D_T(g_1 \cdot g_1^*) = 0, D_T(h_1 \cdot h_1^*) = 0, D_T(g_1 \cdot h_1^*) = 0, \quad (2.6.10)$$

$$D_T(h_1 \cdot g_1^*) = 0, D_T(g_1 \cdot h_1) = 0$$

$\eta^3$

$$(D_Z + \varepsilon D_T^3)(g_1 \cdot f_2) = 0 \quad (D_Z + \varepsilon D_T^3)(h_1 \cdot f_2) = 0 \quad (2.6.11)$$



$\eta^4$

$$D_T^2 (f_2 \cdot f_2) = 0 \quad (2.6.12)$$

Solutions which are consistent with Eqs. (2.6.9)-(2.6.12) are

$$g_1 = \exp(\lambda_1 + \eta_0) \quad h_1 = \sin \phi \exp(\lambda_1 + \varepsilon_0) \quad (2.6.13)$$

$$f_2 = \left( \frac{A_1}{k_1^2} \right) \exp(2\lambda_1)$$

where

$$\lambda_1 = k_1 (T - \varepsilon k_1^2 Z) \quad \text{and} \quad A_1 = \frac{1}{2} [\exp(\eta_0^* + \eta_0) + \exp(\varepsilon_0^* + \varepsilon_0)] \quad (2.6.14)$$

$\eta_0$  and  $\varepsilon_0$  are complex constants and  $k_1$  is a real constant. Using Eqs. (2.6.13) and (2.6.14) in (2.6.8) and then in (2.6.3), after absorbing  $\eta$  the one-soliton solution obtained as

$$Q_1 = B_1 k_1 \operatorname{sech}(k_1 T - \varepsilon k_1^3 Z + \theta_0) \quad (2.6.15)$$

$$Q_2 = B_2 k_1 \operatorname{sech}(k_1 T - \varepsilon k_1^3 Z + \theta_0)$$

where

$$\theta_0 = \frac{1}{2} \ln \left( \frac{A_1}{k_1^2} \right) \quad B_1 = \sqrt{\frac{\exp(2\eta_0)}{4A_1}}, \quad B_2 = \sqrt{\frac{\exp(2\varepsilon_0)}{4A_1}}$$

Using Eq.(2.6.1), one-soliton solution of Eq.(2.4.3) is found to be:

$$q_1 = B_1 k_1 \exp \left[ i \left( \frac{Z}{3\varepsilon} + \frac{T}{27\varepsilon^2} \right) \right] \operatorname{sech}(k_1 T - \varepsilon k_1^3 Z + \theta_0) \quad (2.6.16)$$

$$q_2 = B_2 k_1 \exp \left[ i \left( \frac{Z}{3\varepsilon} + \frac{T}{27\varepsilon^2} \right) \right] \operatorname{sech}(k_1 T - \varepsilon k_1^3 Z + \theta_0)$$

## 2.6.2 Two-soliton solutions

The two-soliton solutions can be obtained by terminating the series expansion for  $F, G, H$  as

$$F = 1 + \eta^2 f_2 + \eta^4 f_4, \quad G = \eta g_1 + \eta^3 g_2, \quad H = \eta h_1 + \eta^3 h_3 \quad (2.6.17)$$

and proceeding as before gives:

$$g_1 = \exp(\lambda_1 + \eta_0) + \exp(\lambda_2 + \eta_0) \quad h_1 = \exp(\lambda_1 + \varepsilon_0) + \exp(\lambda_2 + \varepsilon_0)$$

$$g_3 = A_1 \frac{(k_1 - k_2)^2}{(k_1 + k_2)^2} \left[ \frac{\exp(2\lambda_1 + \lambda_2 + \eta_0)}{k_1^2} + \frac{\exp(\lambda_1 + 2\lambda_2 + \eta_0)}{k_2^2} \right]$$

$$h_3 = A_1 \frac{(k_1 - k_2)^2}{(k_1 + k_2)^2} \left[ \frac{\exp(2\lambda_1 + \lambda_2 + \varepsilon_0)}{k_1^2} + \frac{\exp(\lambda_1 + 2\lambda_2 + \varepsilon_0)}{k_2^2} \right]$$

$$f_2 = A_1 \left[ \frac{\exp(2\lambda_1)}{k_1^2} + 8 \frac{\exp(\lambda_1 + \lambda_2)}{(k_1 + k_2)^2} + \frac{\exp(2\lambda_2)}{k_2^2} \right]$$

$$f_4 = \frac{A_1 (k_1 - k_2)^4 \exp(2\lambda_1 + 2\lambda_2)}{k_1^2 k_2^2 (k_1 + k_2)^4} \quad (2.6.18)$$

where

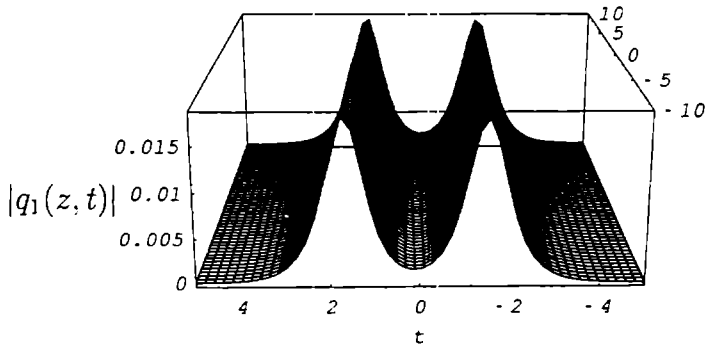
$$\lambda_j = k_j T - \varepsilon k_j^3 Z \quad j = 1, 2 \quad (2.6.19)$$

Here  $k_j$  is a real constant. Using Eqs. (2.6.17)-(2.6.19) in Eqs. (2.6.3) and (2.6.1), the two-soliton solutions of Eq. (2.4.3) are found to be

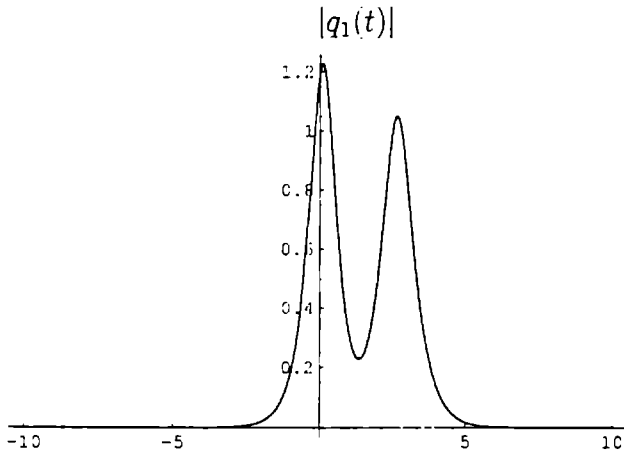
$$u = \frac{G}{F} \exp \left[ i \left( \frac{Z}{3\epsilon} + \frac{T}{27\epsilon^2} \right) \right] \quad (2.6.20)$$

$$v = \frac{H}{F} \exp \left[ i \left( \frac{Z}{3\epsilon} + \frac{T}{27\epsilon^2} \right) \right]$$

Both 1SS and 2SS are in exact agreement with Eq.(2.4.3). Three dimensional and two dimensional plots of 2SS are given in Figs. 2.1(a) and (b) respectively.



(a)



(b)

Fig. 2.1: (a) Three dimensional evolution of the two-soliton solution (2.6.20) (b) two dimensional evolution.

## 2.7 Asymptotic analysis

If the two solitary waves solutions shown in Fig. 2.1 retain their shape and velocity after interaction, i.e. undergo elastic collisions, solitary waves are said to be solitons. Theoretically this can be verified by applying asymptotic analysis to the Eqs. (2.6.18) and (2.6.19). In order to prove that the above solution is indeed the two-soliton solution, Eqs. (2.6.18) and (2.6.19) are rewritten in terms of the new variable  $\rho_1 = T - \varepsilon k_1^2 Z$  and allow the variable  $Z \rightarrow \pm\infty$

$$Q_1 = B_1 k_1 \operatorname{sech}(k_1 T - \varepsilon k_1^3 Z + \lambda') \quad (2.7.1)$$

$$Q_2 = B_2 k_1 \operatorname{sech}(k_1 T - \varepsilon k_1^3 Z + \lambda')$$

where the phase factor

$$\lambda' = \ln \left[ \frac{(k_2 - k_1)^2}{k_1 (k_1 + k_2)^2} \right] \quad (2.7.2)$$

It is obvious from the one-soliton solution (2.7.1) that except for the phase shift of magnitude  $\lambda'$ , the form of the solutions in the limits  $+\infty$  and  $-\infty$  are the same. The presence of another set of one-soliton solutions in (2.6.18) and (2.6.19) with a similar behavior can also be shown by allowing the variable  $Z \rightarrow \pm\infty$  after introducing the new variable  $\rho_2 = T - \varepsilon k_2^2 Z$ . When  $Z \rightarrow \pm\infty$ ,

$$Q_1 = B_1 k_2 \operatorname{sech}(k_2 T - \varepsilon k_2^3 Z + \lambda') \quad (2.7.3)$$

$$Q_2 = B_2 k_2 \operatorname{sech}(k_2 T - \varepsilon k_2^3 Z + \lambda')$$

Thus it is clear that two solitary waves interact in a completely elastic fashion. The only vestige of their interaction is the change in their phase-shift. Each

solitary like wave, (2.7.1) and (2.7.3), which occurs as  $Z \rightarrow \pm\infty$ , and which interact in the special way, is called soliton; and therefore the solutions described by Eq. (2.6.18) and (2.6.19) are exact two-soliton solutions.

## 2.8 Lax pair for CHNLS equations

The linear eigen value problem associated with Eq.(2.6.2) is

$$\psi_T = U\psi \quad \psi_Z = V\psi \quad \psi = (\psi_1 \ \psi_2)^T \quad (2.8.1)$$

where

$$U = \begin{pmatrix} -i\chi & Q_1 & Q_1^* & Q_2 & Q_2^* \\ -Q_1^* & i\chi & 0 & 0 & 0 \\ -Q_1 & 0 & i\chi & 0 & 0 \\ -Q_2^* & 0 & 0 & i\chi & 0 \\ -Q_2 & 0 & 0 & 0 & i\chi \end{pmatrix} \quad (2.8.2)$$

$$\begin{aligned}
V = & \frac{8i\varepsilon\chi^2}{5} \begin{pmatrix} -4 & 0 & 0 & 0 & 0 \\ 0 & 1 & 0 & 0 & 0 \\ 0 & 0 & 1 & 0 & 0 \\ 0 & 0 & 0 & 1 & 0 \\ 0 & 0 & 0 & 0 & 1 \end{pmatrix} + 4\varepsilon\chi^2 \begin{pmatrix} 0 & Q_1 & Q_1^* & Q_2 & Q_2^* \\ -Q_1^* & 0 & 0 & 0 & 0 \\ -Q_1 & 0 & 0 & 0 & 0 \\ -Q_2^* & 0 & 0 & 0 & 0 \\ -Q_2 & 0 & 0 & 0 & 0 \end{pmatrix} \\
& -2i\varepsilon\chi \begin{pmatrix} -2A & -Q_{1T} & -Q_{1T}^* & -Q_{2T} & -Q_{2T}^* \\ -Q_{1T} & |Q_1|^2 & (Q_1^*)^2 & Q_1^*Q_2 & Q_1^*Q_2^* \\ -Q_{1T}^* & Q_1^2 & |Q_1|^2 & Q_1Q_2 & Q_1Q_2^* \\ -Q_{2T} & Q_1Q_2^* & Q_1^*Q_2^* & |Q_2|^2 & (Q_2^*)^2 \\ -Q_{2T}^* & Q_1Q_2 & Q_1^*Q_2 & Q_2^2 & |Q_2|^2 \end{pmatrix} \\
& +\chi \begin{pmatrix} 0 & a_{12} & a_{13} & a_{14} & a_{15} \\ a_{21} & a_{22} & 0 & a_{24} & a_{25} \\ a_{31} & 0 & a_{33} & a_{34} & a_{35} \\ a_{41} & a_{42} & a_{43} & a_{44} & 0 \\ a_{51} & a_{52} & a_{53} & 0 & a_{55} \end{pmatrix}
\end{aligned} \tag{2.8.3}$$

where

$$\begin{aligned}
a_{12} &= 4 A Q_1 + Q_{1TT}, \quad a_{13} = 4 A Q_1^* + Q_{1TT}^*, \quad a_{14} = 4 A Q_2 + Q_{2TT}, \\
a_{15} &= 4 A Q_2^* + Q_{2TT}^*, \quad a_{21} = -4 A Q_1^* - Q_{1TT}^*, \quad a_{22} = Q_1Q_{1T}^* - Q_1^*Q_{1T}, \\
a_{24} &= Q_2Q_{1T}^* - Q_1^*Q_{2T}, \quad a_{25} = Q_2^*Q_{1T}^* - Q_1^*Q_{2T}^*, \quad a_{31} = -4 A Q_1 - Q_{1TT}, \\
a_{33} &= Q_1^*Q_{1T} - Q_1Q_{1T}^*, \quad a_{34} = Q_2Q_{1T} - Q_1Q_{2T}, \quad a_{35} = Q_2^*Q_{1T} - Q_1Q_{2T}^*, \\
a_{41} &= -4 A Q_2 - Q_{2TT}, \quad a_{42} = Q_1Q_{2T}^* - Q_2^*Q_{1T}, \quad a_{43} = Q_1^*Q_{2T} - Q_2^*Q_{1T}^*, \\
a_{44} &= Q_2Q_{2T}^* - Q_2^*Q_{2T}, \quad a_{51} = -4 A Q_2 - Q_{2TT}, \quad a_{52} = Q_1Q_{2T} - Q_2Q_{1T},
\end{aligned}$$

$$a_{53} = Q_1^* Q_{2T} - Q_2 Q_{1T}^*, \quad a_{55} = Q_2^* Q_{2T} - Q_2 Q_{2T}^*$$

$$\text{with } A = |Q_1|^2 + |Q_2|^2$$

The compatibility condition  $U_Z - V_T + [U, V] = 0$  gives rise to Eq. (2.6.2). The construction of Lax pair confirms that Eq. (2.6.2) and thereby the CHNLS Eq. (2.4.3) is indeed completely integrable.

## 2.9 Conclusion

In this chapter, coupled NLS equation with higher-order dispersive and nonlinear effects are considered. By choosing the parameters, Painlevé singularity structure analysis is done and established the integrability. By introducing the suitable transformation, CHNLS equations have been transformed into complex modified K-dV equations. Using Hirota bilinearisation technique, both one-soliton and two-soliton solutions are found out. By using asymptotic analysis, it is found that two-soliton solutions undergo elastic collisions and thus verified that they are indeed two-soliton solutions. Also constructed Lax pairs using AKNS formalism which confirms the integrability of CHNLS equations proved by Painlevé analysis. Thus, with these results, it is shown that the CHNLS equations which describe the wave propagation of two fields in fibre systems with all higher-order effects such as TOD, Kerr dispersion, and delayed nonlinear response, will allow soliton-type propagation.

# Chapter 3

## Effect of frequency chirping on soliton formation

### 3.1 Introduction

Generation of stable ultrashort optical pulses find important applications in ultrahigh-bit-rate optical communication systems, measurement of ultrafast physical process [72], optoelectronic terahertz time domain spectroscopy [73], optoelectronic sampling [74,75] etc. It is possible to generate ultrashort pulses directly from semiconductor lasers [76, 77]. But for these applications of ultrashort pulses, optical pulses with high energies are required and that are not readily available from laser producing ultrashort pulses. It is then necessary to compress the pulse internally. The important pulse compression techniques are soliton-effect compressors [39, 78, 79], compression by adiabatic amplification [11, 12], higher-order soliton compression [45], compression using dispersion-decreasing fiber [11, 12, 80] etc. In this chapter, a new approach is presented, the effect of initial frequency chirp, to compress the pulse.



## 3.2 Formulation of the problem

In an ideal soliton-based communication systems, input pulse launched into the fiber should be chirped, have a hyperbolic-secant shape. In practice, pulse deviate from the ideal requirements necessary to launch the fundamental soliton. The effect of initial frequency chirp during the formation of soliton can be studied using the equation [81]

$$iq_z + q_{tt} + 2 |q|^2 q = \alpha_1(z)t^2q + i\alpha_2(z)q \quad (3.2.1)$$

where  $q(z, t)$  is the slowly varying pulse of the axial field. Equation (3.2.1) contains arbitrary functions  $\alpha_1(z)$  and  $\alpha_2(z)$ . Above equation in the present form does not give soliton solution. Using singularity structure analysis, the integrability condition(s) of the above equation required for the formation of soliton solution is discussed in the next section.

## 3.3 Singularity structure analysis

This analysis ensures that solution of Eq. (3.2.1) is single valued around any movable noncharacteristics manifold when expressed locally as a Laurent series. For this purpose, solution Eq. (3.2.1) is assumed to be of the form:

$$q(z, t) = \phi^\delta \sum_{j=0}^{\infty} q_j(t) \phi^j(z, t), \quad q_0 \neq 0 \quad (3.3.1)$$

with

$$\phi(z, t) = t + \psi(z) = 0 \quad (3.3.2)$$

where  $\psi(t)$  is an arbitrary analytic function of  $t$ ,  $q_j(t)$  ( $j = 0, 1, 2, \dots$ ), in the neighborhood of a noncharacteristic movable singularity manifold defined by  $\phi = 0$ . To investigate the integrability properties of Eq. (3.2.1), it is written in terms of two complex functions  $a$  and  $b$  by defining  $q = a$ ,  $q^* = b$ . Consequently, the following equations are obtained:

$$ia_z + a_{tt} + a^2b = \alpha_1(z)t^2a + i\alpha_2(z)a \quad (3.3.3)$$

$$-ib_z + b_{tt} + b^2a = \alpha_1(z)t^2b - i\alpha_2(z)b$$

where  $a_0, b_0 \neq 0$ ,  $\delta$  is a negative integer and  $a_j$  and  $b_j$  are a set of expansion coefficients analytic in the neighborhood of the non-characteristic singular manifold  $\phi(z, t) = 0$ .

Looking at the leading order behavior, substituting  $a \simeq a_0\phi^{\delta_1}$  and  $b \simeq b_0\phi^{\delta_2}$  in Eq. (3.3.3) and equating the most dominant terms, gives

$$\begin{aligned} \delta_1 = \delta_2 &= -1 \\ a_0b_0 &= -1 \end{aligned} \quad (3.3.4)$$

For finding the powers at which the arbitrary functions can enter into the series, substituting the expressions:

$$a = a_0\phi^{-1} + a_j\phi^{j-1}, \quad (3.3.5)$$

$$b = b_0\phi^{-1} + b_j\phi^{j-1}$$

in Eq. (3.3.3) and comparing the lowest-order terms, a system of two linear algebraic equations in  $(a_j, b_j)$  are obtained. In matrix form it may be conveniently written as:

$$[A(j)][X] = 0 \quad (3.3.6)$$

where

$$[X] = (a_j, b_j)^T$$

$$[A(j)] = \begin{pmatrix} (j-1)(j-2) - 4 & 2a_0^2 \\ 2b_0^2 & (j-1)(j-2) - 4 \end{pmatrix} \quad (3.3.7)$$

Condition for non-trivial solution for  $a_j$  and  $b_j$  is that:

$$|A(j)| = 0. \quad (3.3.8)$$

On solving Eq. (3.3.8), the resonance values are obtained as  $j = -1, 0, 3, 4$ . The resonance at  $j = -1$  corresponds to the arbitrariness of the singular manifold  $\phi(z, t)$ . The resonance at  $j = 0$  corresponds to the fact that any one of the two functions  $a_0$  or  $b_0$  are arbitrary as seen in Eq. (3.3.4). The existence of arbitrary functions at other resonance values can be proved by substituting the full Laurent expansion into Eq. (3.3.3). On equating the coefficients of  $(\psi^{-2}, \psi^{-2})$ , the following equations are obtained:

$$a_1 = \frac{-ia_0\psi_z}{2} \quad (3.3.9)$$

$$b_1 = \frac{ib_0\psi_z}{2}$$

Now, collecting the coefficients of  $(\psi^{-1}, \psi^{-1})$  and on solving:

$$a_2 = (a_0/6)[-ia_{0z}b_0 - \psi_z^2/2 - \alpha_1(z)t^2 - 3i\alpha_2(z)] \quad (3.3.10)$$

$$b_2 = (b_0/6)[ib_{0z}a_0 - \psi_z^2/2 - \alpha_1 t^2 + 3i\alpha_2]$$

Further, from the coefficients of  $(\psi^0, \psi^0)$  and  $(\psi^1, \psi^1)$ , it is clear that Eq. (3.3.3) admits sufficient number of arbitrary functions when the condition:

$$\alpha_{2z} = 2(\alpha_2^2 + \alpha_1) \quad (3.3.11)$$

is satisfied and which corresponds to  $j = 3$  and  $j = 4$  respectively. Thus the general solution (a, b) of Eq. (3.3.3) admits the required number of arbitrary functions, without the introduction of any movable critical manifold, thereby satisfying the P property and hence Eq. (3.2.1) is integrable under the condition (3.3.11). In the present calculation,  $\alpha_2$  is considered as a constant parameter. Then the condition (3.3.11) becomes:

$$\alpha_1 = -\alpha_2^2. \quad (3.3.12)$$

From Eq. (3.3.12), it is obvious that when  $\alpha_2$  is considered as a constant parameter,  $\alpha_1$  also behaves as a constant parameter. For this case,  $\alpha_1$  describes the effect of frequency chirping [81] whereas  $\alpha_2$  describes fiber loss.

### 3.4 Linear eigen value problem

The Lax pair assures the complete integrability of a nonlinear system. Before constructing Lax Pair of Eq. (3.2.1) for the case (3.3.12), a variable transformation:

$$q(z, t) = Q(z, t) \exp\left(\frac{i\alpha_2 t^2}{2}\right) \quad (3.4.1)$$

is introduced. Then Eq. (3.2.1) becomes:

$$iQ_z + Q_{tt} + 2|Q|^2 Q - 2i\alpha_2 t Q_t - 2i\alpha_2 Q = 0. \quad (3.4.2)$$

Now it is convenient to construct Lax pair for Eq. (3.4.2). The linear eigen value problem associated with Eq. (3.4.2) is:

$$\psi_t = U\psi, \quad \psi_z = V\psi, \quad \psi = (\psi_1, \psi_2)^T \quad (3.4.3)$$

where

$$U = \begin{pmatrix} -i\lambda & Q \\ -Q^* & i\lambda \end{pmatrix} \quad (3.4.4)$$

$$V = 2i\lambda^2 \begin{pmatrix} -1 & 0 \\ 0 & 1 \end{pmatrix} + 2\lambda \begin{pmatrix} -i\alpha_2 t & Q \\ -Q^* & i\alpha_2 t \end{pmatrix} + i \begin{pmatrix} |Q|^2 & Q_t - 2i\alpha_2 t Q \\ Q_t^* + 2i\alpha_2 t Q^* & -|Q|^2 \end{pmatrix} \quad (3.4.5)$$

$\lambda$  is the non-isospectral parameter given by

$$\lambda = \lambda_1 + i\lambda_2 = \lambda_0 \exp(2\alpha_2 z) \quad (3.4.6)$$

Now the relation  $U_z - V_t + [U V] = 0$ , gives rise to the Eq. (3.4.2). Thus the complete integrability of Eq. (3.4.2) is confirmed by Lax pair and thereby Eq. (3.2.1) for the case (3.3.12).

### 3.5 Soliton solution

Soliton solution of the Eq. (3.4.2) can be constructed with the help of linear eigen value problem and Bäcklund transformation. To construct the Bäcklund transformation of Eq. (3.4.2), a new variable known as pseudopotential,  $\Gamma$ , is introduced:

$$\Gamma = \frac{\psi_1}{\psi_2} \quad (3.5.1)$$

Differentiating Eq. (3.5.1) and using Eq. (3.4.3):

$$\Gamma_t = -2i\lambda\Gamma + Q + \Gamma^2 Q^* \quad (3.5.2)$$

$$\Gamma_z = -4i\lambda^2\Gamma + 4i\lambda t\Gamma + 2i|Q|^2\Gamma + 2\lambda(Q + Q^*\Gamma^2) + i(Q_t - Q_t^*) \quad (3.5.3)$$

To construct Bäcklund transformation (BT), new transformations in the form  $\Gamma \rightarrow \Gamma'$ ,  $\lambda \rightarrow \lambda^*$ ,  $Q \rightarrow Q'$  is introduced and which keep the form of Eqs. (3.5.2) and (3.5.3) invariant. The simplest transformation can be tried by setting  $\Gamma' = \Gamma$  and after some simplification, the BT of Eq. (3.4.2) is obtained in the form:

$$Q' = Q + \frac{4\lambda_2\Gamma}{1 + |\Gamma|^2} \quad (3.5.4)$$

In Eq. (3.5.4), the primed quantity refers to  $N$ -soliton solution and unprimed quantities refer to  $(N-1)$  soliton solutions. Using Eq. (3.5.4), one can in principle generate  $N$ -soliton solutions.

To find  $\Gamma$ , consider the trivial case  $Q = 0$ , then the equation  $\psi_t = U\psi$  becomes

$$\psi_{1t} = -i\lambda\psi_1 \quad (3.5.5)$$

$$\psi_{2t} = i\lambda\psi_2$$

and equation  $\psi_z = U\psi$  becomes

$$\psi_{1z} = (-2i\lambda^2 + 2i\lambda t)\psi_1 \quad (3.5.6)$$

$$\psi_{2z} = (2i\lambda^2 - 2i\lambda t)\psi_2$$

On solving Eqs. (3.5.5) and (3.5.6)

$$\psi_1(z, t) = c_1(0) \exp \left[ -2i \int \lambda^2 dz - i\lambda t \right] \quad (3.5.7)$$

$$\psi_2(z, t) = c_2(0) \exp \left[ 2i \int \lambda^2 dz + i\lambda t \right]$$

Substituting Eq. (3.5.7) in Eq. (3.5.1), pseudopotential is obtained as:

$$\Gamma = \frac{c_1(0)}{c_2(0)} \exp \left[ -2i\lambda_1 t + 2\lambda_2 t - 4i \int (\lambda_1^2 - \lambda_2^2) dz + 8 \int \lambda_1 \lambda_2 dz \right] \quad (3.5.8)$$

where  $\lambda_1 = \lambda_1(0) \exp[2\alpha_2 z]$  and  $\lambda_2 = \lambda_2(0) \exp[2\lambda z]$ . Substituting Eq. (3.5.8) in Eq. (3.5.4), the one-soliton solution of Eq. (3.4.2) is found to be:

$$Q = 2\lambda_2\chi \exp \left[ -2i\lambda_1 t - 4i \int (\lambda_1^2 - \lambda_2^2) dz \right] \operatorname{sech} \left[ 2\lambda_2 t + 8 \int \lambda_1 \lambda_2 dz + \theta \right] \quad (3.5.9)$$

where  $\chi = \sqrt{\frac{|c_2(0)|^2}{|c_1(0)|^2}}$  and  $\theta = \frac{1}{2} \ln \left[ \frac{|c_1(0)|^2}{|c_2(0)|^2} \right]$

One soliton solution of Eq. (3.2.1) is obtained by substituting the above solution in Eq. (3.4.1).

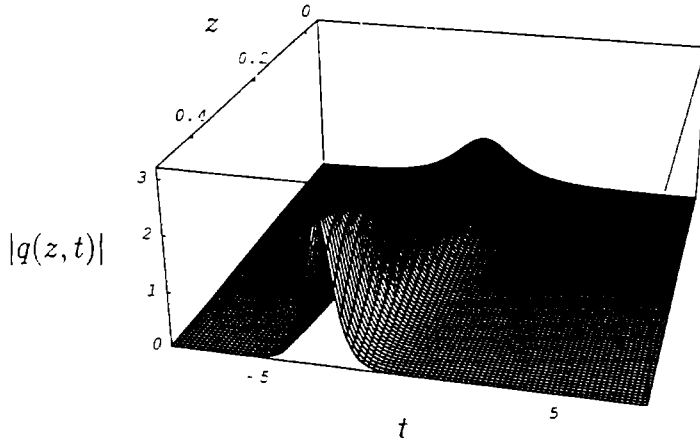
$$q(z, t) = 2\lambda_2\chi \exp \left[ -2i\lambda_1 t - 4i \int (\lambda_1^2 - \lambda_2^2) dz + \frac{i\alpha_2 t^2}{2} \right] \operatorname{sech} \left[ 2\lambda_2 t + 8 \int \lambda_1 \lambda_2 dz + \theta \right] \quad (3.5.10)$$

From Eq. (3.5.10), input pulse (at the input,  $z = 0$  and  $\alpha_1(z) = 0$ ) can be described as:

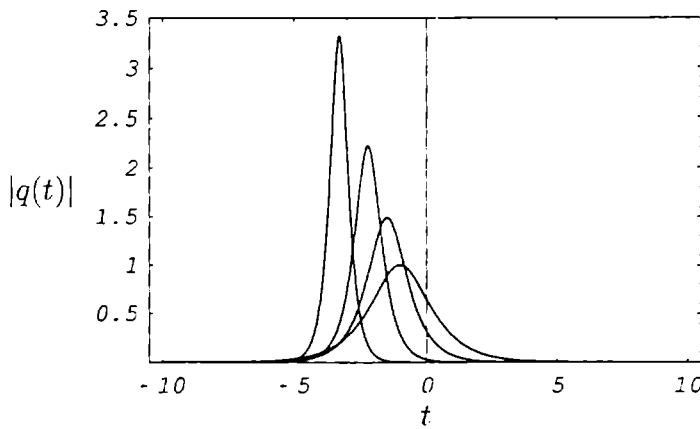
$$q(0, t) = 2\lambda_2(0)\chi \exp \left[ -2i\lambda_1(0)t + \frac{i\alpha_2 t^2}{2} \right] \operatorname{sech} [2\lambda_2(0)t + \theta] \quad (3.5.11)$$

The term  $\alpha_2$  is known as the chirp parameter. From Eq. (3.5.11), it is obvious that input pulse is initially unchirped. By properly choosing the value of chirp parameter, the effect of initial frequency chirping can be effectively used for pulse compression technique eventhough fiber loss is present. For  $\alpha_2 = -1$ , three dimensional and two dimensional evolution of the input pulse described by Eq. (3.5.11) are shown in Figs. 3.1(a) and 3.1(b). From the figure, it is clear that at each stage of propagation, the product of pulse width and pulse amplitude is found to be conserved due to which area occupied by the pulse envelope remains preserved which is an important property of soliton [82].





(a)



(b)

Fig. 3.1: (a) Three dimensional evolution of soliton pulse described by Eq. (3.5.10) (b) Two dimensional nature of the soliton pulse at each stage of propagation

### 3.6 Compression factor

The compression achieved by the input pulse can be described in terms of compression factor. It is defined as the ratio of the FWHM of the soliton pulse at the beginning of the fiber,  $\tau_0$ , to that at the end of the fiber,  $\tau_L$ . The higher the

value of compression factor, the more the pulse compressed. Using Eq. (3.5.10), the pulsewidth  $\tau$  can be defined as

$$\operatorname{sech} [\xi + 2\lambda_2\tau] = \frac{1}{2} \quad (3.6.1)$$

where  $\xi = 8 \int \lambda_1 \lambda_2 dz + \theta$ . Pulsewidth depends on the value of  $\xi$  which merely translates the pulse and doesn't change its width. Now  $t_{peak}$  can be defined as

$$\operatorname{sech} [t_{peak} + \xi] = 1 \quad (3.6.2)$$

Equation (3.6.2) gives  $t_{peak} = -\xi$ . Then  $\tau$  can be defined as

$$\operatorname{sech} [t_{peak} + \xi + 2\lambda_2\tau] = \frac{1}{2} \quad (3.6.3)$$

or

$$\tau = \frac{\operatorname{sech}^{-1} \left( \frac{1}{2} \right)}{2\lambda_2} \quad (3.6.4)$$

The compression factor is then given by

$$C_f = \frac{\lambda_2(L)}{\lambda_2(0)} \quad (3.6.5)$$

Thus the compression achieved initially unchirped pulse can be evaluated using the Eq. (3.6.5) for a given length of fiber.

### 3.7 Conclusion

In this chapter, propagation of initially unchirped pulse with the inclusion of fiber loss have been considered to study the effect of frequency chirping on the soliton formation in the presence of fiber loss. At first, an equation is formulated to describe the propagation of initially unchirped pulses through lossy fiber by Painlevé analysis. Using linear eigen value problem and Bäcklund transformation, soliton solution is generated. By the proper choice of chirp parameter, the effect of frequency chirping has been successfully used to compress the soliton pulse by dominating the effect of fiber loss. Here the important soliton property of area conservation is maintained during each stage of propagation. Compression factor achieved by the pulse has been derived and can be calculated for a given fiber length.

# Chapter 4

## Soliton propagation in a real fiber with amplification and effective phase modulation

### 4.1 Introduction

Soliton formation and the compression achieved by the pulse during propagation in presence of initial frequency chirping have some limitations. The effect of initial frequency chirping appears as a perturbation. Soliton formation is possible for small values of chirp parameter  $\alpha_2$ , and gets disturbed for larger values of  $\alpha_2$ . Only for negative values of chirp parameter, frequency chirping can be effectively used for pulse compression. For positive values, instead of compression, pulse gets broadened. In addition, this method is convenient with sources that inherently produce unchirped pulses. In this chapter, a general method is suggested as a compression technique for completely integrable systems.

## 4.2 Formulation of the problem

The use of inline electro-optic phase modulators is known as a rather simple way to control soliton transmission [82, 83]. Insertion of modulators with properly designed filters result in substantial suppression of the Gordon-Haus timing jitter [82,83]. This is desirable for increasing the transmission capacity of communication systems. Mezentsev and Turtisyn have modelled a system which describes pulse propagation with inline phase-modulators. Pulse propagation through such system is described by modified NLS equation of the form

$$iq_z + q_{tt} + 2 |q|^2 q - \alpha_1(z)t^2 q = 0 \quad (4.2.1)$$

where the term  $\alpha_1(z)t^2 q$  electro-optic phase modulation [82].

Solitons do not face distortion from the Kerr nonlinearity or group dispersion. However the fiber loss contributes to their distortion. A simple solution to this problem is to provide proper measures to compensate for the loss, such as optical amplification. In the presence of phase modulation, fiber loss and amplification, the nonlinear Schrödinger equation that describes pulse propagation is modified to [83]:

$$iq_z + q_{tt} + 2 |q|^2 q = \alpha_1(z)t^2 q + i\alpha_2(z)q \quad (4.2.2)$$

where  $\alpha_2(z) = G(z) + \Gamma$  Here  $\Gamma$  is the normalized fiber loss.  $G(z)$  represents gain of the amplifier, which, in general is a function of the distance  $z$  and is also normalized. The above equation describes the propagation of soliton pulse for the condition (3.3.11) discussed in the previous chapter. It is difficult to study Eq. (4.2.2) in the present form. Introducing a variable transformation:

$$q(z, t) = Q(z, t) \exp\left(-\frac{i\alpha_2 t^2}{2}\right) \quad (4.2.3)$$

and using the condition (3.3.11), Eq. (4.2.2) can be expressed as:

$$iQ_z + Q_{tt} + 2|Q|^2 Q - 2i\alpha_2 t Q_t - 2i\alpha_2 Q = 0 \quad (4.2.4)$$

### 4.3 Linear eigen value problem

The linear eigen value problem associated with Eq. (4.2.4) is:

$$\psi_t = U\psi \quad \psi_z = V\psi \quad \psi = (\psi_1 \ \psi_2)^T \quad (4.3.1)$$

where:

$$U = \begin{pmatrix} -i\gamma & Q \\ -Q^* & i\gamma \end{pmatrix} \quad (4.3.2)$$

$$V = 2i\gamma^2 \begin{pmatrix} -1 & 0 \\ 0 & 1 \end{pmatrix} + 2\gamma \begin{pmatrix} -i\alpha_2 t & Q \\ -Q^* & i\alpha_2 t \end{pmatrix} + i \begin{pmatrix} |Q|^2 & Q_t - 2i\alpha_2 t Q \\ Q_t^* + 2i\alpha_2 t Q^* & -|Q|^2 \end{pmatrix} \quad (4.3.3)$$

where  $\gamma$  is the non-isospectral parameter given by

$$\gamma = \gamma_1 + i\gamma_2 = \gamma_0 \exp\left(2 \int \alpha_2 dz\right) \quad (4.3.4)$$

Now the compatibility relation  $U_z - V_t + [U \ V] = 0$  gives rise to Eq. (4.2.4).

This assures the complete integrability of the Eq. (4.2.4). Now the exact soliton solution can be constructed analytically which is discussed in the next section.

## 4.4 Hirota bilinearization and soliton solution

Hirota's bilinear method [53] is followed to construct soliton solution. For NLS type equations, the transformations used to construct Hirota's bilinear equations have the form:

$$Q = \frac{G(z, t)}{F(z, t)} \quad (4.4.1)$$

where  $G(z, t)$  is a complex function and  $F(z, t)$  is a real function. Using the transformation (4.4.1), Eq. (4.2.4) can be decoupled in the form:

$$[iD_z + D_t^2 - 2i\alpha_2 t D_t - 2i\alpha_2](G.F) = 0 \quad (4.4.2)$$

$$D_t^2(F.F) = 2|G|^2$$

where the Hirota bilinear operators  $D_z$  and  $D_t$  are defined in Eq. (2.6.5). To construct one-soliton solution (1SS),  $F$  and  $G$  takes the form:

$$F = 1 + \eta^2 f_2, \quad G = \eta g_1 \quad (4.4.3)$$

Substituting Eq.(4.4.3) in Eq.(4.4.2) and then collecting coefficients of  $\eta$  and  $\eta^2$ , gives

$\eta$

$$[iD_z + D_t^2 - 2i\alpha_2 t D_t - 2i\alpha_2](g_1.1) = 0 \quad (4.4.4)$$

$\eta^2$

$$D_t^2(1.f_2 + f_2.1) = 2|g_1|^2 \quad (4.4.5)$$

$\eta^3$

$$[iD_z + D_t^2 - 2i\alpha_2 t D_t - 2i\alpha_2](g_1.f_2) = 0 \quad (4.4.6)$$

$\eta^4$ 

$$D_t^2 (f_2 \cdot f_2) = 0 \quad (4.4.7)$$

Equations (4.4.4)-(4.4.7) can be solved by assuming

$$g_1 = 4\beta_2 \exp(\mu) \quad (4.4.8)$$

$$f_2 = \exp(\mu + \mu^*)$$

where

$$\mu = -2i\beta_1 t - 4i \int (\beta_1^2 - \beta_2^2) dz + 2\beta_2 t + 8 \int \beta_1 \beta_2 dz + \mu_0 \quad (4.4.9)$$

with  $\beta_1(z) = \beta_1(0) \exp(2 \int \alpha_2 dz)$  and  $\beta_2(z) = \beta_2(0) \exp(2 \int \alpha_2 dz)$ . Using Eqs. (4.4.9), (4.4.8), (4.4.3) and (4.4.1), after absorbing  $\eta$ , the 1SS of Eq. (4.2.4) can easily be worked out as:

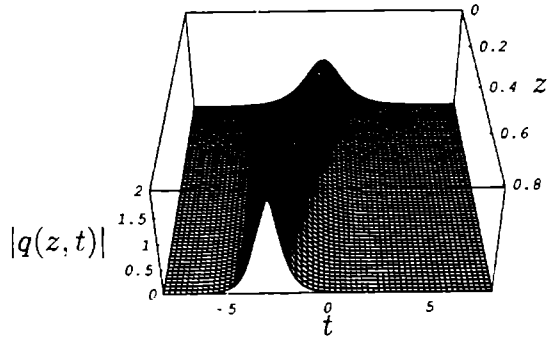
$$Q = 2\beta_2 \exp \left[ -2i\beta_1 t - 4i \int (\beta_1^2 - \beta_2^2) dz \right] \operatorname{sech} \left[ 2\beta_2 t + 8 \int \beta_1 \beta_2 dz + \mu_0 \right] \quad (4.4.10)$$

Using the transformation (4.2.3), the 1SS of Eq. (4.2.2) is obtained as:

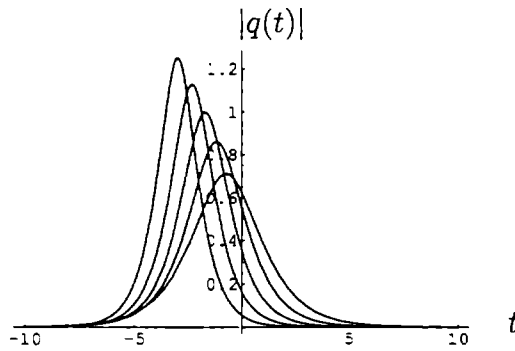
$$q = 2\beta_2 \exp \left[ -2i\beta_1 t - 4i \int (\beta_1^2 - \beta_2^2) dz + \frac{i\beta_2 t^2}{2} \right] \operatorname{sech} \left( 2\beta_2 t + 8 \int \beta_1 \beta_2 dz + \mu_0 \right) \quad (4.4.11)$$

Using the above equation, pulse propagation through lossy with amplification and effective phase modulation can be studied. Figure 4.1 shows the evolution of





(a)



(b)

Fig. 4.1: (a) Three dimensional evolution of the soliton pulse described in Eq. (4.4.12) for  $\beta_1(0) = 1$ ,  $\beta_2(0) = 0.5$ , and  $\alpha_2(z) = z + 0.01$  (b) Two dimensional evolution of soliton pulse.

soliton pulse in such a system. Figure shows that due to the interplay between fiber loss, gain, and phase modulation, pulse gets compressed during the propagation. Here compression is in such a way that area of the pulse is maintained at each stage of propagation [82]. The compression factor achieved by the pulse is given by

$$C_f = \frac{\beta_2(L)}{\beta_2(0)} \quad (4.4.12)$$

## 4.5 Pulse propagation in normal dispersive regime

In the wavelength range shorter than zero-dispersion wavelength  $\gamma_d$ , called normal dispersive regime, the soliton solution given by Eq. (1.5.17) doesn't exist. However, even in this range of wavelength, the portion without light which is produced by chopping a continuous light wave, is known to form a soliton. Such a soliton solution is called dark soliton solution [40, 85]. Recently there is an increased interest in dark solitons because of the possible applications in optical logic devices [86] and waveguide optics as dynamic switches and junctions [87]. They are also considered for signal processing and communication applications because of their inherent stability [88]. In fact, the influence of noise and fibre loss on dark soliton is much lesser than that on bright solitons [89].

The nonlinear Schrödinger equation describing dark solitons is obtained from Eq. (1.4.45) by changing the sign of  $(\beta_2)$  and is given by

$$iq_z - q_{tt} + 2|q|^2 q = 0 \quad (4.5.1)$$

Now proceeding to the case of the normal GVD regime, Eq. (4.2.2) can be written as

$$iq_z - q_{tt} + 2|q|^2 q = \alpha(z)t^2 q + i\alpha_2(z)q \quad (4.5.2)$$

## 4.6 Integrability analysis

System described by the Eq. (4.5.2) support dark solitons only if it is integrable in nature. In the present form, Eq. (4.5.2) will not describe dark soliton propagation. Before proceeding to arrive the integrability condition, a variable

transformation is introduced:

$$q(z, t) = Q(z, t) \exp\left(\frac{i\alpha_2 t^2}{2}\right) \quad (4.6.1)$$

Then Eq. (4.5.2) becomes

$$iQ_z - \frac{\alpha_2 z t^2 Q}{2} - Q_{tt} + 2|Q|^2 Q - 2i\alpha_2 t Q_t - 2i\alpha_2 Q - (\alpha - \alpha_2^2) t^2 Q = 0 \quad (4.6.2)$$

The linear eigen value problem associated with Eq. (4.6.2) is:

$$U = \begin{pmatrix} -\frac{i\gamma}{2} & -iQ \\ iQ^* & \frac{i\gamma}{2} \end{pmatrix} \quad (4.6.3)$$

$$V = \gamma^2 \begin{pmatrix} \frac{i}{2} & 0 \\ 0 & -\frac{i}{2} \end{pmatrix} + \gamma \begin{pmatrix} -i\alpha_2 t & iQ \\ -iQ^* & i\alpha_2 t \end{pmatrix} + \begin{pmatrix} i|Q|^2 & -Q_t - 2i\alpha_2 t Q \\ -Q_t^* + 2i\alpha_2 t Q^* & -i|Q|^2 \end{pmatrix} \quad (4.6.4)$$

where  $\gamma$  has the same meaning. Now the relation  $U_z - V_t + [U, V] = 0$  leads to:

$$iQ_z - Q_{tt} + 2|Q|^2 Q + 2i\alpha_2 t Q_t + 2i\alpha_2 Q = 0 \quad (4.6.5)$$

From Eqs. (4.6.5) and (4.6.2), it is clear that Eq. (4.5.2) admits complete integrability when the condition:

$$\alpha_{2z} = -2(\alpha - \alpha_2^2) \quad (4.6.6)$$

is satisfied.

## 4.7 Dark solitons

Similar to the case of nonlinear Schrödinger equations in the anomalous dispersive regime, Hirota's technique can also be applied to obtain dark soliton solutions. By applying Hirota's bilinear method, Eq. (4.6.5) can be decoupled as:

$$[iD_z - D_t^2 - 2i\alpha_2 t D_t - 2i\alpha_2 + \nu](G.F) = 0 \quad (4.7.1)$$

$$(D_t^2 - \nu)(F.F) = -2|G|^2$$

$\nu$  is a function to be determined.

To construct dark soliton solution, assume:

$$G = g_0(1 + \eta g_1) \quad F = 1 + \eta f_1 \quad (4.7.2)$$

Substituting Eq. (4.7.2) in (4.7.1) and collecting the coefficients of  $\eta^0$

$$[iD_z - D_t^2 - 2i\alpha_2 t D_t - 2i\alpha_2 + \nu](g_0.1) = 0 \quad (4.7.3)$$

$$\nu = 2|g_0|^2$$

Equation (4.7.3) can be solved by assuming:

$$g_0 = 2\alpha_0 \exp \left[ \int (2\alpha_2 + i\nu) dz \right] \quad (4.7.4)$$

where  $\alpha_0$  is a constant. Then

$$\nu = 2|g_0|^2 = 8\alpha^2 = 8\alpha_0^2 \exp[4 \int \alpha_2 z] \quad (4.7.5)$$

Substituting Eq. (4.7.2) in (4.7.1) and on collecting coefficients of  $\eta$  and  $\eta^2$ , gives

$\eta$ :

$$[iD_z + D_t^2 - 2i\alpha_2 t D_t](1.f_1 + g_1.1) = 0 \quad (4.7.6)$$

$$(D_t^2 - \mu)(1.f_1 + f_1.1) = -4g_1 |g_0|^2$$

$\eta^2$

$$[iD_z + D_t^2 - 2i\alpha_2 t D_t](g_1.f_1) = 0 \quad (4.7.7)$$

$$(D_t^2 - \mu)(1.f_1 + f_1.1) = -2g_1 |g_0|^2$$

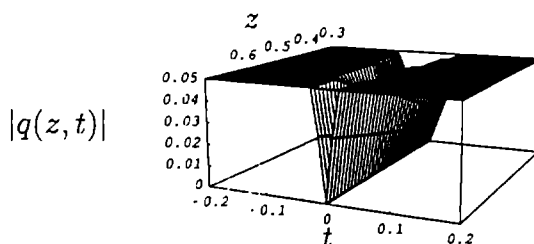
Equations (4.7.6) and (4.7.7) are solved by assuming

$$g_1 = -\exp(4\alpha_2 t + 2\eta_0) \quad f_1 = -g_1 \quad (4.7.8)$$

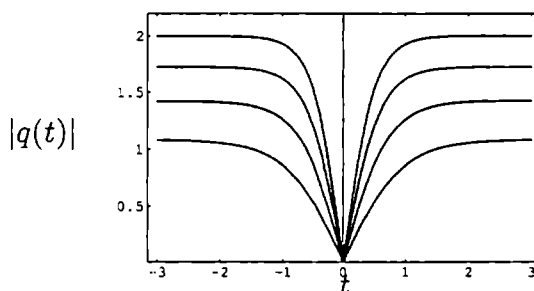
where  $\eta_0$  is a constant. From Eqs. (4.7.8), (4.7.4), (4.7.2), (4.6.1), and (4.4.1), after absorbing  $\eta$ , dark soliton solution of Eq. (4.5.2) is obtained as:

$$q = 2\alpha \exp \left[ i \left( \int 8\alpha^2 dz - \frac{\alpha_2 t^2}{2} \pm \pi \right) \right] \tanh(2\alpha t + \eta_0) \quad (4.7.9)$$

Thus exact dark soliton solution by following the Hirota technique is obtained. Here also, it is observed that the product of the pulse width and pulse amplitude is found to be conserved due to which the area occupied by the pulse envelope remains preserved with the inclusion of loss, gain and phase modulation. This is clearly depicted in Figs. 4.2(a) and 4.2(b). Thus dark soliton pulse also experiences compression.



(a)



(b)

Fig. 4.2: (a) Three dimensional plot of the dark soliton solution (4.3.18) (b) shows the two dimensional plot  $|q(t)|$  for  $z = 0.4, 0.6, 0.8, 1.0$

## 4.8 Conclusion

Modified NLS equations in anomalous and normal dispersive regimes with phase modulation, loss, and amplification are considered. Integrability conditions from AKNS method are arrived in both cases and constructed bright and dark soliton solutions. Solutions of equations (4.2.2) and (4.5.2) explain how the pulse compression can be achieved by keeping soliton property of area conservation when it is transmitted through the fibre with loss, gain and phase modulation.

# Chapter 5

## Propagation of soliton pulse through dispersion-decreasing fiber

### 5.1 Introduction

A novel technique of pulse compression makes use of optical fibers whose dispersion decreases along the direction of propagation [43, 44]. The pulse compression mechanism of dispersion-decreasing fibers (DDFs) has been used to generate train of ultrashort pulses [46, 47, 90-92]. The basic idea consists of injecting a continuous wave (cw) beam with weak sinusoidal modulation imposed on it into an optical fiber exhibiting gain [90]. Since decreasing dispersion is equivalent to an effective gain, such fibers can be used in place of a fiber amplifier [46]. As sinusoidal signal is amplified, individual pulses within each modulation cycle are also compressed. The combined effect of GVD, SPM, and effective gain is to convert a nearly cw signal into a train-of high-quality pulse train of ultrashort solitons [45].

In comparison with other compression techniques, the required DDF length are

significantly shorter and much larger compression factors can be achieved. Very-high-quality pulse compression is possible and input power requirements are significantly lower. Furthermore, the proportion of pedestal energy is significantly less and the compressed output pulse propagates like a fundamental soliton.

## 5.2 Mathematical formulation of the problem

The concept of dispersion-decreasing fiber can be established mathematically by using the NLS Eq. (1.5.3). Pulse propagation through dispersion-decreasing fiber can be studied by using the equation [45, 93]:

$$iq_z + \beta_1(z) q_{tt} + 2\beta_2(z) |q|^2 q = 0 \quad (5.2.1)$$

where  $q$  represents the normalized envelope amplitude,  $\beta_1(z)$  governs dispersion variation along the fibre,  $\beta_2(z)$  is the nonlinear parameter which also varies with distance along the direction of propagation. The above equation is also known as nonuniform NLS equation.

By making the following transformations:

$$q(z, t) = Q(\eta, t) \sqrt{\beta_1/\beta_2} \quad (5.2.2)$$

$$\eta = \int_0^z \beta_1(z') dz'$$

Equation (5.2.1) is reduced to:

$$iQ_\eta + Q_{tt} + 2Q|Q|^2 - i\alpha(\eta)Q = 0 \quad (5.2.3)$$



where:

$$\alpha(\eta) = -\sqrt{\frac{\beta_2}{\beta_1}} \frac{d}{d\eta} \left( \sqrt{\frac{\beta_1}{\beta_2}} \right) \quad (5.2.4)$$

is the effective gain coefficient. Equation (5.2.3) shows that the effect of nonuniform parameters is mathematically equivalent to adding a gain term to the NLS equation. Thus the problem of nonlinear light propagation through the fiber with nonuniform parameters is reduced to the case of uniform fiber with an amplification. Equation (5.2.3) shows that the effect of nonuniform parameters is mathematically equivalent to adding a gain term to the NLS equation and which can be used to discuss pulse compression [44].

### 5.3 Singularity analysis and soliton solution

Equation (5.2.3) in the present form will not give describe soliton propagation. To find the condition under which Eq. (5.2.3) produces soliton solution, singularity analysis is carried out along the lines of Weiss *et al* with simplification due to Kruskal and involves seeking a solution of given partial differential equation in the form

$$Q(\eta, t) = \phi^\delta \sum_{j=0}^{\infty} Q_j(t) \phi^j(\eta, t), Q_0 \neq 0 \quad (5.3.1)$$

with

$$\phi(\eta, t) = t + \psi(\eta) \quad (5.3.2)$$

where  $\psi(\eta)$  is an arbitrary analytic function of  $\eta$ ,  $Q_j(t)$  ( $j = 0, 1, 2, \dots$ ), in the

neighborhood of a non-characteristic movable singularity manifold defined by  $\phi = 0$ .

To investigate the integrability properties of Eq. (5.2.3), it is rewritten in terms of two complex functions  $a$  and  $b$  by defining  $Q = a$ ,  $Q^* = b$ .

$$ia_\eta + a_{tt} + 2a^2b - i\alpha a = 0 \tag{5.3.3}$$

$$-ib_\eta + b_{tt} + 2ab^2 + i\alpha b = 0$$

where  $a_0, b_0 \neq 0$ ,  $\delta$  is a negative integer and  $a_j$  and  $b_j$  are a set of expansion coefficients analytic in the neighborhood of the non-characteristic singular manifold defined by  $\phi(\eta, t) = 0$ . Looking at the leading order behavior, substitute  $a \simeq a_0\phi^{\delta_1}$ ,  $b \simeq b_0\phi^{\delta_2}$  in Eq. (5.3.3) and balancing the dominant terms, gives:

$$\delta_1 = \delta_2 = -1, \tag{5.3.4}$$

$$a_0b_0 = -1.$$

For finding the powers at which the arbitrary functions can enter into the series, substitute the expressions:

$$a \simeq a_0\phi^{-1} + a_j\phi^{j-1} \tag{5.3.5}$$

$$b \simeq b_0\phi^{-1} + b_j\phi^{j-1}$$

in Eq. (5.3.3) and comparing the lowest-order terms, a system of two linear algebraic equations in  $(a_j, b_j)$  is obtained. In matrix form, it may be conveniently written as

$$[A(j)][X] = 0 \tag{5.3.6}$$

where

$$[X] = (a_j, b_j)^T, \quad (5.3.7)$$

and

$$[A(j)] = \begin{pmatrix} (j-1)(j-2) - 4 & 2a_0^2 \\ 2b_0^2 & (j-1)(j-2) - 4 \end{pmatrix} \quad (5.3.8)$$

To have a nontrivial solution for  $a_j$  and  $b_j$ , Eq. (5.3.8) must satisfy the condition:

$$|A(j)| = 0 \quad (5.3.9)$$

On solving Eq. (5.3.9), the resonance values obtained are  $j = -1, 0, 3, 4$ . The resonance at  $j = -1$  corresponds to the arbitrariness of the singular manifold  $\phi(\eta, t)$ . The resonance at  $j = 0$  corresponds to the fact that any one of the two functions  $a_0$  or  $b_0$  is arbitrary as seen in Eq. (5.3.4). From the coefficients of  $(\phi^0, \phi^0)$  and  $(\phi^1, \phi^1)$ , it is clear that Eq. (5.3.3) admits sufficient number of arbitrary functions which correspond to  $j = 3$  and  $j = 4$  respectively provided  $\alpha(\eta)$  must satisfy the condition:

$$\alpha(\eta) = -\frac{1}{2(\eta + \eta_0)} \quad (5.3.10)$$

where  $\eta_0$  is an arbitrary integration constant. Using Eqs. (5.2.4) and (5.3.10), the integrability condition can be redefined as

$$\frac{\beta_1}{\beta_2} = c^2 (\eta + \eta_0) \quad (5.3.11)$$

where  $c$  is the constant of integration. Again introduce a new variable transformation:

$$Q(\eta, t) = \frac{-1}{(\eta + \eta_0)} U(Z, T) \exp\left(\frac{it^2}{4(\eta + \eta_0)}\right) \quad (5.3.12)$$

$$Z = \frac{-1}{(\eta + \eta_0)}, \quad T = \frac{-t}{(\eta + \eta_0)}$$

which transform Eq. (5.2.3) to NLSE for the condition (5.3.10)

$$iU_Z + U_{TT} + 2U|U|^2 = 0 \quad (5.3.13)$$

Using the exact soliton solution of the Eq. (5.3.13) [71]:

$$U = 2k_2\chi_1 \exp(-4i(k_1^2 - k_2^2)Z - 2ik_1T) \operatorname{sech}[\theta + 8k_1k_2Z + 2k_2T], \quad (5.3.14)$$

where  $\theta$  is the phase factor,  $k_1$ ,  $k_2$ , and  $\chi_1$  are arbitrary constants, the fundamental soliton solution of the Eq. (5.2.1) can be calculated as:

$$q(z, t) = 2\lambda_2\chi_1 \sqrt{\frac{\beta_1}{\beta_2}} \exp(-i\sigma) \operatorname{sech}\left[\theta + 8 \int \lambda_1\lambda_2 d\eta + 2\lambda_2 t\right] \quad (5.3.15)$$

where  $\sigma = \frac{-\alpha t^2}{2} + 4 \int (\lambda_1^2 - \lambda_2^2) d\eta + 2\lambda_1 t$ ,  $\lambda_1 = k_1 \exp[2 \int \alpha d\eta]$ , and  $\lambda_2 = k_2 \exp[2 \int \alpha d\eta]$ .

Equation (5.3.15) is the exact soliton solution of the Eq. (5.2.1) which can be used to analyze the pulse propagation through the fiber with variable dispersion.

## 5.4 Analysis of pulse propagation through different profiles

Here we study the propagation of soliton pulse described by Eq. (5.3.15) through different dispersion decreasing fibers. The profiles considered are linear, hyperbolic, exponential, logarithmic, and Gaussian. These profiles can be expressed in

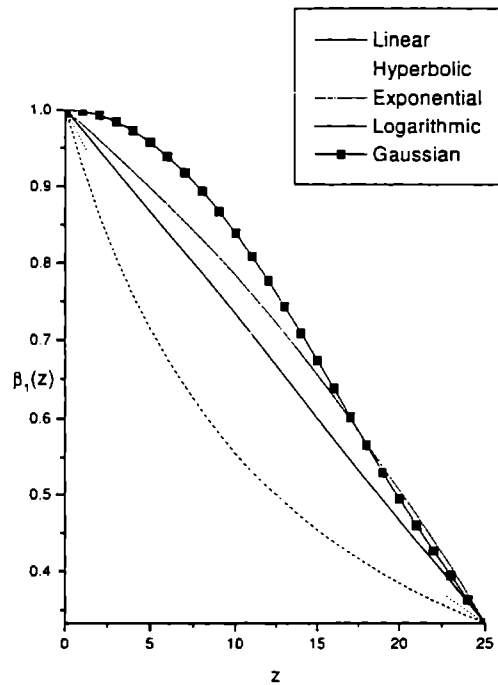


Fig. 5.1: Schematics of dispersion profiles

terms of the parameters  $1/\beta$  ( value of  $\beta_1$  at  $z = L$ ) and length of the fibre  $L$  are

$$\begin{aligned}
 \text{Linear} \quad \beta_1(z) &= \left(\frac{1-\beta}{\beta L}\right)z + 1 \\
 \text{Hyperbolic} \quad \beta_1(z) &= \frac{L}{(\beta-1)z+L} \\
 \text{Exponential} \quad \beta_1(z) &= \exp\left(-\frac{\ln\beta}{L}z\right) \\
 \text{Logarithmic} \quad \beta_1(z) &= \ln\left(e + \frac{z}{L}(e^{1/\beta} - e)\right) \\
 \text{Gaussian} \quad \beta_1(z) &= \exp\left(-\frac{\ln\beta}{L^2}z^2\right)
 \end{aligned} \tag{5.4.1}$$

By using Eq. (5.3.11), the nature of nonlinear coefficient,  $\beta_2(z)$ , corresponding to each profile given in Eq. (5.4.1) can be determined. In these normalized profiles, dispersion coefficient  $\beta_1(z)$  monotonically decreases from an initial value,  $\beta_1(0) = 1$ , to a final value of  $1/\beta$  after a length  $L$  of DDF. The ratio of dispersion  $\beta_1(0)/\beta_1(L)$  is defined as  $\beta$ . These dispersion profiles are illustrated in Fig. (5.1).

By keeping the value of  $\beta = 3$  and fiber length  $L = 25$  unit, we study the soliton pulse propagation through fiber with various dispersion decreasing profiles described in equation (5.4.1). Figures (5.2-5.6) show the pulse amplitude of soliton pulse through different profiles at various distances  $z = 18, 21$  and  $25$ .

Pulse propagation through various profiles show that as the fiber length increases, pulse gets compressed adiabatically by conserving the soliton area i.e. the product of pulse amplitude and pulse width is maintained at each stage of propagation along the fiber, which is an important property of soliton [81]. Analysis also shows that compressed pulses are completely free from the pedestals

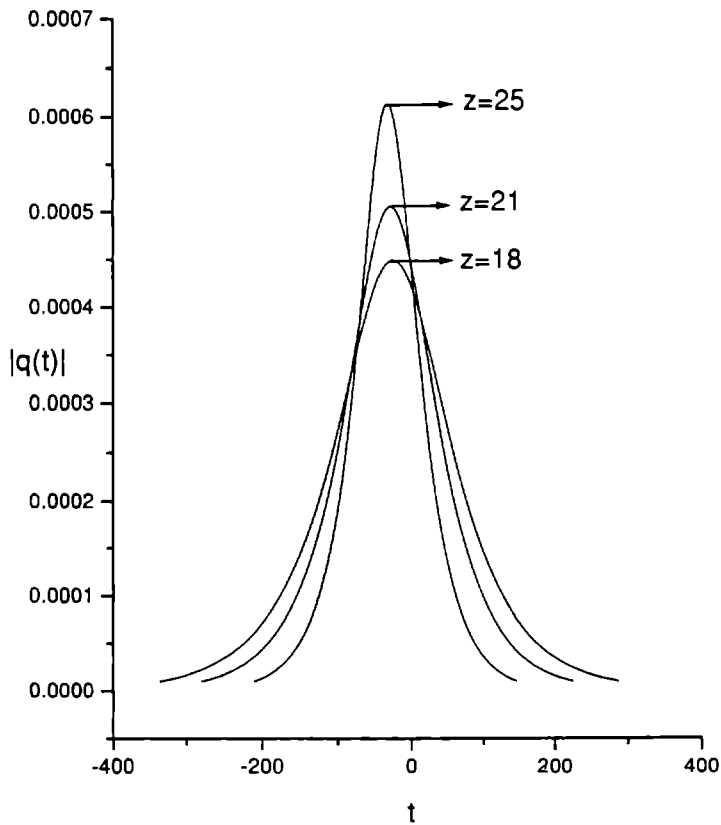


Fig. 5.2: Shows the nature of the pulse through linear profile at various distances

which makes the compressed pulse in the fiber highly stable. Since we are discussing the pulse propagation in an ideal lossless fibre, soliton energy also gets conserved. Pulse amplitude through different profiles at  $z = 25$  is compared and is shown in Fig. 5.7. From the figure, it is clear that pulse gets compressed to its maximum value and obtained maximum amplitude when it is propagated through fiber whose dispersion decreases in the Gaussian form.

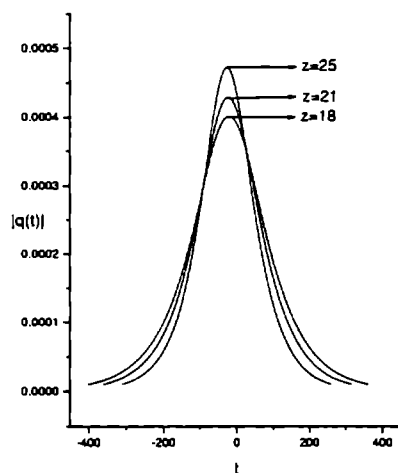


Fig. 5.3: Shows the nature of the pulse through hyperbolic profile at various distances

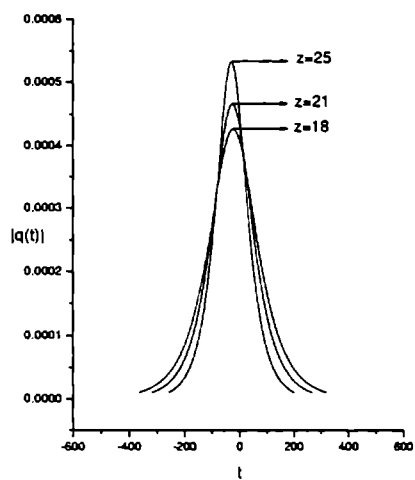


Fig. 5.4: Shows the nature of the pulse through exponential profile at various distances



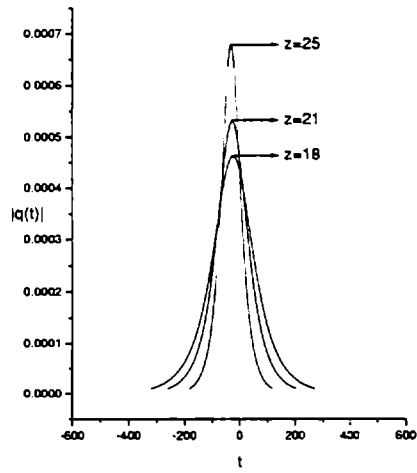


Fig. 5.5: Shows the nature of the pulse through logarithmic profile at various distances

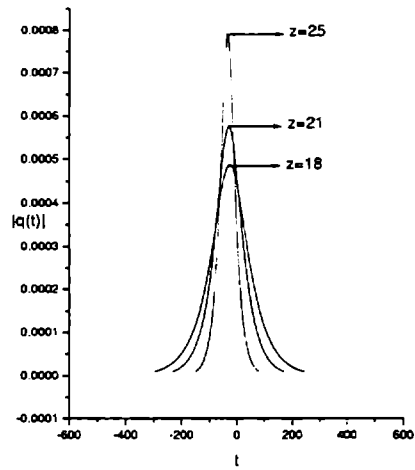


Fig. 5.6: Shows the nature of the pulse through Gaussian profile at various distances

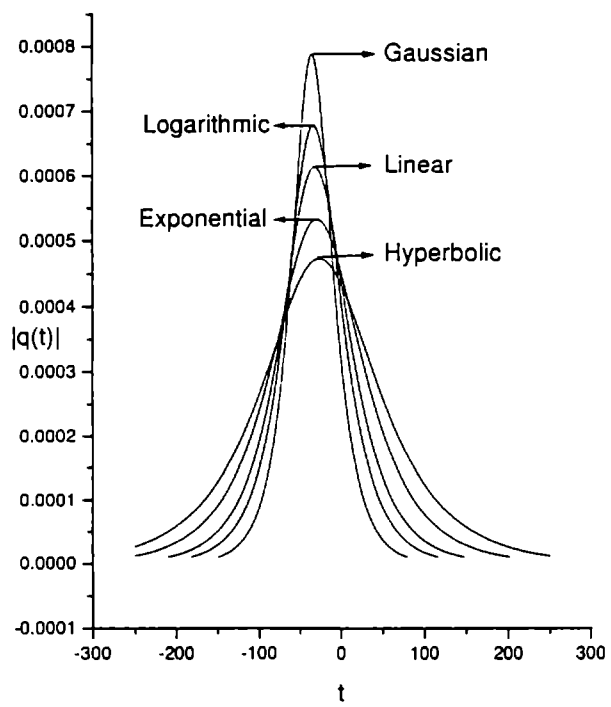


Fig. 5.7: Shows the comparison of the nature of the pulse through five different profiles at  $z = 25$

## 5.5 Compression factor

Soliton compression factor,  $C_f$ , achieved by the DDF can be defined as the ratio of the FWHM of the soliton pulse at the beginning of the DDF,  $\tau_0$ , to that at the end of the DDF,  $\tau_L$ . It is given by

$$C_f = \frac{\tau_0}{\tau_L} = \frac{\lambda_2(L)}{\lambda_2(0)} \quad (5.5.1)$$

Since the value of pulse width is constant at the beginning of each dispersion decreasing fiber, the value of the compression factor at the fiber length  $L$  in each profile can be compared. Table 5.1 shows the comparison of compression factor after the fiber length  $L = 25$ .

Nature of profiles	$C_f$
Linear	4.8
Hyperbolic	2.847
Exponential	3.616
Logarithmic	5.87
Gaussian	7.913

Table 5.1

Analytical calculations also show that pulse gets compressed to its maximum value when it is propagated through fiber with dispersion varies in the Gaussian form. Using Eq. (5.5.1), the variation of compression factor with fiber length through each profile can be studied. The variations are illustrated in Fig. (5.8) for a fiber length  $L = 25$ .

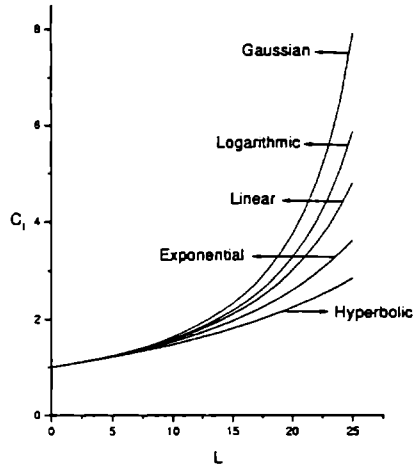


Fig. 5.8: Comparison in the variation of compression factor

## 5.6 Pulse propagation through birefringent DDF

In the previous sections, the propagation of single mode through DDF has been considered. But when the degenerate modes exist, interaction of degenerate modes can be described by a system of nonuniform coupled nonlinear Schrödinger equations (CNLS) of the form [94]:

$$iq_{1z} + \beta_1(z) q_{1tt} + 2\beta_2(z) (|q_1|^2 + |q_2|^2) q_1 = 0 \quad (5.6.1)$$

$$iq_{2z} + \beta_1(z) q_{2tt} + 2\beta_2(z) (|q_1|^2 + |q_2|^2) q_2 = 0$$

where  $q_1$  and  $q_2$  are the normalized modes,  $\beta_1(z)$  and  $\beta_2(z)$  are the normalized second-order dispersion coefficient and nonlinear coefficient and  $z$  and  $t$  are the normalized distance and time respectively.

By the following transformations:

$$q_1(z, t) = Q_1(\eta, t) \sqrt{\beta_1/\beta_2} \quad q_2(z, t) = Q_2(\eta, t) \sqrt{\beta_1/\beta_2} \quad (5.6.2)$$

$$\eta = \int_0^z \beta_1(z') dz'$$

Equation (5.6.1) is reduced to

$$iQ_{1\eta} + Q_{1tt} + 2Q_1(|Q_1|^2 + |Q_2|^2) - i\alpha(\eta)Q_1 = 0 \quad (5.6.3)$$

$$iQ_{2\eta} + Q_{2tt} + 2Q_2(|Q_1|^2 + |Q_2|^2) - i\alpha(\eta)Q_2 = 0$$

where

$$\alpha(\eta) = -\sqrt{\frac{\beta_2}{\beta_1}} \frac{d}{d\eta} \left( \sqrt{\frac{\beta_1}{\beta_2}} \right) \quad (5.6.4)$$

Integrability condition of Eq. (5.6.3) is:

$$\alpha(\eta) = -\frac{1}{2(\eta + \eta_0)} \quad (5.6.5)$$

where  $\eta_0$  is an arbitrary integration constant. From Eqs. (5.6.4) and (5.6.5), the integrability condition can be redefined as:

$$\sqrt{\frac{\beta_2}{\beta_1}} \frac{d}{d\eta} \left( \sqrt{\frac{\beta_1}{\beta_2}} \right) = \frac{1}{2(\eta + \eta_0)} \quad (5.6.6)$$

Using the variable transformation

$$\begin{aligned} Q_1(\eta, t) &= \frac{-1}{(\eta+\eta_0)} U_1(Z, T) \exp\left(\frac{it^2}{4(\eta+\eta_0)}\right) \\ Q_2(\eta, t) &= \frac{-1}{(\eta+\eta_0)} U_2(Z, T) \exp\left(\frac{it^2}{4(\eta+\eta_0)}\right) \end{aligned} \quad (5.6.7)$$

$$Z = \frac{-1}{(\eta+\eta_0)} \quad T = \frac{-t}{(\eta+\eta_0)}$$

Equation (5.6.3) can be transformed to the well-known CNLSE.

$$iU_{1Z} + U_{1TT} + 2U_1(|U_1|^2 + |U_2|^2) = 0 \quad (5.6.8)$$

$$iU_{2Z} + U_{2TT} + 2U_2(|U_1|^2 + |U_2|^2) = 0$$

Exact soliton solution of Eq. (5.6.8) is

$$U_1 = 2k_2\chi_1 \exp(-4i(k_1^2 - k_2^2)Z - 2ik_1T) \operatorname{sech}[8k_1k_2Z + 2k_2t + \theta] \quad (5.6.9)$$

$$U_2 = 2k_2\chi_2 \exp(-4i(k_1^2 - k_2^2)Z - 2ik_1T) \operatorname{sech}[8k_1k_2Z + 2k_2t + \theta]$$

where  $k_1$ ,  $k_2$ ,  $\chi_1$  and  $\chi_2$  are arbitrary real constants  $\theta$  is the phase factor. By using Eqs. (5.6.7) and (5.6.2), the fundamental soliton solution of Eq. (5.6.1) is obtained as

$$q_1(z, t) = 2\lambda_2\chi_1 \sqrt{\frac{\beta_1}{\beta_2}} \exp(-i\sigma) \operatorname{sech}[8 \int \lambda_1\lambda_2 d\eta + 2\lambda_2t + \theta] \quad (5.6.10)$$

$$q_2(z, t) = 2\lambda_2\chi_2 \sqrt{\frac{\beta_1}{\beta_2}} \exp(-i\sigma) \operatorname{sech}[8 \int \lambda_1\lambda_2 d\eta + 2\lambda_2t + \theta]$$

where  $\lambda_1$ ,  $\lambda_2$ , and  $\sigma$  are defined in Sec. 5.4 and  $\theta$  is the phase factor. Above

soliton solutions help to study the pulse propagation through birefringent single mode fiber with various dispersion profiles.

From Eq. (5.6.10), input pulse launched at the fiber (at the input,  $z = 0$  and  $\beta_1(z) = 1$ ) is given by

$$q(0, t) = \frac{2k_2}{\sqrt{\eta_0}} \chi_1 \exp\left(-\frac{it^2}{2\eta_0} - \frac{2ik_1 t}{\eta_0}\right) \operatorname{sech}\left[\theta + \frac{2k_2 t}{\eta_0}\right] \quad (5.6.11)$$

$$q(0, t) = \frac{2k_2}{\sqrt{\eta_0}} \chi_2 \exp\left(-\frac{it^2}{2\eta_0} - \frac{2ik_1 t}{\eta_0}\right) \operatorname{sech}\left[\theta + \frac{2k_2 t}{\eta_0}\right]$$

## 5.7 Adiabatic soliton pulse compression in DDF with various dispersion profiles

For a given value of fiber length, pulse compression achieved by input soliton pulse through various dispersion-decreasing profiles, described in Eq. (5.4.1), can be studied by substituting Eq. (5.6.10) in Eq. (5.4.1). Keeping the ratio of dispersion  $\beta = 3$  and fiber length  $L = 25$ , pulse propagation through different profiles at various distances ( $z = 18$  and  $25$ ) are shown in Figs. 5.9-5.13.

In all cases, it is obvious that as the pulse propagates, pulse amplitude increases whereas pulse gets compressed. It is also clear from the solution that pulse amplitude increases in the exponential form while pulse width decreases exponentially. Thus the important soliton property of conservation of pulse area is maintained during propagation in the fiber.

Figure 5.14 shows the comparison of the pulse after a given distance, say  $z = 25$ , through five different dispersion-decreasing profiles. Comparison shows that pulse gets compressed to its maximum value when it is propagated through the fiber whose dispersion varies in the Gaussian form. Therefore, in an ideal birefringent

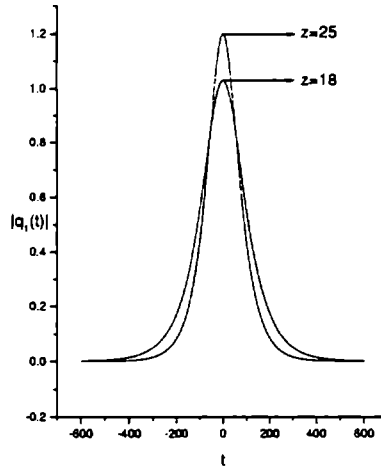


Fig. 5.9: Shows the nature of the pulse through linear profile at various distances

DDF, Gaussian profile is found to be the optimum dispersion profile for achieving maximum pulse compression in the integrable limit. The coupled solution  $q_2(z, t)$ , also gives the same result.

Here also, an interesting phenomena can be observed that compressed pulses are completely free from pedestals. This makes the pulse in the fiber highly stable as the presence of pedestals not only leads to a deterioration in the quality of pulse and energy characteristics of the compression, but it also makes the compressed pulse unstable due to the nonlinear interaction of the pedestal with the compressed pulse.

Compression factor,  $C_f$ , achieved by the birefringent DDF is given by

$$C_f = \frac{\lambda_2(L)}{\lambda_2(0)} \quad (5.7.1)$$

Table 5.2 shows the comparison of compression factor over a fiber length  $L = 25$ .



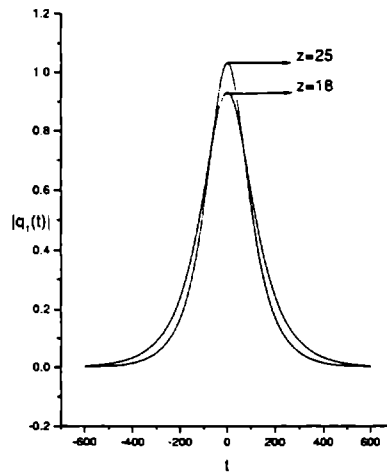


Fig. 5.10: Shows the nature of the pulse through hyperbolic profile at various distances

Nature of profiles	$C_f$
Linear	3.0
Hyperbolic	2.219
Exponential	2.543
Logarithmic	3.372
Gaussian	3.685

Table 5.2

Thus, analytical calculations also show that maximum value of compression is obtained when pulse is propagated through the fiber with dispersion varies in the Gaussian form. In the uncoupled situation also, it was found that Gaussian profile is the optimum profile for achieving maximum pulse compression. Variations in the compression factor for a given value of fiber length ( $L = 25$ ) are illustrated in Fig. 5.15.

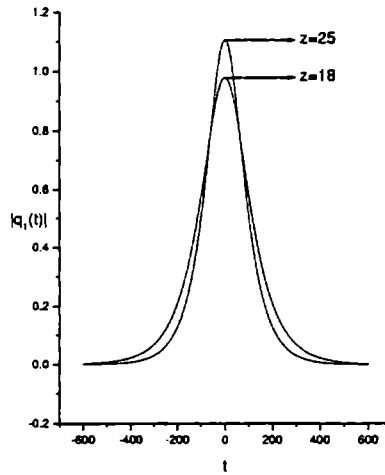


Fig. 5.11: Shows the nature of the pulse through exponential profile at various distances

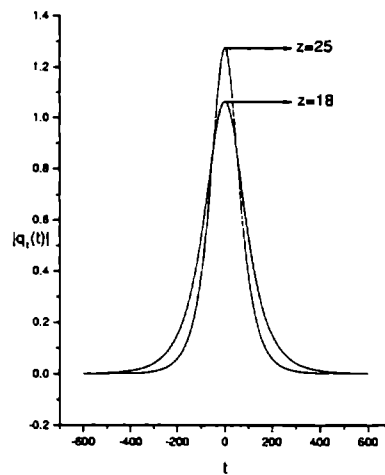


Fig. 5.12: Shows the nature of the pulse through logarithmic profile at various distances

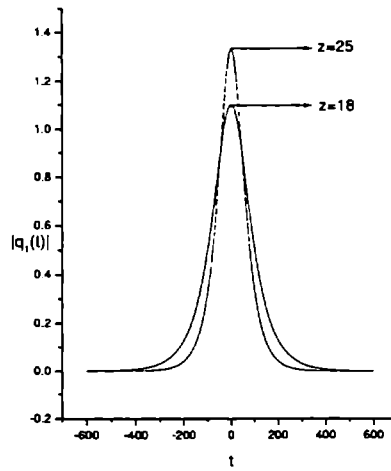


Fig. 5.13: Shows the nature of the pulse through Gaussian profile at various distances

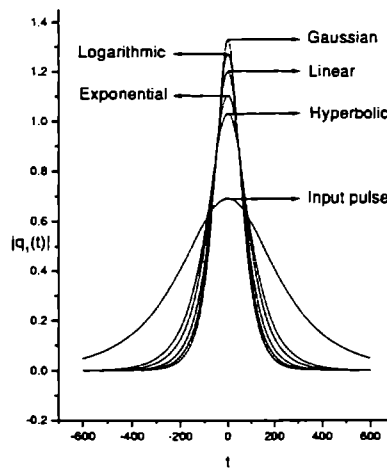


Fig. 5.14: Shows the comparison of the nature of the pulse through five different profiles at  $z = 25$

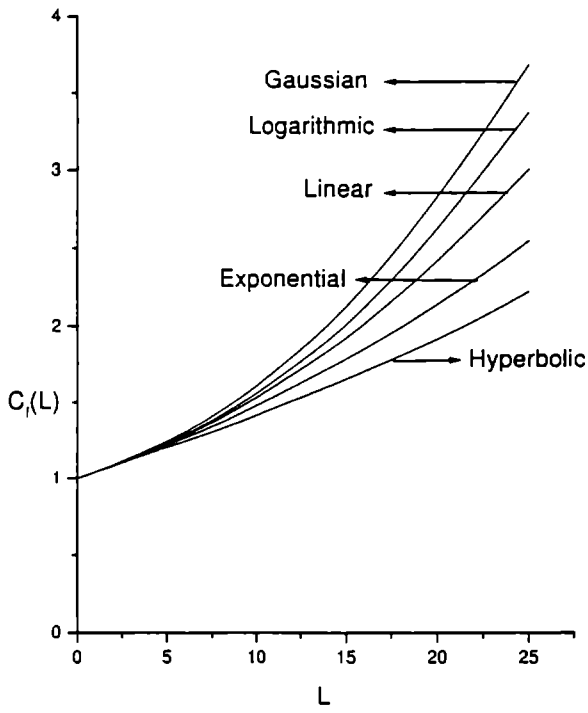


Fig. 5.15: Comparison in the variation of compression factor

## 5.8 Conclusion

In this chapter, propagation of both single mode and degenerative modes through fiber with variable dispersion has been studied. Pulse propagation through the fiber with variable dispersion is described by nonuniform NLS equation. Integrability condition of the nonuniform NLS equation is obtained using singularity structure analysis. By making the suitable transformations, nonuniform NLS equation can be transformed to the well-known NLS equation in the integrable limit. From the known soliton solution of uniform NLS equation, the fundamental soliton solution of nonuniform NLS equation has been obtained.

Effect of various dispersion-decreasing profiles, namely linear, hyperbolic, exponential, logarithmic, and Gaussian on soliton pulse propagation has been analyzed both graphically and analytically. Graphical analysis show that as pulse propagates through various dispersion decreasing profiles, pulse amplitude gets increased and pulse gets compressed adiabatically in each case by conserving the soliton property of area conservation. Out of the five different profiles considered, Gaussian profile is found to be the optimum dispersion profile for achieving maximum soliton pulse compression in the integrable limit in both cases. Theoretical evaluation of compression factor also show that maximum value of compression is obtained when pulse is propagated through the fiber with dispersion varies in the Gaussian form. Furthermore, it is also noted an important feature that compressed pulses are completely free from pedestals in each case. This improves the quality of compressed pulse and also makes the pulse highly stable which helps the compressed pulse in the application of ultra-high-bit rate optical communication systems.

# Chapter 6

## Soliton propagation through dispersion-decreasing fiber with fiber loss

### 6.1 Introduction

In the previous chapter, the propagation of soliton pulses through optical fiber with variable dispersion under ideal conditions had been discussed. However, in a real fiber, the light wave propagates with finite loss. In this chapter, the condition needed for an optical pulse to become a soliton pulse in a lossy dispersion-decreasing fiber is discussed.

### 6.2 Basic equation

Mathematically, the pulse propagation through DDF with the inclusion of fiber loss is accounted for by adding a loss term to Eq. (5.2.1) so that it takes the form [95]:

$$iq_z + \beta_1(z) q_{tt} + 2\beta_2(z) |q|^2 q + i\Gamma q = 0 \quad (6.2.1)$$

where  $\Gamma$  is the normalized fiber loss. Equation (6.2.1) in the present form is difficult for the integrability analysis. Using the transformation:

$$q(z, t) = Q(\eta, t) \sqrt{\beta_1/\beta_2} \quad (6.2.2)$$

$$\eta = \int_0^z \beta_1(z') dz',$$

Eq. (6.2.1) can be transformed to a simple form:

$$iQ_\eta + Q_{tt} + 2Q|Q|^2 - i\alpha(\eta)Q = 0 \quad (6.2.3)$$

where

$$\alpha(\eta) = -\sqrt{\frac{\beta_2}{\beta_1}} \frac{d}{d\eta} \left( \sqrt{\frac{\beta_1}{\beta_2}} \right) - \frac{\Gamma}{\beta_1} \quad (6.2.4)$$

Now it is convenient to find the integrability condition of Eq. (6.2.3). Here, an alternative method of linear eigen value problem is applied to determine the condition needed for an optical pulse to become a soliton pulse.

### 6.3 Linear eigenvalue problem and soliton solution

The Lax pair assures the complete integrability of a nonlinear system and is especially used to obtain integrability condition and N-soliton solution by means of inverse scattering transform (IST) method. The linear eigen value problem associated with Eq. (6.2.3) is

$$\psi_t = U\psi, \quad \psi_\eta = V\psi, \quad \psi = (\psi_1 \ \psi_2)^T \tag{6.3.1}$$

where

$$U = \begin{pmatrix} -i\lambda & u \\ -u^* & i\lambda \end{pmatrix} \tag{6.3.2}$$

$$V = 2i\lambda^2 \begin{pmatrix} -1 & 0 \\ 0 & 1 \end{pmatrix} + 2\lambda \begin{pmatrix} i\alpha t & u \\ -u^* & -i\alpha t \end{pmatrix} \tag{6.3.3}$$

$$+ i \begin{pmatrix} |u|^2 & u_t + 2i\alpha t u \\ u_t^* - 2i\alpha t u^* & -|u|^2 \end{pmatrix}$$

with

$$u = Q \exp\left(-\frac{i\alpha t^2}{2}\right) \tag{6.3.4}$$

The form of the non-isospectral parameter  $\lambda$  is

$$\lambda = \lambda_0 \exp\left(2 \int \alpha d\eta\right) \tag{6.3.5}$$

The compatibility condition, viz,  $U_\eta - V_t + [UV] = 0$ , gives rise to Eq. (6.2.3) provided

$$\alpha(\eta) = -\frac{1}{2(\eta + \eta_0)} \tag{6.3.6}$$

where  $\eta_0$  is an arbitrary constant. The condition (6.3.6) is known as the integrability condition of Eq. (6.2.3). From Eqs. (6.2.4) and (6.3.6), the condition can





be redefined as

$$\sqrt{\frac{\beta_2}{\beta_1}} \frac{d}{d\eta} \left( \sqrt{\frac{\beta_1}{\beta_2}} \right) + \frac{\Gamma}{\beta_1} = \frac{1}{2(\eta + \eta_0)} \quad (6.3.7)$$

By using another variable transformation of the form:

$$Q(\eta, t) = \frac{-1}{(\eta + \eta_0)} U(Z, T) \exp\left(\frac{it^2}{4(\eta + \eta_0)}\right) \quad (6.3.8)$$

$$Z = \frac{-1}{(\eta + \eta_0)} \quad T = \frac{-t}{(\eta + \eta_0)}$$

Eq. (6.2.3) can be transformed to the well-known NLSE:

$$iU_Z + U_{TT} + 2U|U|^2 = 0 \quad (6.3.9)$$

Exact soliton solution of the Eq. (6.3.9) is known and is given by [71]

$$U = 2k_2\chi_1 \exp\left(\frac{i\alpha t^2}{2} - 4i(k_1^2 - k_2^2)Z - 2ik_1T\right) \operatorname{sech}[\theta + 8k_1k_2Z + 2k_2t] \quad (6.3.10)$$

where  $\theta$  is the phase factor, and  $k_1$ ,  $k_2$ , and  $\chi_1$  are arbitrary constants. On substituting Eq. (6.3.10) in Eqs. (6.3.8) and (6.2.2), the fundamental soliton solution of Eq. (6.2.1) is obtained as

$$q(z, t) = 2\lambda_2\chi_1 \sqrt{\frac{\beta_1}{\beta_2}} \exp(-i\sigma) \operatorname{sech}\left[\theta + 8 \int \lambda_1\lambda_2 d\eta + 2\lambda_2t\right] \quad (6.3.11)$$

where  $\sigma = \frac{-\alpha t^2}{2} + 4 \int (\lambda_1^2 - \lambda_2^2) d\eta + 2\lambda_1t$ ,  $\lambda_1 = k_1 \exp[2 \int \alpha d\eta]$ , and  $\lambda_2 = k_2 \exp[2 \int \alpha d\eta]$ .

Equation (6.3.11) is an exact soliton solution describing the pulse propagation through the variable dispersion fibre with loss. From Eq. (6.3.11), initial pulse at the input core (at the input,  $z = 0$ ,  $\beta_1(z) = 0$ , and  $\Gamma = 0$ ) is given by

$$q(0, t) = \frac{2k_2}{\sqrt{\eta_0}} \exp\left(-\frac{it^2}{2\eta_0} - \frac{2ik_1t}{\eta_0}\right) \operatorname{sech}\left[\theta + \frac{2k_2t}{\eta_0}\right] \quad (6.3.12)$$

## 6.4 Soliton pulse propagation through various profiles

The dispersion-decreasing profiles considered are described in Eq. (5.4.1). On solving Eq. (6.3.7),  $\beta_2$  is obtained as

$$\beta_2(z) = \frac{\beta_1}{(\eta + \eta_0)} \exp(2\Gamma z) \quad (6.4.1)$$

From Eq. (6.4.1), the nonlinear coefficient  $\beta_2(z)$  can be determined corresponding to each dispersion profile,  $\beta_1(z)$ . Using Eqs. (5.4.1), (6.3.11) and (6.4.1), the effect of fiber loss when input pulse, described by Eq. (6.3.12), propagates through various profiles can be studied.

### 6.4.1 Critical fiber loss

Keeping the value of  $\beta = 3$  and fiber length  $L = 25$ , nature of the pulse through linear profile at  $z = 18$  and  $25$  for different values of fiber loss are shown in Fig. 6.1 (a-c). Figure 6.1 (b) shows the nature of the pulse propagation for  $\Gamma = 0.021879$ . For this value, it is clear that amplitude remains constant as it propagates where as pulse gets compressed.

It is interesting to note that at this value, the important soliton property of conservation of pulse area is not maintained during propagation and is considered as the critical value of fiber loss represented by  $\Gamma_c$ . It is also clear from Fig. 6.1 (b)

that when the loss exceeds  $\Gamma_c$ , pulse area is not maintained during propagation whereas from Fig. 6.1 (c), it is obvious that area of the pulse gets maintained when the loss is less than the critical value.

Figures 6.2(a-c), 6.3(a-c), 6.4(a-c), 6.5(a-c) show the variation in the amplitude and pulse width of soliton pulse through hyperbolic, exponential, logarithmic and Gaussian profiles respectively for different values of  $\Gamma$ . From these graphs, it is clear that pulse gets compressed adiabatically by conserving the soliton property of the wave profile only when fiber loss is less than the critical value and gets violated when the loss is greater than or equal to critical value  $\Gamma_c$ . It is also noted that critical value of loss is different for different dispersion profiles and are given in table 6.1.

Nature of profile	$\Gamma_c$
Linear	0.021879
Hyperbolic	0.0147418
Exponential	0.0175173
Logarithmic	0.0255561
Gaussian	0.0270237

Table 6.1

#### 6.4.2 Compression factor

Figure 6.6 shows the nature of soliton pulse at a particular distance (say,  $z = 25$ ) through various profiles for a given value loss equal to 0.01 (which is less than the critical value of loss in each case).

Comparison shows that in the integrable limit, maximum value of pulse compression is obtained when pulse is propagated through the fiber whose dispersion

varies in the Gaussian form.

Soliton compression factor,  $C_f$ , achieved by the DDF given by

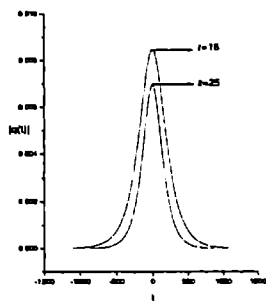
$$C_f = \frac{\tau_0}{\tau_L} = \frac{\lambda_2(L)}{\lambda_2(0)} = \frac{\eta_0}{\eta(L) + \eta_0} \quad (6.4.2)$$

Since the value of pulse width is constant at the beginning of each dispersion decreasing fiber, the compression achieved by the soliton pulse at the fiber length  $L$  in each profile can be compared. Table 6.2 shows the comparison of compression factors over a fiber length  $L = 25$ .

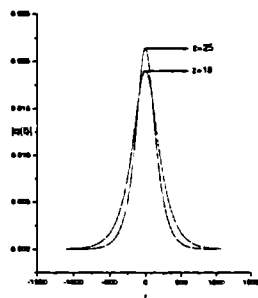
Nature of profiles	$C_f$
Linear	3.0
Hyperbolic	2.219
Exponential	2.543
Logarithmic	3.372
Gaussian	3.685

Table 6.2

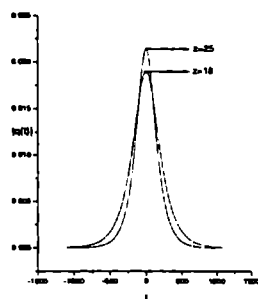
Analytical calculations also show that maximum value of compression is obtained when pulse is propagated through Gaussian profile. Using Eq. (6.4.2), the variation of compression factor with fiber length in profile can be studied. Its variation for a given value of fiber length ( $L = 25$ ) are illustrated in Fig. 6.7 From Eq. (6.4.2), it is obvious that  $C_f$  depends on the value of  $\beta$ . So, by varying the value  $\beta$ , pulse with desired value of compression factor  $C_f$  for a given length of fiber can be generated. As an example, by taking  $\beta = 1.391$  and keeping other parameters remain constant, compression factor equal to 10 can be achieved by propagating the pulse through Gaussian profile over a fiber length  $L = 25$ .



(a)

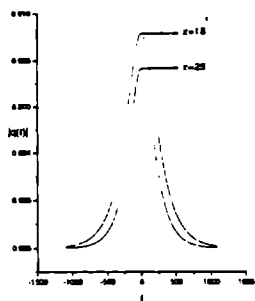


(b)

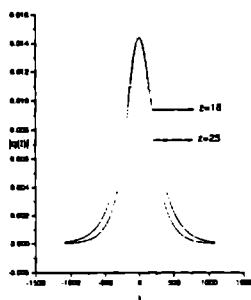


(c)

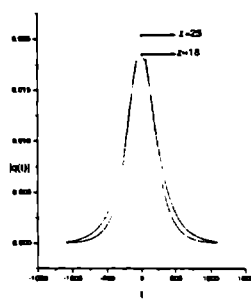
Fig. 6.1: Pulse propagation through linear profile for fiber loss  $\Gamma$  (a)  $> \Gamma_c$  (b)  $= \Gamma_c$  (c)  $< \Gamma_c$



(a)

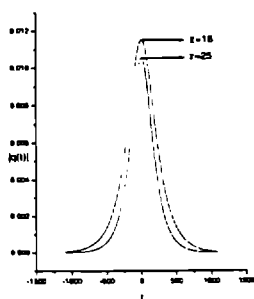


(b)

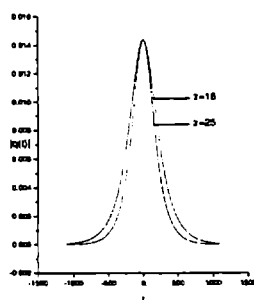


(c)

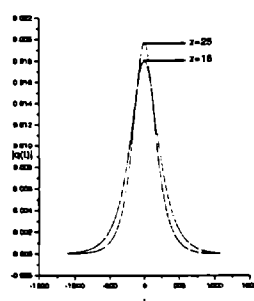
Fig. 6.2: Pulse propagation through hyperbolic profile for fiber loss  $\Gamma$  (a)  $> \Gamma_c$  (b)  $= \Gamma_c$  (c)  $< \Gamma_c$



(a)

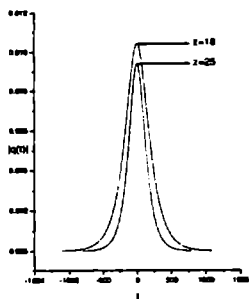


(b)

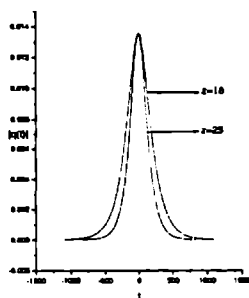


(c)

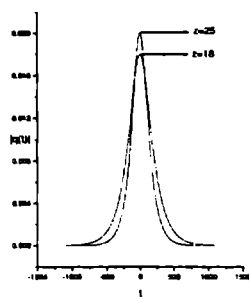
Fig. 6.3: Pulse propagation through exponential profile for fiber loss  $\Gamma$  (a)  $> \Gamma_c$  (b)  $= \Gamma_c$  (c)  $< \Gamma_c$



(a)



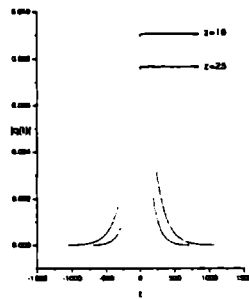
(b)



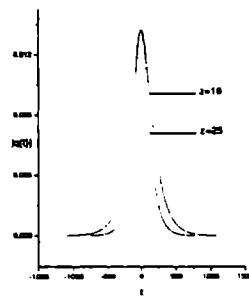
(c)

Fig. 6.4: Pulse propagation through logarithmic profile for fiber loss  $\Gamma$  (a)  $> \Gamma_c$  (b)  $= \Gamma_c$  (c)  $< \Gamma_c$

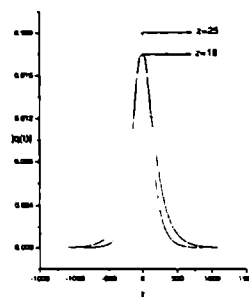




(a)



(b)



(c)

Fig. 6.5: Pulse propagation through Gaussian profile for fiber loss  $\Gamma$  (a)  $> \Gamma_c$  (b)  $= \Gamma_c$  (c)  $< \Gamma_c$

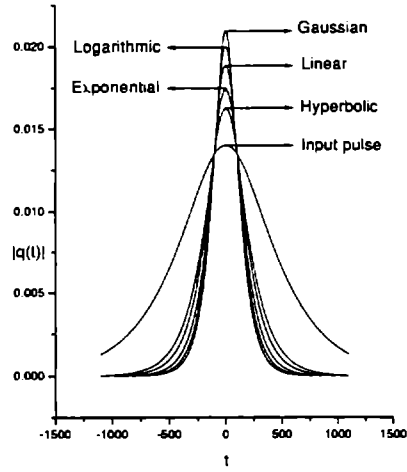


Fig. 6.6: Shows the comparison of the nature of the pulse through five different profiles at  $z = 25$  for  $\Gamma < \Gamma_c$

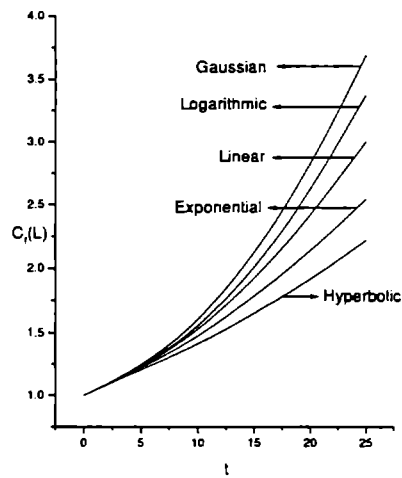


Fig. 6.7: Comparison in the variation of compression factor

## 6.5 Pulse propagation through a birefringent DDF

When a pulse is propagated through a lossy birefringent single mode fiber, it can be described by a coupled nonlinear Schrödinger (CNLS) equation of the form [96]

$$iq_{1z} + \beta_1(z) q_{1tt} + 2\beta_2(z) (|q_1|^2 + |q_2|^2) q_1 + i\Gamma q_1 = 0 \quad (6.5.1)$$

$$iq_{2z} + \beta_1(z) q_{2tt} + 2\beta_2(z) (|q_1|^2 + |q_2|^2) q_2 + i\Gamma q_2 = 0$$

where  $q_1$ ,  $q_2$ ,  $\beta_1(z)$ ,  $\beta_2(z)$ , and  $\Gamma$  have the usual meaning.

By making the following transformations:

$$q_1(z, t) = Q_1(\eta, t) \sqrt{\beta_1/\beta_2} \quad q_2(z, t) = Q_2(\eta, t) \sqrt{\beta_1/\beta_2} \quad (6.5.2)$$

$$\eta = \int_0^z \beta_1(z') dz'$$

Equation (6.5.1) can be reduced to a uniform coupled NLS equation of the form:

$$iQ_{1\eta} + Q_{1tt} + 2Q_1 (|Q_1|^2 + |Q_2|^2) - i\alpha(\eta) Q_1 = 0 \quad (6.5.3)$$

$$iQ_{2\eta} + Q_{2tt} + 2Q_2 (|Q_1|^2 + |Q_2|^2) - i\alpha(\eta) Q_2 = 0$$

where

$$\alpha(\eta) = -\sqrt{\frac{\beta_2}{\beta_1}} \frac{d}{d\eta} \left( \sqrt{\frac{\beta_1}{\beta_2}} \right) - \frac{\Gamma}{\beta_1} \quad (6.5.4)$$

Integrability analysis of Eq. (6.5.3) gives the result:

$$\alpha(\eta) = -\frac{1}{2(\eta + \eta_0)} \quad (6.5.5)$$

where  $\eta_0$  is an arbitrary constant. From Eqs. (6.5.4) and (6.5.5), the integrability condition can be rewritten as:

$$\sqrt{\frac{\beta_2}{\beta_1}} \frac{d}{d\eta} \left( \sqrt{\frac{\beta_1}{\beta_2}} \right) + \frac{\Gamma}{\beta_1} = \frac{1}{2(\eta + \eta_0)} \quad (6.5.6)$$

## 6.6 Lax pairs and soliton solutions

The linear eigen value problem associated with Eq. (6.5.3) is:

$$\psi_t = U\psi \quad \psi_\eta = V\psi \quad \psi = (\psi_1 \ \psi_2 \ \psi_3)^T \quad (6.6.1)$$

where

$$U = \begin{pmatrix} -i\lambda & u_1 & u_2 \\ -u_1^* & i\lambda & 0 \\ -u_2^* & 0 & i\lambda \end{pmatrix} \quad (6.6.2)$$

$$V = 2i\lambda^2 \begin{pmatrix} -1 & 0 & 0 \\ 0 & 1 & 0 \\ 0 & 0 & 1 \end{pmatrix} + 2\lambda \begin{pmatrix} i\alpha t & u_1 & u_2 \\ -u_1^* & -i\alpha t & 0 \\ -u_2^* & 0 & -i\alpha t \end{pmatrix} \quad (6.6.3)$$

$$+ i \begin{pmatrix} |u_1|^2 + |u_2|^2 & u_{1t} + 2i\alpha t u_1 & u_{2t} + 2i\alpha t u_2 \\ u_{1t}^* - 2i\alpha t u_1^* & -|u_1|^2 & -u_2 u_1^* \\ u_{2t}^* - 2i\alpha t u_2^* & -u_1 u_2^* & -|u_2|^2 \end{pmatrix}$$

and

$$u_1 = Q_1 \exp\left(-\frac{i\alpha t^2}{2}\right) \quad u_2 = Q_2 \exp\left(-\frac{i\alpha t^2}{2}\right) \quad (6.6.4)$$

The non-isospectral parameter  $\lambda$  is given by

$$\lambda = \lambda_0 \exp \left( 2 \int \alpha d\eta \right) \quad (6.6.5)$$

such that the compatibility condition  $U_\eta - V_t + [U V] = 0$  gives rise the Eq. (6.5.3). Using the transformation:

$$\begin{aligned} Q_1(\eta, t) &= \frac{-1}{(\eta + \eta_0)} U_1(Z, T) \exp \left( \frac{it^2}{4(\eta + \eta_0)} \right) \\ Q_2(\eta, t) &= \frac{-1}{(\eta + \eta_0)} U_2(Z, T) \exp \left( \frac{it^2}{4(\eta + \eta_0)} \right) \end{aligned} \quad (6.6.6)$$

$$Z = \frac{-1}{(\eta + \eta_0)} \quad T = \frac{-t}{(\eta + \eta_0)}$$

Eq. (6.5.3) can be transformed to CNLSE:

$$iU_{1Z} + U_{1TT} + 2U_1 (|U_1|^2 + |U_2|^2) = 0 \quad (6.6.7)$$

$$iU_{2Z} + U_{2TT} + 2U_2 (|U_1|^2 + |U_2|^2) = 0$$

Exact soliton solution of Eq. (6.6.7) is:

$$U_1 = 2k_2 \chi_1 \exp(-4i(k_1^2 - k_2^2)Z - 2ik_1T) \operatorname{sech}[8k_1k_2Z + 2k_2T] \quad (6.6.8)$$

$$U_2 = 2k_1 \chi_1 \exp(-4i(k_1^2 - k_2^2)Z - 2ik_1T) \operatorname{sech}[8k_1k_2Z + 2k_2T]$$

where  $\theta$  is the phase factor,  $k_1, k_2, \chi_1, \chi_1$  are arbitrary constants. By using Eqs.

(6.6.2) and (6.6.6), the fundamental soliton solution of Eq. (6.5.1) is obtained as

$$q_1(z, t) = 2\lambda_2\chi_1 \left( \frac{c_2^*}{c_1^*} \right) \exp \left( -\frac{i\alpha t^2}{2} - 4i \int (\lambda_1^2 - \lambda_2^2) d\eta - 2i\lambda_1 t \right) \sqrt{\frac{\beta_1}{\beta_2}} \operatorname{sech} h [8 \int \lambda_1 \lambda_2 d\eta + 2\lambda_2 t]$$

$$q_2(z, t) = 2\lambda_2\chi_2 \left( \frac{c_3^*}{c_1^*} \right) \exp \left( -\frac{i\alpha t^2}{2} - 4i \int (\lambda_1^2 - \lambda_2^2) d\eta - 2i\lambda_1 t \right) \sqrt{\frac{\beta_1}{\beta_2}} \operatorname{sech} h [8 \int \lambda_1 \lambda_2 d\eta + 2\lambda_2 t]$$
(6.6.9)

where  $\sigma = \frac{-\alpha t^2}{2} + 4 \int (\lambda_1^2 - \lambda_2^2) d\eta + 2\lambda_1 t$ ,  $\lambda_1 = k_1 \exp[2 \int \alpha d\eta]$ , and  $\lambda_2 = k_2 \exp[2 \int \alpha d\eta]$ .

Above soliton solutions help to describe the pulse propagation through a lossy birefringent single mode fiber with variable dispersion.

From Eq. (6.6.9), input pulse (at the input,  $z = 0$ ,  $\beta_1(z) = 1$ , and  $\Gamma = 0$ ) can be described as:

$$q_1(0, t) = \frac{2k_2}{\sqrt{\eta_0}} \left( \frac{c_2^*}{c_1^*} \right) \exp \left( -\frac{it^2}{2\eta_0} - \frac{2ik_1 t}{\eta_0} \right) \operatorname{sech} h \left[ \frac{2k_2 t}{\eta_0} \right]$$
(6.6.10)

$$q_1(0, t) = \frac{2k_2}{\sqrt{\eta_0}} \left( \frac{c_3^*}{c_1^*} \right) \exp \left( -\frac{it^2}{2\eta_0} - \frac{2ik_1 t}{\eta_0} \right) \operatorname{sech} h \left[ \frac{2k_2 t}{\eta_0} \right]$$

## 6.7 Critical loss and optimum dispersion profile

Compression of the input soliton pulse described by Eq. (6.6.10) through fibers with various dispersion-decreasing profiles, explained in Eq. (5.4.1), can be studied graphically with the help of Eqs. (6.6.9) and (5.4.1). Keeping the ratio of dispersion  $\beta = 3$  and fiber length  $L = 25$ , pulse propagation through various dispersion profiles for different fiber losses have been analyzed. Figures 6.8(a-c) show the variation in the amplitude and pulsewidth of the input pulse when it is propagated through linearly decreasing dispersion fiber with decreasing fiber losses at  $z = 18$  and  $25$ . From these figures, it is obvious that when  $\Gamma$  is greater than or equal to  $\Gamma_c$ , pulse area will not be conserved where as for  $\Gamma < \Gamma_c$ , area of the pulse is maintained during propagation. In linear case, value of critical loss is

found to be  $\Gamma_c = 0.02188$  and nature of the pulse when it is propagated through the fiber having  $\Gamma = \Gamma_c$  and  $\Gamma > \Gamma_c$  are shown in Fig. 6.8(b) and 6.8(a). From these figures, it is clear that soliton pulse area is conserved only when the loss is less than the critical value, which is shown in Fig. 6.8(c), and gets violated when the fiber loss is greater than or equal to critical value. Figs. 6.9(a-c), 6.10(a-c), 6.11(a-c), and 6.12(a-c) shows the pulse propagation through hyperbolic, exponential, logarithmic, and Gaussian profiles respectively for different losses. These analysis shows that critical value is different for different dispersion profiles. In all cases, it is observed that pulse area is maintained only when the fiber loss is less than the critical value. Table 6.3 gives the numerical value of  $\Gamma_c$  corresponding to each dispersion profiles.

Nature of profile	$\Gamma_c$
Linear	0.02188
Hyperbolic	0.01474
Exponential	0.01752
Logarithmic	0.02556
Gaussian	0.02702

Table 6.3

Here an interesting phenomena is noted that in each case, compressed pulses are completely free from pedestals. This makes the compressed pulse in the fiber highly stable as the presence of pedestals not only leads to a deterioration in the quality of pulse and energy characteristics of the compression, but it also makes the compressed unstable due to the nonlinear interaction of the pedestal with the compressed pulse. Fig. (6.13) shows the comparison of the nature of

the pulse after a given distance, say  $z = 25$ , through five different dispersion-decreasing profiles for a relatively small fiber loss, say  $\Gamma = 0.01$ , (which is less than the critical value in each case). Comparison shows that maximum value of pulse compression is obtained when pulse is propagated through the fiber whose dispersion varies in the Gaussian form. Therefore, from the graphical analysis, it is clear that Gaussian profile is found to be the optimum dispersion profile for achieving maximum pulse compression in the birefringent fiber.

Soliton compression factor,  $C_f$ , achieved by the DDF is given by

$$C_f = \frac{\tau_0}{\tau_L} = \frac{\lambda_2(L)}{\lambda_2(0)} \quad (6.7.1)$$

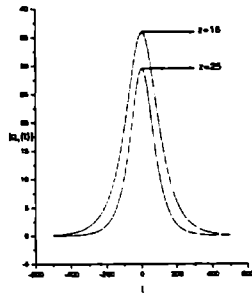
Table 6.4 shows the comparison of compression factor over a fiber length  $L = 25$ .

Nature of profiles	$C_f$
Linear	4.8
Hyperbolic	2.847
Exponential	3.616
Logarithmic	5.87
Gaussian	7.913

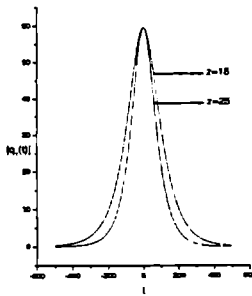
Table 6.4

Analytical calculations also show that maximum value of compression is obtained when pulse is propagated through the fiber with dispersion varies in the Gaussian nature. Variations in the compression factor for a given value of fiber length ( $L = 25$ ) are illustrated in Fig. 6.14.

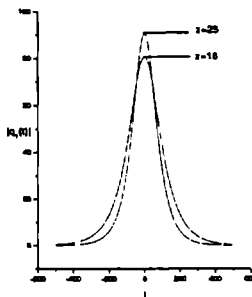




(a)

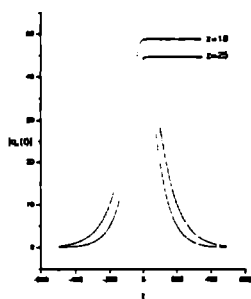


(b)

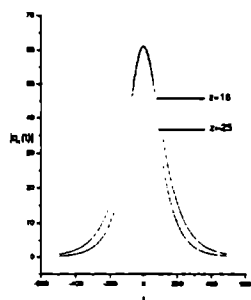


(c)

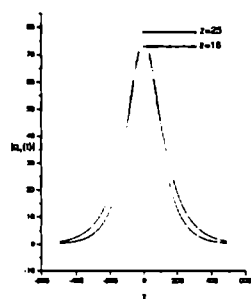
Fig. 6.8: Pulse propagation through linear profile for fiber loss  $\Gamma$  (a)  $> \Gamma_c$  (b)  $= \Gamma_c$  (c)  $< \Gamma_c$



(a)

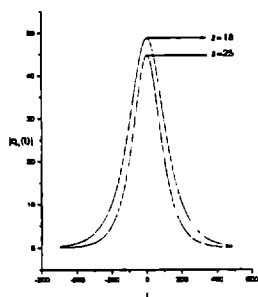


(b)

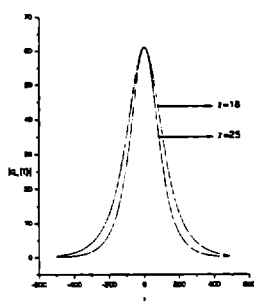


(c)

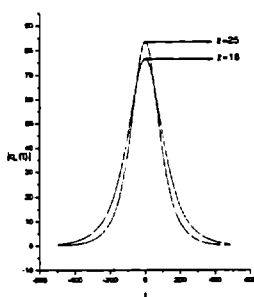
Fig. 6.9: Pulse propagation through hyperbolic profile for fiber loss  $\Gamma$  (a)  $> \Gamma_c$  (b)  $= \Gamma_c$  (c)  $< \Gamma_c$



(a)

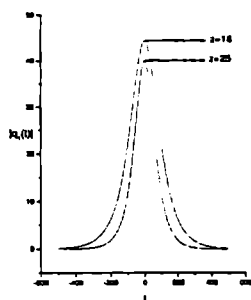


(b)

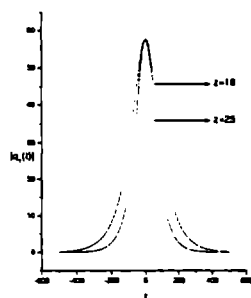


(c)

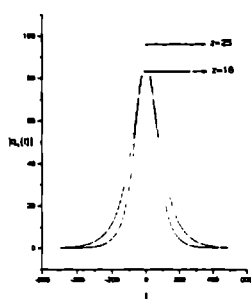
Fig. 6.10: Pulse propagation through exponential profile for fiber loss  $\Gamma$  (a)  $> \Gamma_c$  (b)  $= \Gamma_c$  (c)  $< \Gamma_c$



(a)

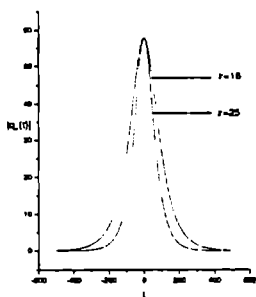


(b)

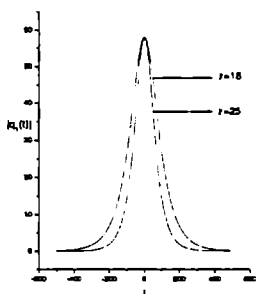


(c)

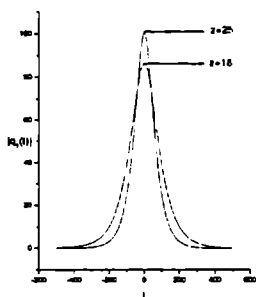
Fig. 6.11: Pulse propagation through logarithmic profile for fiber loss  $\Gamma$  (a)  $> \Gamma_c$  (b)  $= \Gamma_c$  (c)  $< \Gamma_c$



(a)



(b)



(c)

Fig. 6.12: Pulse propagation through Gaussian profile for fiber loss  $\Gamma$  (a)  $> \Gamma_c$  (b)  $= \Gamma_c$  (c)  $< \Gamma_c$

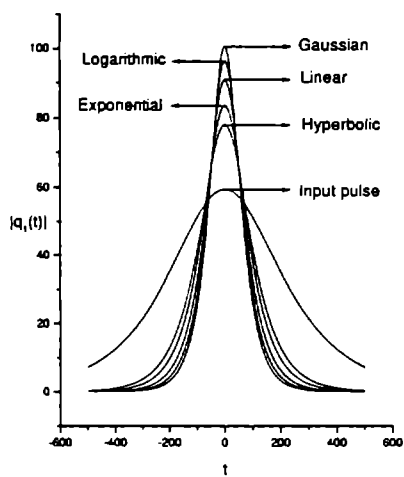


Fig. 6.13: Shows the comparison of the nature of the pulse through five different profiles at  $z = 25$  for  $\Gamma < \Gamma_c$

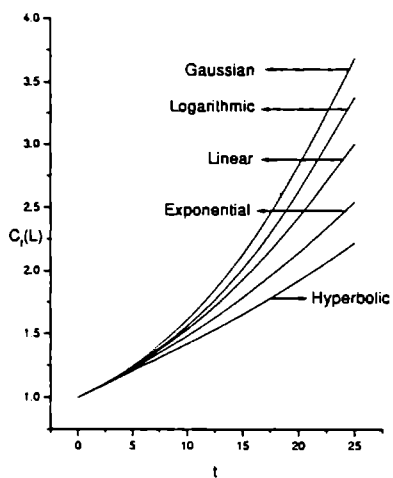


Fig. 6.14: Comparison in the variation of compression factor

## 6.8 Results and Discussions

In this chapter, the pulse propagation through lossy fiber with variable dispersion supporting both single and degenerative fields are considered. In the general case, the propagation equations we have considered will not describe soliton transmission. The condition required for the soliton propagation has been determined using integrability analysis. Exact soliton solution is constructed. Soliton pulse propagation through the fiber with various profiles for different values of fiber loss have been analyzed graphically. Graphical results show that there exists a critical value of fiber loss for each profiles and the critical value is found to be different for different profiles. Significance of critical value is that the soliton property of the conservation of soliton area is maintained when pulse is propagated below the critical value of fiber loss. When the loss exceeds this critical value, area conservation is not maintained at all.

Pulse propagation through different profiles for the fiber loss less than critical value have been analyzed graphically. Graphical results show that out of the five different profiles considered, Gaussian profile is found to be the optimum profile for the soliton pulse compression technique in the integrable limit. Arrived the compression factor achieved by the dispersion-decreasing fiber and obtained maximum value when pulse is propagated through Gaussian profile. Thus the theoretical values are in well agreement with the graphical result. Since soliton solutions considered have the fundamental nature, there should not appear any type of pedestals along with the compressed pulse. This makes the pulse in the fiber highly stable and also improves the quality of the compressed pulse.

# Chapter 7

## Conclusion

The results and conclusion of the thesis are summarized below.

1) Well-known nonlinear Schrödinger equation has been succeeded in explaining the propagation of pico-second optical pulses in single-mode optical fibers. But, when the pulses are so short, of the order of femtosecond, it is necessary to include higher-order effects such as third-order dispersion, self-steepening, and stimulated inelastic scattering. Propagation of femtosecond pulses with the inclusion of higher-order effects have been considered in chapter two. In general, such a system does not support soliton propagation. Using Painlevé analysis, condition required for the existence of soliton in the system described by coupled higher-order nonlinear Schrödinger equation have been obtained. Its integrability nature is confirmed by constructing Lax pairs. Both one and two-soliton solutions are generated using Hirota's technique. Two-soliton interactions are studied and shown that their interaction is elastic in nature.

2) Generation of stable, ultra-short optical pulses has become an important topic in view of their application in future ultrahigh-bit rate optical communication systems. Various methods are presented for the generation of ultra-short pulses in exactly integrable system. In an ideal communication systems, input pulse launched



into the fiber should be unchirped. But, in actual practice, pulse launched into the fiber need not be chirped and gets deviated from the ideal requirements necessary for formation of fundamental soliton. Condition required for the formation of soliton pulse when initially unchirped pulse propagate through lossy fiber is obtained. It is found that soliton formation is due to the effect of initial frequency chirp. It is also found that due to initial frequency chirp, soliton pulse gets compressed during propagation by keeping the important soliton property of area conservation.

3) The use of dispersion-decreasing fibers (DDFs) in particular have been recognized to be very useful for high-quality and stable pulse compression and soliton train generation. Condition for the existence of soliton in DDFs has been studied. Single mode optical fiber with various dispersion-decreasing profiles, namely linear, hyperbolic, exponential, logarithmic, and Gaussian have been considered. Graphical analysis shows that as pulse propagates through various dispersion decreasing profiles, pulse amplitude gets increased and pulse gets compressed adiabatically in each case by keeping the soliton property of area conservation. Out of the five different profiles considered, Gaussian profile is found to be the optimum dispersion profile for achieving maximum soliton pulse compression. Theoretical evaluation of compression factor also shows that maximum value of compression is obtained when pulse is propagated through the fiber with dispersion varies in the Gaussian form. Furthermore, an important feature is that compressed pulses are completely free from pedestals in each case. Same results have been also obtained from the birefringent DDFs.

4) In real DDFs, the light wave propagates with finite loss. It is found that such system also belongs to the class of integrable systems. Pulse propagation

through fiber with various dispersion-decreasing profiles, namely, linear, hyperbolic, exponential, logarithmic, and Gaussian for different values of fiber loss has been studied. It is found that there exists a critical value of fiber loss in each profiles and is different for different profiles. Significance of critical loss is found that the soliton property of the conservation of pulse area is maintained only when pulse is propagated below the critical loss. When the loss exceeds the critical value, area conservation is not maintained at all. Graphical analysis shows that out of the five different profiles considered, Gaussian profile is found to be the optimum profile for the soliton pulse compression technique in the integrable limit. Theoretical evaluation of the compression factor is in well agreement with the graphical result. Since the solitons considered have the fundamental nature, there should not appear any type of pedestals along with the compressed pulse. This makes the pulse in the fiber highly stable and improves the quality of the compressed pulse.

# Bibliography

- [1] A. Hasegawa and Y. Kodama, *Solitons in Optical Communications*, (Clarendon Press, Oxford, 1995).
- [2] G. P. Agrawal, *Nonlinear Fiber Optics* (Academic Press, San Diego, 2001).
- [3] G. P. Agrawal, *Application of Nonlinear Fiber Optics* (Academic Press, San Diego, 2001).
- [4] N. N. Akhmediev and A. Ankiewicz, *Solitons-Nonlinear Pulses and Beams* (Chapman and Hall, London, 1997).
- [5] M. J. Ablowitz, G. Biondini, and L. A. Ostrovsky, *Chaos* **10**, 471 (2000).
- [6] A. Hasegawa, *Chaos* **10**, 475 (2000).
- [7] A. Hasegawa, *Pramana J. Phys.* **57**, 1097 (2001).
- [8] M. N. Islam, *Opt. Lett.* **14**, 1257 (1989).
- [9] M. N. Islam, *Opt. Lett.* **15**, 417 (1990).
- [10] C. R. Menyuk, M. N. Islam, and J. P. Gordon, *Opt. Lett.* **16**, 566 (1991).
- [11] S. V. Chernikov, P. V. Mamyshev, *J. Opt. Soc. Amer. B* **8**, 1633 (1991).

- [12] S. V. Chernikov, D. J. Richardson, E. M. Dianov, D. N. Payne, *Electron Lett.* **28**, 1842 (1992).
- [13] A. L. Steele, *Electron. Lett.* **29**, 1971 (1993)
- [14] B. C. Collings, S.T. Cundiff, N. N. Akhmediev, J. M. Soto-Crespo, K. Bergman and W. H. Knox, *J. Opt. Soc. Am. B* **17**, 354 (2000).
- [15] J. M. Soto-Crespo, N. N. Akhmediev, B. C. Collings, S. T. Cundiff, K. Bergman and W. H. Knox, *J. Opt. Soc. Am. B* **17**, 366 (2000).
- [16] A. D. Kim, J. N. Kuntz, and D. J. Muraki, *IEEE J. Quantum Electron.* **36**, 366 (2000).
- [17] Y. Gong, P. Shuma, T. Hianga, Chenga, Q. Wena and D. Tang, *Opt. Commun.* **200**, 389 (2001).
- [18] N. S. Bergano and C. R. Davidson, *J. lightwave Tech.* **14**, 1299 (1996).
- [19] A. Ghatak and K. Thyagarajan, *Introduction to Fiber Optics* (Cambridge University Press, Cambridge, U.K, 1999).
- [20] S. R. Nagel, J. B. MacChesney, and K. L. Walker *Optical Fiber Communications*, Vol.1 (Academic Press, Orlando, 1985).
- [21] Y. R. Shen, *Principles of Nonlinear Optics* (Wiley, New York, 1984).
- [22] P. N. Butcher and D. N. Cotter, *The Elements of Nonlinear Optics*, (Cambridge University Press, Cambridge, U.K, 1990).
- [23] W. Zhao and E. Bourkoff, *IEEE J. Quantum Electron* **QE-24**, 365 (1988).
- [24] R. W. Boyd, *Nonlinear Optics* (Academic Press, San Diego, CA, 1992).

- [25] B. H. Stolen and C. Lin, *Phys. Rev. A* **17**, 1448 (1978).
- [26] S. A. Akhmanov, R. V. Khokklov, and A. P. Sukhorukov, *Laser Handbook* (North-Holland, Amsterdam, 1972).
- [27] S. Song, C. T. Allen, K. R. Demarest, and R. Hui, *J. Lightman Tech.* **17**, 2285 (1999).
- [28] D. Grischkowsky, E. Courtens, and J. A. Armstrong, *Phys. Rev. Lett.* **31**, 422 (1973).
- [29] Y. Kodama and A. Hasegawa, *IEEE J. Quantum Electron.* **23**, 510 (1987).
- [30] R. H. Stolen, *Optical Fiber Communications* (Academic Press, New York, 1979).
- [31] A. Hasegawa and Y. Kodama, *Proc. IEEE* **69**, 1145 (1981).
- [32] A.C. Newell, *Nonlinear Optics* (Addison-Wesley Publishing company, California, 1992).
- [33] P. Damient, *Wave Transmission and Fiber Optics* (MacMillian, New York, 1990).
- [34] M. Schubert and B. Wilhelmi, *Nonlinear Optics and Quantum Electronics* (Wiley, New York, 1986).
- [35] G. P. Agrawal, *Supercontinuum Laser Source*, Ed. R. R. Alfano (Springer-Verlag, Heidelberg, 1989)
- [36] H. A. Haus, *Waves and Fields in Optoelectronics* (Prentice-Hall, Englewood Cliffs, 1984)

- [37] P. M. Morse and H. Feshbach, *Methods of Theoretical Physics*, (McGrawHill, New York, 1953).
- [38] A. Hasegawa and F. Tappert, *Appl. Phys. Lett.* **23**, 142 (1973).
- [39] L. F. Mollenauer, R. H. Stolen and G. P. Gordon, *Phys. Rev. Lett.* **45**, 1095 (1980).
- [40] A. Hasegawa and F. Tappert, *Appl. Phys. Lett.* **23**, 171 (1973).
- [41] J. A. Rao and A. A. Rangawala, *Solitons-Introduction and Applications*, Ed. M. Lakshmanan (Springer-Verlag, Germany, 1998).
- [42] A. A. Rangawala and J. A. Rao, *Phys. Lett. A* **112**, 188 (1985).
- [43] H. H. Kuehl, *J. Opt.Soc. Am. B* **5**, 709 (1988).
- [44] S. V. Chernikov, E. M. Dianov, D. J. Richardson, and D. N. Payne, *Opt. Lett.* **18**, 476(1993).
- [45] P. V. Mamyshev, *Optical solitons-Theory and Experiment* Ed. J. R. Taylor (Cambridge University Press, Cambridge, U.K, 1992).
- [46] P. V. Mamyshev, S. V. Chernikov, and E. M. Dianov, *IEEE J. Quantum Electron.* **27**, 2347 (1991).
- [47] E. A. Swanson and S. R. Chinn, *IEEE Photon. Technol. Lett.* **6**, 796 (1994).
- [48] J. Weiss, M. Tabor and G.J. Carnevale, *J. Math. Phys.* **24** 522 (1983)
- [49] M. D. Kruskal and N. Joshi, *Soliton theory, Painlevé property and integrability* (University of New South Wales, Australia, 1991).
- [50] K. Porsezian, *Pramana-J. of Phys.* **143**, 48 (1997).

- [51] C. S. Gardner, J. M. Greene, M. D. Kruskal, and R. M. Miura, *Phys. Rev. Lett.* **19**, 1905 (1967)
- [52] P. D. Lax, *Commun. Pure Appl. Math.* **21**, 467 (1968).
- [53] M. J. Ablowitz, D. J. Kaup, A. C. Newell, and H. Segur, *Stud. Appl. Math.* **53**, 249 (1974)
- [54] R. Hirota, *Solitons*, Ed. R. K. Bullough and P. J. Caudrey (Springer, Berlin, 1980).
- [55] H. H. Chen, *Backlund Transformation*, Ed. A. Dold and B. Eckmann, (Springer-Verlag, Berlin, 1974).
- [56] M. Miyagi and S. Nishida, *Appl. Opt.* **18**, 678 (1979).
- [57] N. Tzoar and M. Jain, *Phys. Rev. A* **23**, 1266 (1981).
- [58] D. Anderson and M. Lisak, *Phys. Rev. A* **27**, 1393 (1983).
- [59] D. N. Christodoulidis and R. I. Joseph, *Appl. Phys. Lett.* **47**, 76 (1985).
- [60] E. A. Golovchenko, E. M. Dianov, A. N. Prokhorov, and V. N. Serkin, *JETP Lett.* **42**, 87 (1985).
- [61] F. M. Mitschke and L. F. Mollenauer, *Opt. Lett.* **11**, 659 (1986).
- [62] J. P. Gordon, *Opt. Lett.* **11**, 662 (1986).
- [63] K. Ohkuma, Y. H. Ichikawa, and Y. Abe, *Opt. Lett.* **22**, 516 (1987).
- [64] Y. Kodama and K. Nozaki, *Opt. Lett.* **12**, 1038 (1987).
- [65] R. Radhakrishnan and M. Laksmanan, *Phys. Rev. E*, **54**, 2949 (1996).

- [66] W. Hodel and H. P. Weber, *Opt. Lett.* **12**, 924 (1987).
- [67] K. Tai, A. Hasegawa, and N. Bekki, *Opt. Lett.* **13**, 392 (1996).
- [68] R. Hirota, *J. Math. Phys.* **14**, 805 (1973).
- [69] N. Sasa and J. Satsuma, *J. Phy. Soc. Jpn.* **60**, 409 (1991).
- [70] K. Porsezian, M. Daniel and M. Lakshmanan, *Non-Linear Evolution Equations and Dynamical Systems*, Ed V. C. Makankov (World Scientific, Singapore, 1993).
- [71] M. N. Vinoj and V. C. Kuriakose, *Phys. Rev. E*, **62**, 8719 (2000).
- [72] D. H. Auston and M. C. Nuss, *IEEE J. Quantum Electron.* **24**, 184 (1988).
- [73] B. B. Hu and M. C. Nuss, *Opt. Lett.* **20**, 1716 (1995).
- [74] J. Valdmains and G. Mourou, *IEEE J. Quantum Electron.* **22**, 69 (1986).
- [75] T. Nagatsuma, M. Yaita, M. Shinagawa, K. Kato, A. Kozen. K. Iwatsuki, and K. Suzuki, *Electron. Lett.* **30**, 814 (1994).
- [76] S. Arahira, S. Oshiba, Y. Matsui, T. Kunni, and Y. Ogawa, *Appl. Phys. Lett.* **64**, 1917 (1994)
- [77] A. G. Weber, M. Schell, G. Fischbeck, and D. Bimberg, *IEEE J. Quantum Electron.* **28**, 2220 (1992).
- [78] J. T. Ong, R. Takahashi, M. Tsuchiya, S. H. Wong, R. T. Shara, Y. Ogawa, and T. Kamiya, *IEEE J. Quantum Electron.* **29**, 1701 (1993).
- [79] K. A. Ahmed, K. C. Chan, and H. F. Liu, *IEEE J. Select. Topics Quantum Electron.* **1**, 592 (1995).



- [80] H. H. Kuehl, *J. Opt. Soc. Am. B* **5**, 709 (1988).
- [81] M. N. Vinoj, V. C. Kuriakose, and K. Porsezian, *Chaos, Solitons, and Fractals*, **12**, 2569 (2001).
- [82] J. D. Moores, *Opt. Lett.* **21**, 555 (1996).
- [83] V. K. Mezentsev and S. K. Turitsyn, *Opt. Commun.* **146**, 225 (1998).
- [84] M. N. Vinoj and V. C. Kuriakose, *Pramana-J. of Phys.* **57**, 987 (2001).
- [85] P. Emplit, J. P. Hamaide, F. Reynaud, C. Froehly, and A. Barthelemy, *Opt. Commun.* **62**, 374 (1987).
- [86] G. A. Swartzlander, *Opt. Lett.* **17**, 493 (2001).
- [87] B. Luther-Davies and Y. Xiaoping, *Opt. Lett.* **17**, 496 (1992).
- [88] D. Krokul, N. J. Halas, G. Giuliani, and D. Grisehowsky, *Phys. Rev. Lett.* **60**, 29 (1988).
- [89] Y. S. Kivshar and B. Luther-Davies, *Phys. Rep.* **298**, 81 (1998).
- [90] E. M. Dianov, P. V. Mamyshev, A. M. Prokhorov, and S. V. Chernikov, *Opt. Lett.* **14**, 1008 (1989).
- [91] S. V. Chernikov, J. R. Taylor, P. V. Mamyshev, and E. M. Dianov, *Electron. Lett.* **28**, 931 (1994).
- [92] S. V. Chernikov, J. R. Taylor, and R. Kashyap, *Electron. Lett.* **29**, 1788 (1992).
- [93] M. N. Vinoj, A. U. Seema, and V. C. Kuriakose, *J. of Nonlinear Optical Physics and Materials* (to appear).

- [94] M. N. Vinoj and V. C. Kuriakose, (submitted to Pramana-J. of Phys.)
- [95] M. N. Vinoj and V. C. Kuriakose, J. Opt. A: Pure Appl. Opt. (to appear)
- [96] M. N. Vinoj and V. C. Kuriakose, Opt. Commun. (to appear)

